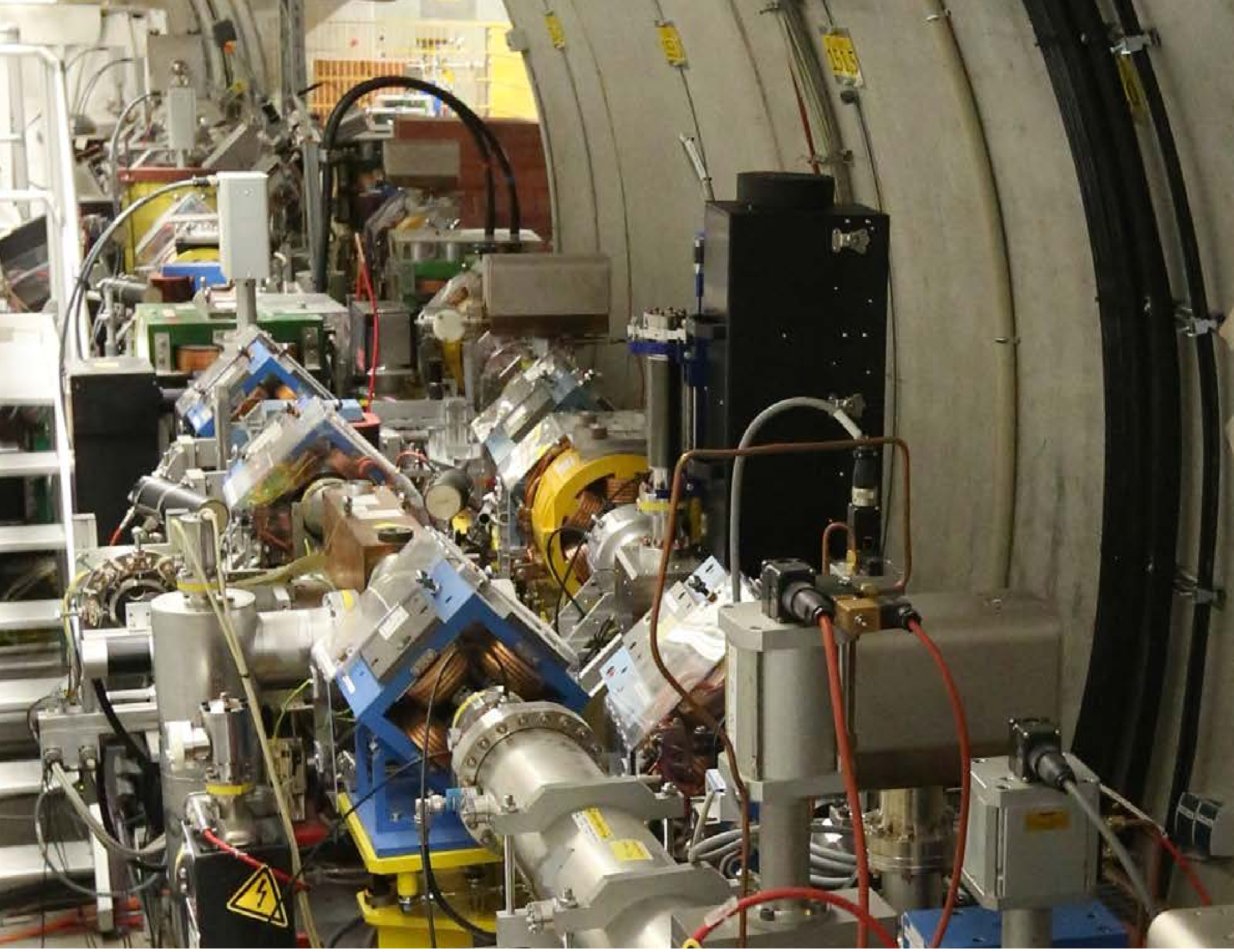

ACCELERATORS 2014.

Highlights
and Annual Report

Accelerators | Photon Science | Particle Physics

Deutsches Elektronen-Synchrotron
A Research Centre of the Helmholtz Association

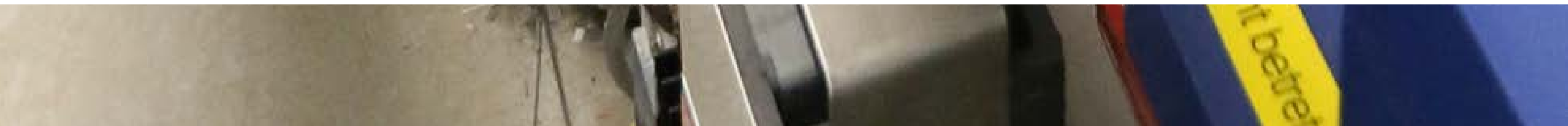

Cover

One of the highlights of 2014 was the first lasing of the new FLASH2 undulator beamline on 20 August. The photograph shows the FLASH1 beamline on the left and the new extraction beamline of FLASH2 on the right. (Titelphoto: Dirk Nölle, DESY)

ACCELERATORS 2014.

Highlights and
Annual Report

Contents

The year 2014 at DESY.

Chairman's foreword

As a member of the Helmholtz Association, the DESY research centre plays a leading role in the Helmholtz research field "Matter". In preparation of the so-called third Helmholtz programme-oriented funding period (POF III), which sets the financial frame for the coming five years from 2015 to 2019, the research field "Matter" has been radically reorganised in order to meet the challenges of the future. The three novel research programmes within "Matter" promote enhanced cooperation between hitherto separate scientific disciplines and between several Helmholtz research centres. One example is the newly formed research programme "Matter and the Universe", which – for the first time – integrates particle physics, astroparticle physics and the physics of hadrons and nuclei. Another prime example is the novel research programme "Matter and Technologies", which strategically joins forces across Helmholtz centres to strengthen the development of enabling technologies for future particle accelerators, for advanced particle and photon detectors and for computing infrastructures.

In spring 2014, the POF III Helmholtz evaluation confirmed the outstanding quality within the research field "Matter", including DESY's substantial contributions. The international peer review panels awarded highest marks to all research activities, including DESY's user facilities – the synchrotron radiation source PETRA III and the soft X-ray free-electron laser FLASH – as well as to the X-ray free-electron laser European XFEL, which is currently under construction. With the resulting new budget lines, which foresee an annual increase of 3% for our research programmes and of 4% for the operation of our user facilities, we have a very solid base for fulfilling our mission.

Based on its core competencies as a world-leading accelerator laboratory, DESY's strategy is to devise and develop forefront accelerator facilities on site and to be a key player in European and international large-scale projects. Currently, work at DESY focuses on the construction of the accelerator for the European XFEL and on the commissioning of the re-assembled PETRA III storage ring, its two new experimental halls and the second FLASH experimental hall.

The construction of the European XFEL is ongoing. Major parts of the infrastructure, such as the electron injector and the radio frequency system, have been installed in the tunnel. The first modules are already mounted, and the serial production of further modules is running smoothly. DESY is making every effort to meet the overall goal of closing the tunnel by mid-2016. The excellent work of our accelerator team and its friendly and effective collaboration with the members of the Accelerator Consortium are key factors for success.

DESY's soft X-ray laser FLASH is a world-leading user facility with outstanding scientific output, and it continues to be a

View into the main tunnel of the European XFEL X-ray laser with first accelerator modules

Representatives of the Helmholtz Association touring the tunnels of the European XFEL X-ray laser on the occasion of the evaluation for the third programme-oriented funding period (PoF III)

pathfinder for free-electron laser (FEL) science and technology. With the simultaneous operation of two independent undulator chains, FLASH is leading the worldwide efforts towards multi-user operation of FEL facilities.

Further important activities at DESY are its participation in the upgrade programme of the experiments at the Large Hadron Collider (LHC) at CERN near Geneva as well as in the implementation of the Cherenkov Telescope Array (CTA), a new international gamma-ray observatory. DESY has allocated considerable resources from its base budget for these two mission-critical projects and is currently seeking additional funding.

DESY is embarking into an exciting and brilliant future. The novel research infrastructures at DESY enable radically new ways of exploring matter and materials at relevant length and time scales, opening a new gate to the design of tailored functional materials and better drugs, and to new discoveries in the nanoworld. In order to exploit these opportunities for scientific breakthroughs, DESY has started to expand its own research capabilities and launched new interdisciplinary research cooperations on the DESY campus. The Center for Free-Electron Laser Science (CFEL) and the new Centre for Structural Systems Biology (CSSB) are two highlights hereof.

At the same time, DESY has already redirected considerable financial resources for the future operation of the European XFEL. A challenge that DESY is currently facing is to ensure that the long-term German contribution to the European XFEL operation is secured without further reductions imposed onto DESY's research. I am optimistic that the current negotiations with DESY's funding and advisory bodies will deliver a practical solution.

In future, DESY will take a more strategic approach to technology transfer. To better leverage the potential for innovation, the Senate of Hamburg, DESY and the University of Hamburg decided to build up a new business incubator on the DESY campus. This innovation centre will foster and facilitate enterprise foundations, and start-ups will get support within an inspiring scientific and technological environment. Two start-up companies initiated by DESY scientists are already being co-funded by the Helmholtz Association. The X-Spectrum company will enter the market with a high-technology X-ray detector, and Class 5 Photonics will build very flexible femtosecond lasers generating short, high-power pulses.

I am delighted to thank all our dedicated accelerator staff and our collaborators for their excellent work and commitment.

Helmut Dosch
Chairman of the DESY Board of Directors

Accelerators at DESY.

Introduction

Regarding DESY's accelerator activities, the year 2014 was characterised by much and decisive progress in our large-scale projects and our research and development programme.

The PETRA III synchrotron radiation facility was shut down as planned for most of the year for the extension project, which comprises the construction of new beamlines in the North and East sections. Removal of the machine and tunnel sections, construction of the new tunnels and experimental halls and re-installation of the accelerator components proceeded very well and within the foreseen schedule. By the end of the year, the work was essentially completed. Re-commissioning of the machine will take place in early 2015, fully in accord with the project plan, and first users in the Max von Laue experimental hall can expect photon beams by the end of the first quarter of 2015. While getting PETRA III back into routine operation is the primary goal, investigations of possible performance improvements for the future are also continuing. It was found that limitations of the achievable (already very small) horizontal emittance are not only caused by the focusing strengths in the regular PETRA III arcs but also by the beam optics of the "new eighth" section. First concepts to mitigate these limitations have been worked out, and the potential of PETRA III for even smaller emittances will be further explored in the future. The shutdown of PETRA III was a good opportunity to perform improvements on the pre-accelerators, which had been on the to-do list for quite a while. In particular, installing an additional new injector gun in the LINAC II pre-accelerator was an important measure to eliminate a potentially serious operation reliability risk by providing a backup for the electron beam source. This work, together with other refurbishments, was completed well in time to get the pre-accelerator chain back into operation to deliver beam for the PETRA III re-commissioning in 2015.

The FLASH free-electron laser (FEL) facility resumed routine user operation with the FLASH1 undulator beamline in early 2014 and delivered self-amplified spontaneous emission (SASE) FEL beams with good performance and high reliability until the end of the year. In parallel, work on the new FLASH2 beamline was completed, and beam commissioning took place. After stable and reproducible extraction of the beam into the new beamline was demonstrated, it became quickly clear that FLASH2 studies could almost entirely be done in parallel to FLASH1 user operation without perturbing the latter, thus demonstrating early on the concept of splitting the beam pulse between the two beamlines. FLASH2 commissioning proceeded very efficiently, leading to a first SASE FEL beam in the movable-gap undulator on 20 August 2015, while FLASH1 kept on routinely serving users. Simultaneous operation of two FEL beamlines with one accelerator was thus proven for the first time worldwide, an important result and invaluable experience also for the later user operation of the European XFEL X-ray laser facility. Construction of the FLASH2 photon beamline will continue and, in the course of 2015, the first experiments will be carried out in the new FLASH2 experimental hall.

Although longer interruptions of FLASH operation due to failures in the radio frequency (RF) gun, as occasionally experienced previously, did not occur in 2014, work on better long-term system reliability is ongoing. Modifications in the cathode area seem to have significantly improved the situation, and systematic studies of the RF window have started to reduce the probability of failure, which is important for FLASH but even more so for the long-pulse and high-gradient gun operation parameter regime needed for optimum performance of the European XFEL. The PITZ photoinjector test facility at the DESY location in Zeuthen is strongly involved in these important activities.

Undulator of FLASH2, the new beamline at DESY's FLASH free-electron laser facility

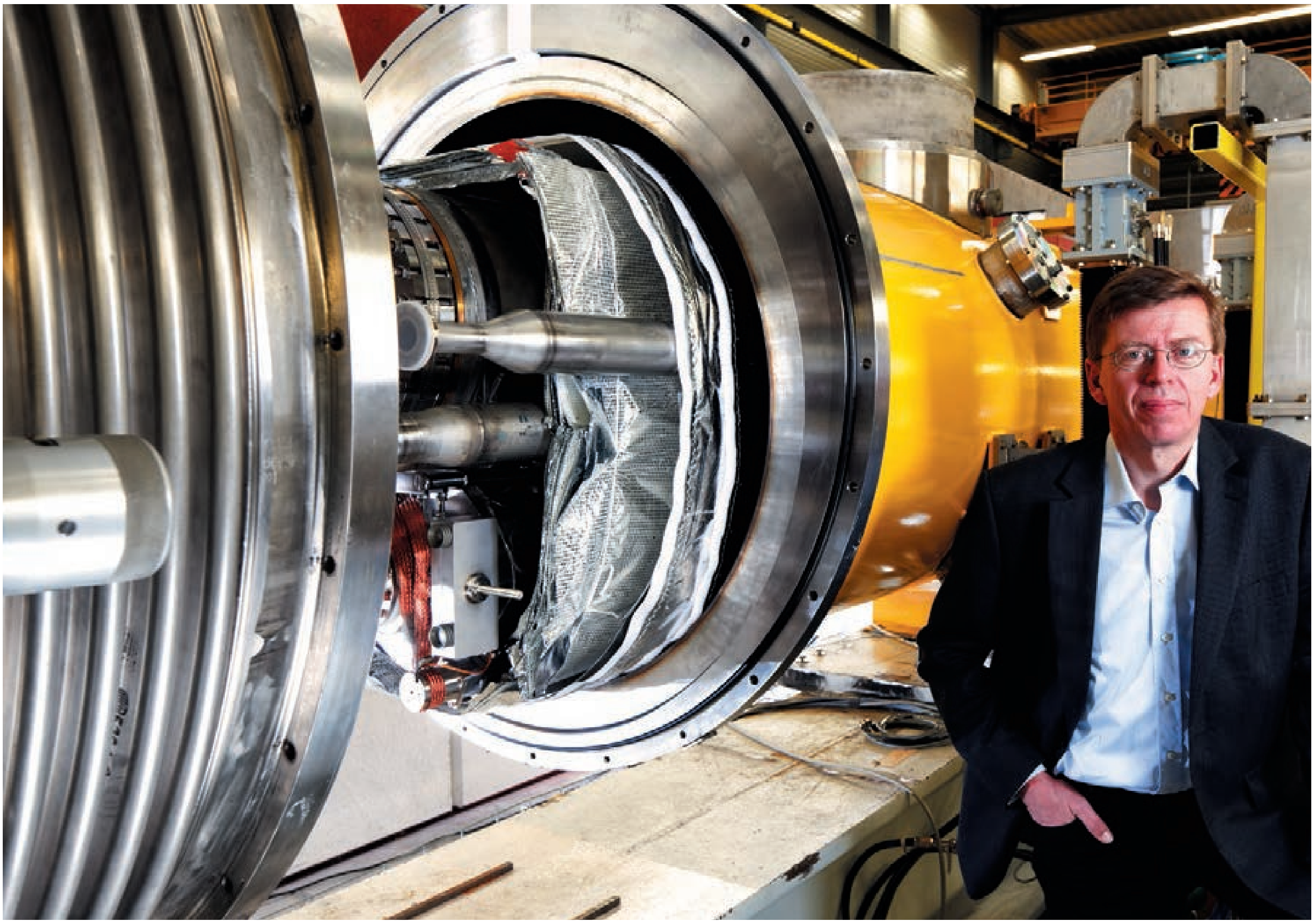

In the European XFEL accelerator construction project, a breakthrough was achieved in the production of superconducting accelerator modules. After overcoming earlier challenges and problems, the assembly, which takes place at CEA in Saclay, France, was ramped up during the year and reached the foreseen rate of one module per week delivered to DESY consistently in the last quarter of 2014. The module tests at the Accelerator Module Test Facility (AMTF) at DESY also picked up speed and, by the end of 2014, a considerable fraction of the 24 delivered modules had undergone the cool-down, conditioning and RF test procedure. A reduction in accelerating gradient relative to previous single-cavity tests is observed for some of the cavities, but thanks to the high performance reached in the cavity production, the achieved average gradient per module is within the European XFEL specifications. By the end of 2014, several accelerator modules had been installed into the European XFEL accelerator tunnel in their foreseen positions, and the procedures for making the necessary module interconnections were being established. A major focus in the project is now on accelerating module assembly, tests and installation simultaneously so that every possible effort is made to complete the construction of the superconducting linear accelerator by summer 2016, in accordance with the project schedule. Besides the modules, these efforts involve a large number of other components – such as RF and vacuum systems, magnets and power supplies, diagnostics and controls, etc. – and a large part of the accelerator division and infrastructure groups at DESY are working heavily and with great engagement towards this challenging goal.

Regarding our accelerator research activities, the evaluation of the Accelerator Research and Development (ARD) topic as part of the “Matter and Technologies” programme proposal for the third programme-oriented funding period (POF III, 2015–2019) of the Helmholtz Association was certainly a highlight in 2014. Together with our partners in five other Helmholtz centres and two Helmholtz institutes, we presented a convincing research strategy and received very positive comments and excellent ratings from the group of international reviewers. The R&D on superconducting RF technology in continuous-wave mode (with possible future applications at FLASH and the European XFEL) and the development of laser plasma acceleration, two activities that are being strongly ramped up at DESY, were identified by the reviewers as particularly important and are to be given highest priority in the execution of the programme.

Enjoy reading more about our exciting accelerator activities on the following pages!

Reinhard Brinkmann
Director of the Accelerator Division

News and events.

News and events.

A busy year 2014

February

Happy birthday, DESY synchrotron!

The particle accelerator "Deutsches Elektronen-Synchrotron" celebrated its 50th birthday. Half a century ago, electrons completed their first lap around the newly built DESY ring accelerator. This marked the start of the particle acceleration era in Hamburg, which eventually saw the DESY research centre (which is named after the synchrotron) develop into Germany's largest accelerator centre and become a pioneer in technologies for particle detectors and experiments with synchrotron radiation.

On 26 February 1964, DESY Director Willibald Jentschke celebrated the successful start of the DESY accelerator together with the accelerator team.

On 25 February 1964, shortly before midnight, the first particles repeatedly rounded the 300 m diameter synchrotron. After two weeks of sometimes frustrating efforts by the accelerator team, everything went very quickly. The first electrons reached an energy of 2.5 GeV in about 8000 rounds, and on the following day already, it was possible to obtain 5 GeV, just 1 GeV short of the final design energy.

Eventful years of operation followed, with all kinds of particle physics experiments and with the world's first characterisation studies of synchrotron radiation, whose high value for research was first recognised at DESY. Since then, the synchrotron has been serving as a pre-accelerator for the large-scale particle accelerators DORIS, PETRA and HERA. Moreover, it is still in demand as a test beam source for the investigation of future detectors. Even on its 50th birthday, the DESY synchrotron went on operating, reliably accelerating electrons to 6.3 GeV.

April

Russian Ambassador visits DESY and European XFEL

On 29 April, the Ambassador of the Russian Federation to Germany, Vladimir M. Grinin, visited DESY and European XFEL. On a tour of the PETRA III synchrotron radiation source and the construction site of the European XFEL X-ray free-electron laser, Ambassador Grinin got an impression of the diversity of collaborations between DESY researchers and Russian institutes. "Especially regarding our research infrastructures – in particular at the European XFEL and the German–Russian beamline at PETRA III – we have jointly achieved a new level of collaboration, in which the competence and reliability of our Russian partners are essential," DESY Director Helmut Dosch said on the occasion.

The PETRA III extension, which is currently under construction, will be equipped with a German–Russian beamline, due to take up operation in 2016. Russia also contributes over 300 million euro to the European XFEL X-ray laser, making it the second-largest shareholder after Germany. Among other things, about 800 beamline magnets and many cryogenic components for the superconducting accelerator technology come from Russian institutions. The three test benches used to check the super-conducting accelerator modules prior to their installation into the European XFEL tunnel are also provided by Russian institutes. "Russian scientists are delivering a very important contribution to the development of free-electron lasers in general and of the European XFEL in particular," said European XFEL Managing Director Massimo Altarelli.

DESY's cooperation with Russian institutes has a long tradition that goes back almost to the founding era of the research centre. Since 2013, the German–Russian cooperation in the development and application of large-scale research facilities has been concentrated within the Ioffe Röntgen Institute (IRI), which is coordinated by DESY and the National Research Centre Kurchatov Institute in Moscow.

Ambassador Vladimir Grinin (left) together with DESY physicist Wolfgang Drube at PETRA III

X-ray laser flashes measured with record time resolution

Researchers from DESY and the SLAC National Accelerator Laboratory in California, USA, have developed a new pulse monitor to measure individual pulses of X-ray free-electron lasers (FELs) with unprecedented time resolution. At SLAC's Linac Coherent Light Source (LCLS), the scientists achieved a resolution of 1 fs. The previous record for single-shot measurements was 10 fs.

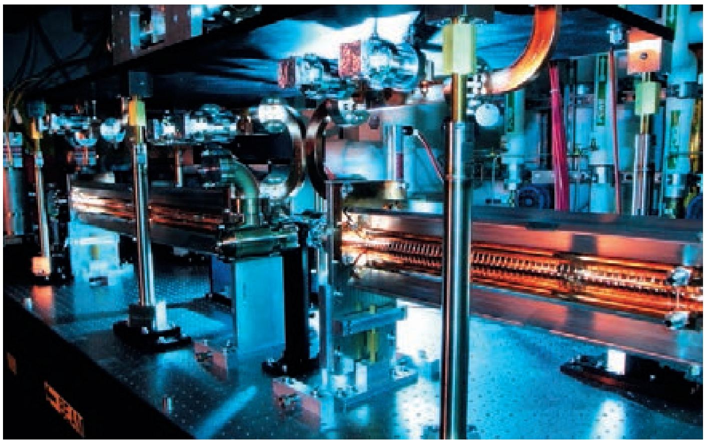

The X-band radio frequency transverse deflector (two 1 m long structures) is the centrepiece of LCLS's new pulse monitor, which provides shot-by-shot pulse information with unsurpassed few-femtosecond time resolution

Owed to their extraordinary power packed into ultrashort light pulses, X-ray FELs promise scientific breakthroughs in many areas, ranging from imaging of single molecules to filming the motion of electrons in atoms and molecules. However, the interpretation of such experiments is challenging because individual X-ray FEL pulses vary in shape and length. The new pulse monitor, which was unveiled in a study published by the journal *Nature Communications*, provides researchers with precise measurements of every single X-ray pulse – crucial information for the analysis of data collected at LCLS and potentially other FELs, including FLASH2, the new beamline at DESY's FLASH facility, and the European XFEL X-ray laser, which is currently under construction in Northern Germany.

X-ray FELs are linear accelerators that bring bunches of electrons to nearly the speed of light before sending them through magnetic structures known as undulators. These cause the electrons to wiggle along their flight path and emit radiation that amplifies into very bright and ultrashort flashes of X-ray laser light. Subsequent FEL pulses are not identical, however. They differ slightly in shape and duration, as both the statistical nature of light production in X-ray FELs and the acceleration process lead to fluctuations between separate shots.

Such irregularities pose a significant challenge for experimenters. Many processes studied with X-ray FELs depend on how they are initiated or sampled by the X-ray pulse, and scientists therefore need to know the exact time-dependent pulse profile. Moreover, applications such as the imaging of single molecules rely on limiting the exposure of samples to damaging X-rays and would thus also profit from a precise knowledge of X-ray pulse durations. Yet, high-resolution pulse monitors for X-ray FELs are not widely available. Until now, researchers estimated LCLS's X-ray pulse lengths indirectly from the lengths of the electron bunches that produce the X-ray pulses – an approximation often not accurate enough for the interpretation of experiments.

With the new pulse monitor, scientists can measure X-ray pulses more directly. The electron beam is diagnosed after it has left the undulators. As the production of X-rays leads to an energy loss of the electrons, the electron bunch carries the "footprint" of the X-ray pulse. The centrepiece of the pulse monitor is an X-band radio frequency transverse deflector, which is located behind the undulators and kicks electrons out of their original flight path. As the deflection differs between the head and tail of the electron bunch, its temporal profile along the accelerator is stretched or "streaked" in a direction perpendicular to it. Different positions in that direction correspond to different times in flight direction.

In a subsequent step, the streaked electron bunch traverses a dipole magnet that stretches the electron beam in yet another direction depending on electron energy – a process similar to a prism turning white light into a colourful spectrum. The end result is a two-dimensional electron bunch pulse profile, with time in one dimension and energy in the other. The researchers then measure this profile when the X-ray FEL produces laser light, and again when lasing is suppressed. The comparison of both profiles enables them to determine the time-dependent energy loss of the electron bunch due to the X-ray pulse. From the energy loss, in turn, they can reconstruct the power profile of the X-ray pulse.

Radio frequency deflectors are routinely used for electron beam diagnostics in front of X-ray FEL undulators. One new approach in the study was to insert a deflector behind the undulator, which enabled the scientists to measure the X-ray pulses' footprints. Another feature of the new device is a tenfold increase in time resolution compared to conventional deflectors.

The pulse monitor is now available to LCLS users, providing them with accurate pulse information that is expected to advance their data analysis. The new tool can capture every single one of LCLS's up to 120 X-ray flashes per second and does not interfere with ongoing X-ray experiments. Besides improving data interpretation, the method can also help to enhance the performance of X-ray FELs. Undulators can be tapered, for example, to increase their X-ray output. However, this process is not yet understood in detail and needs to be optimised. With the new tool, researchers now have a new instrument to look into these details.

Applications of the pulse monitor are not limited to LCLS. It may also be of interest as a diagnostic tool for the new beamline at DESY's FLASH facility, FLASH2, and for the European XFEL X-ray laser. At FLASH2, for instance, the new device could be used to optimise seeding – the initiation of the laser process by an external laser.

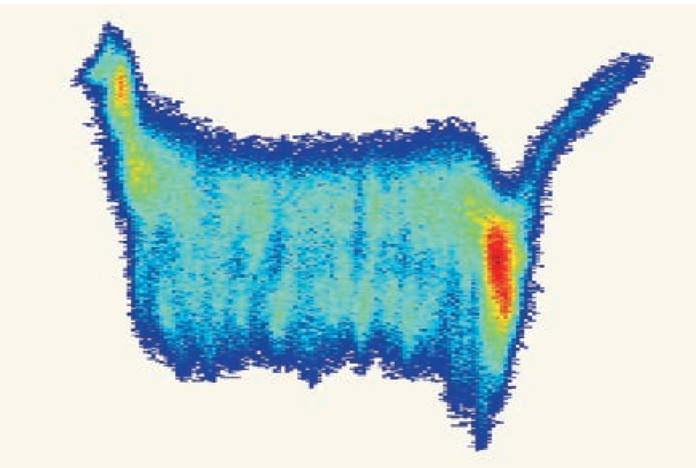

Electron bunch measured at LCLS with time in the horizontal dimension and energy in the vertical dimension. The electron bunch profile carries the "footprint" of the X-ray pulse created by the electron bunch and is used to reconstruct the temporal power profile of the X-ray pulse.

August

FLASH2 generates first laser light

On 20 August, FLASH2, the new undulator line of DESY's FLASH soft X-ray FEL facility, generated its first laser light. The first undulator line FLASH1, which receives electron bunches from the same accelerator, was operated at the same time without restrictions. This makes FLASH the world's first FEL with two laser lines served by one accelerator and operated simultaneously and independently from each other.

FLASH2, the new undulator line of DESY's FLASH facility

The launch of FLASH as the world's first soft X-ray FEL user facility in 2005 heralded the era of research with X-ray lasers. At FLASH, densely packed electron bunches from a superconducting linear accelerator travel at almost the speed of light through periodic magnetic structures called undulators, thereby generating ultrashort and highly intense laser pulses in the X-ray range. From the beginning, FLASH was very much in demand and therefore frequently overbooked.

To meet the rapidly growing user requests for beam time, an extension project was started in autumn 2011. For 30 million euro, FLASH was to be upgraded with a second undulator line and a second experimental hall, allowing for twice as many experiments as before. The basis for this technological feat is provided by the superconducting TESLA accelerator technology employed at FLASH, which makes it possible to serve several undulator lines with one linear accelerator.

The FLASH2 undulators are variable-gap undulators with movable upper and lower halves. Changing the gap of the FLASH2 undulators allows the wavelength of the emitted laser light to be adjusted, while the wavelength of FLASH1 is determined by the energy of the accelerated electrons. The new beamline FLASH2 thus achieved first lasing at 40 nm, while at the same time, FLASH1 delivered laser pulses at 13.5 nm.

In a following test shift, the operators tuned the FLASH2 wavelength down to 22 nm with FLASH1 generating pulses at constant wavelength. During routine operation, FLASH2 will produce wavelengths between 4 and 60 nm.

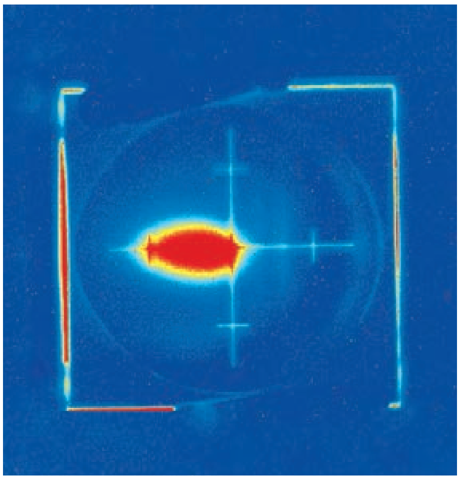

One of the first FLASH2 laser pulses

September

Topping-out celebrations for new PETRA III experimental halls

On 15 September, DESY celebrated the topping-out of two new experimental halls for its PETRA III synchrotron radiation source. The two halls will provide a total space of about 6000 m^2 for up to ten beamlines for experiments with the X-ray radiation generated by PETRA III, plus additional space for offices and labs. The first new beamlines of the 80 million euro project will be ready for operation in autumn 2015.

Construction site of one of the new experimental halls for the PETRA III extension, Hall North

The 2.3 km long PETRA III ring accelerator produces high-intensity, highly collimated X-ray pulses for a wide range of physical, biological and chemical experiments. Fourteen measuring stations, which can accommodate up to thirty experiments, already exist in a 300 m long experimental hall christened “Max von Laue” hall. Using the extremely brilliant X-rays, researchers study innovative solar cells, observe the dynamics of cell membranes or analyse fossilised dinosaur eggs.

Since its start of user operation in 2009, PETRA III has been heavily overbooked. In December 2013, DESY therefore launched the PETRA III extension project to give more scientists access to the facility and broaden its research portfolio through new experimental technologies, such as nanospectroscopy and materials research technologies. The new beamlines and measuring instruments are being constructed in close cooperation with the future user community, in part as collaborative research projects. Three of the future PETRA III beamlines will be realised in an international partnership with Sweden, India and Russia.

Starting in February 2014, approximately 170 m of the PETRA III tunnel and accelerator were dismantled to build the new halls. In August, the accelerator team began to reconstruct the accelerator within the completed tunnel areas. After the civil construction of the experimental halls, technical installation will follow from December 2014, with the accelerator being restarted in parallel. Experiments in the Max von Laue hall will resume in April 2015. The first measuring stations in the new halls will become ready for operation in autumn 2015 and early 2016.

Accelerator operation and construction.

PETRA III.

Paving the way for more light

User operation at DESY's PETRA III synchrotron radiation source in 2014 ended in February. That short user run of only four weeks can be considered an extension of the long run period that started in 2013. It was also the last user operation before a long shutdown period required to implement the PETRA III facility extension project. For this extension, two tunnel segments of about 80 m each in the northern and eastern sections of the PETRA ring were completely reconstructed, and two new experimental halls were built. In the future, synchrotron radiation will be available to users at 10 new beamlines in addition to the already existing 14 beamlines in the Max von Laue experimental hall.

Implementing the PETRA III facility extension project

User operation at PETRA III was resumed after the end-of-year break on 6 January 2014 and ended on 3 February 2014 after only 576 hours scheduled for user runs. Since then, activities at PETRA III have focused on the implementation of the facility extension project, which was originally planned to start in 2013. From 2007 to 2009, the PETRA ring had been converted into a dedicated synchrotron radiation facility with one large experimental hall, referred to as Max von Laue hall, which constitutes one octant of the PETRA ring. All 14 beamlines were located in this octant. The PETRA III facility extension project involves the installation of 10 additional beamlines in two halls in the northern (PXN) and eastern (PXE) sections of the ring. The locations of the two halls, Hall North and Hall East, are shown in Fig. 1.

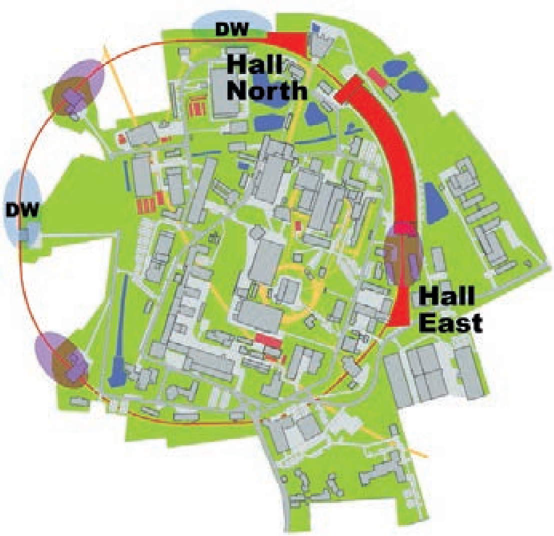

Figure 1

Overview of the PETRA III storage ring showing the new halls North and East. Each hall will house five beamlines.

In January 2014, PETRA III delivered synchrotron radiation to users at all 14 beamlines in the Max von Laue hall with a very good beam availability of 96.96%, exceeding the targeted availability of 95%. The mean time between failures (MTBF) was 33 h. During the short user run in 2014, PETRA III was mainly operated in two distinct "timing modes" with 40 and 60 bunches, which allow users to perform time-resolved experiments and are thus characterised by a larger bunch-to-bunch spacing of 192 ns and 128 ns, respectively. A total of 336 h or 58% of the user time was scheduled for the 40-bunch mode, while 25% of the user time (144 h) was dedicated to the 60-bunch mode. Additionally, 17% of the user time was spent in "continuous mode" with a total current of 100 mA distributed in 960 evenly filled bunches and a bunch-to-bunch spacing of 8 ns. User operation in 2014 may be considered a short extension of the long run period that started in 2013. It was the last user operation before the long shutdown required to implement the facility extension project.

In February, all accelerator components were removed from the two about 80 m long tunnel segments dedicated to the new experimental halls PXN and PXE, and the existing accelerator tunnel was completely removed in those regions. The foundation of the new tunnel segments, which will house several new insertion devices, is formed by a 1 m thick concrete slab. Construction activities for the concrete slab for Hall East are shown in Fig. 2. The new accelerator tunnels were handed over to DESY as scheduled on 30 July (North) and 12 August (East). Since then, the installation of technical infrastructure, accelerator components and beamline front-end components has progressed well, leading to a nearly complete installation of the accelerator at the end of the year, as shown in Fig. 3. While not all cables in the eastern extension section could be

Figure 2

Pouring of the first part of the concrete slabs for the new halls on 29 April 2014 on the construction site of Hall East. The view is towards the old PETRA III tunnel at the end of the eastern long straight section.

Figure 3

Accelerator components installed in the new tunnel segments in the northern and eastern sections of PETRA III. The photograph shows the northern tunnel section on 29 October 2014.

installed in 2014, one important milestone, namely the radiation safety readiness of PETRA III, was successfully established on 16 December. Mounting of power and signal cables in the eastern section and other minor installation activities will be finalized in January 2015 in parallel to the technical commissioning of power supplies in the northern section. The commissioning of PETRA III with beam is scheduled for February 2015, about one year after the end of the user run in 2014.

Challenges ahead

Regular user operation for the 14 beamlines in the Max von Laue hall is scheduled for the end of April 2015. Within only six weeks, stable beam operation has to be reestablished, including the commissioning of the new vacuum components, the beam position monitors and the fast orbit feedback system, which relies on a complete new processing unit. The new magnet lattice implies a new beam optics with a 20% larger emittance of 1.2 nm, which requires further improvements. Furthermore, it is foreseen to install additional collimators in the Hall North-East right before the Max von Laue hall to improve the protection of the insertion devices in the Max von Laue hall against radiation damage.

Contact: Rainer Wanzenberg, rainer.wanzenberg@desy.de
Michael Bieler, michael.bieler@desy.de
Wolfgang Drube, wolfgang.drube@desy.de
Oliver Seeck, oliver.seeck@desy.de

FLASH.

Two beamlines in action

The major highlight of 2014 at DESY's FLASH free-electron laser facility was the first lasing of the new FLASH2 undulator beamline. The new beamline saw its first electron beam in March 2014. First lasing of FLASH2 at 40 nm was achieved on 20 August while FLASH1 was running with 250 pulses at 13.5 nm in preparation for a user experiment. The FLASH team thus unambiguously demonstrated that both beamlines can be operated truly in parallel – both at 10 Hz, sharing the same accelerator. After the construction of FLASH2, the accelerator and FLASH1 photon beamlines had been re-commissioned for user operation. The fifth user period started in February 2014; more than 5000 h of user beamtime are scheduled until May 2015.

First lasing of FLASH2

Beam commissioning of the new FLASH2 beamline started shortly after the permission for operation was granted in February 2014. The first electron beam was transported into the FLASH2 extraction beamline section on 4 March and finally through the whole FLASH2 beamline to the dump on 23 May. Besides the commissioning of loss monitors and essential electron beam diagnostics, such as current and beam position monitors, the first goal was to establish parallel operation with FLASH1. This was achieved at the end of May, opening up the opportunity to operate FLASH2 while FLASH1 is serving user experiments. First lasing at a wavelength of 40 nm was achieved on 20 August while FLASH1 was running with 250 pulses at 13.5 nm in preparation for a user experiment. Since then, FLASH2 commissioning has continued in parallel to FLASH1 user operation, and lasing at several different wavelengths has been established.

This great achievement was made possible by the extraordinary work of the DESY scientific and technical staff.

FLASH's superconducting accelerator is operated with 800 µs long RF pulses at a repetition rate of 10 Hz. During FLASH2 commissioning in 2014, usually the first 400 µs of the RF pulse were used for the FLASH1 beam, serving user experiments. After a gap of 30 µs required for the kicker system to ramp up, the remainder of the RF pulse accelerated the beam for FLASH2.

One important feature is that both beamlines can be served with beam of different characteristics, such as charge, compression and intra-burst repetition rate. This is made possible by using two injector laser systems, together with the possibility to adjust RF parameters like amplitude and phase almost independently for the two parts of the beam. Moreover, the variable-gap undulators of FLASH2 allow photon radiation with different wavelengths to be produced independently of the electron beam energy. Figure 1 shows an aerial view of the entire FLASH facility with the new FLASH2 beamline and the two experimental halls.

FLASH operation

In 2014, FLASH delivered more than 7600 h of scheduled beamtime. Besides the usual shutdown at the end of the year, a brief shutdown in January was required to integrate the personnel safety interlocks of FLASH2 into the FLASH system. The unexpected exchange of the RF gun window in April entailed an additional two-week break of operation.

With 4152 h, FLASH provided more beamtime to users than in any other year before. Another 3381 h were used for machine studies, for improvements and developments of the photon beamlines and for the preparation of user runs. In addition, a few commissioning shifts (96 h) were required in January. 162 h were allocated for regular maintenance. Figure 2 shows the beamtime distribution during user runs in 2014. More than 3000 h of FEL radiation (SASE) were delivered to users. As usual, time was required for tuning and setting up the experiments, including frequent changes of wavelength and bunch pattern, often on a day-by-day basis. This tuning and setup time amounted to a bit more than 20% of the user beamtime. About 40 different wavelengths between 4.3 nm and 41.5 nm were set up, 1 to 400 bunches per burst and different intra-burst repetition rates (from 100 kHz to 1 MHz) were realised.

At 95.8%, the uptime of the facility during user runs was very close to the goal of 96%. Using contingency, we were able to compensate for lost beamtime, so that most users were actually delivered the scheduled beamtime.

Figure 1

Aerial view of the FLASH facility taken in July 2014, including the new tunnel (to the left of the old FLASH tunnel) and the new experimental hall (lower left corner, right next to the old FLASH hall). Adjacent to the two FLASH experimental halls are the curved PETRA III hall (far left) and the construction site of the PETRA III extension Hall North (lower right corner).

RF gun

In early 2014, a small vacuum leak was detected in the RF window of the RF gun. In order not to spoil the superconducting modules, it was decided to change the window during the study period in April, thus affecting the user runs as little as possible. The RF window separates the slightly overpressured air in the RF waveguides (1.5 bar) and the beam vacuum (10^{-10} mbar). RF windows are known to have breakdown issues and are therefore preconditioned with RF parameters similar to those for normal RF gun operation. Nevertheless, more time than expected was required to condition the new window in situ. This led to an unfortunate loss of beamtime of 320 h. The preconditioning of RF windows is being reviewed in order to improve the readiness of spares. The RF gun is now operated stably with an input RF power of 4.5 MW, corresponding to a maximum accelerating field of 50 MV/m at the cathode. The RF pulse length is kept at a conservative 500 μs at a repetition rate of 10 Hz.

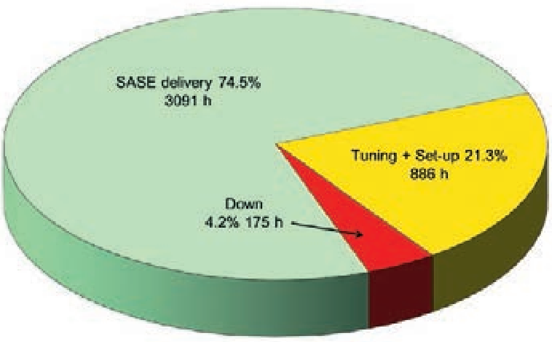

Figure 2

Beamtime distribution during user runs in 2014. The uptime of the facility was 95.8%. Scheduled maintenance during user runs is not included (53 h).

Since autumn 2013, all superconducting modules have been operated with the new MTCA.4-based low-level RF control and feedback system. The system shows an excellent performance. For example, the arrival time jitter of the electron beam after acceleration and compression is now reduced from 60 to 30 fs (rms) without the need for a special beam-based feedback. A similar low-level RF system for the RF gun is in preparation. Since the feedback and low-level controls for the RF gun are different and also more difficult than for superconducting modules, the implementation of the new system for the RF gun requires more time. To gain experience, the new system is presently being run in parallel to the standard system as a monitoring system.

Single-spike lasing

A very promising result towards true single-spike lasing was achieved in May 2014. With a new short-pulse injector laser, electron bunches were compressed down to a few femtoseconds only. The trick is to reduce space charge effects, which counteract the attempt to compress electron bunches, and to reduce the initial bunch duration at the RF gun as much as possible to keep RF tolerances reasonable. From the measured single-shot photon spectra at a wavelength of 7 nm, an average of 1.5 spikes was evaluated. The estimated photon pulse duration was a remarkably small 2.4 fs (rms). This is an order of magnitude shorter than ever produced at FLASH.

Contact: Siegfried Schreiber, siegfried.schreiber@desy.de

PITZ.

Photoinjector tests and further developments

As in 2013, operation of the PITZ photoinjector test facility at DESY in Zeuthen in 2014 focused on preparing the electron sources (guns) for FLASH and the European XFEL. In parallel, preparations for further accelerator studies were undertaken in the framework of the accelerator R&D programme of the Helmholtz Association.

Stability studies for the European XFEL

Stability studies and characterization of Gun 4.4

Gun 4.4, the European XFEL spare gun, was installed at PITZ in autumn 2013. This cavity was equipped with a single preconditioned Thales-type RF window – the best produced until then. Gun performance and stability tests started during the last weeks of 2013, aiming at the longest possible stable operation at full pulse length (650 µs) and full peak power (~6.5 MW). In mid-January 2014, a run at reduced power (6.0 MW) was stable for ~39 h before being stopped by the operator to change the machine settings. Shortly afterwards, operation with electron beam was started and resulted in typically 10–20 h of uninterrupted beam operation at a power level of ≥ 6 MW. Stable operation was then mostly interrupted by light signals in the vacuum system (most of them at the Thales window, only some from the RF input coupler region).

Figure 1

Transport of the new gun setup with two Thales-type RF windows to the PITZ tunnel. The large support structure needed for the T-combiner and the two RF windows (top and bottom) can be seen in the foreground.

The consequent, very tight measurement programme with Gun 4.4 comprised, besides the usual gun characterisation (alignment procedures, measurements of quantum efficiency and beam momentum, transverse phase space characterisation via emittance measurements and tomographic measurements, as well as dark-current studies), also coupler kick studies and bunch characterisation studies for FLASH injector parameters. After some improvements in the gun cooling system, the jitter of the gun RF phase was measured to be ~0.2° (rms).

In early January already, problems in the cathode region appeared, announced by an increased vacuum pressure in the cathode region. Triggered by the observation of a partially destructed cathode spring at Gun 4.3 (which is installed in the European XFEL injector building), the cathode holder and RF spring were exchanged for a gold-coated version in early April 2014 to improve the electrical contact. This opening of the gun vacuum system made a partial reconditioning necessary, which took place over the Easter period at different RF pulse durations. Unfortunately, light signals from the Thales window prevented stable operation for more than 1–2 h above a power level of ~5.5 MW. Finally, a vacuum leak at the Thales window was detected. Beam operation continued at reduced power (5 MW, later 4.5 MW) to get some operation experience with the new RF spring, but really stable operation was not possible, so Gun 4.4 was dismounted from the PITZ beamline. It is now in Hamburg, where it awaits the availability of a replacement Thales window.

Summer shutdown work

At the end of May 2014, a longer shutdown started, during which Gun 4.4 was dismounted and Gun 4.2 installed (see below). The booster cavity was moved towards the gun to gain space for the installation of a plasma cell and related additional beamline components, such as quadrupole magnets for proper beam propagation in the plasma cell environment. For the plasma generation, an ArF laser was installed and commissioned in a new lab. In parallel, a complete re-arrangement of the laser hutch took place to house a new, additional 3D ellipsoidal laser system.

Gun 4.2 and the two-window solution

Gun 4.2 was already used at PITZ and FLASH from 2008 to 2012. It was dismounted from FLASH due to problems with the old RF spring design (watchband design). In autumn 2012, the new RF spring design (contact stripe) was implemented, followed by dry-ice cleaning of the gun. In summer 2014, Gun 4.2 was mounted on a new setup together with two Thales RF windows (Fig. 1). The RF components were partly preconditioned (Thales windows at the RF test stand in Hamburg, T-combiner and 10 MW in-vacuum directional coupler at the T-combiner test stand in Zeuthen). The use of two windows has the advantage that each window gets only half of the total RF power in the gun, which should help to avoid the destruction of this sensitive component that was observed in 2014 during the operation of three different gun setups with a single Thales RF window at FLASH, PITZ and the European XFEL.

Conditioning of the complete new gun setup started on 4 September 2014. Progress was slow, however, due to high light activity on the specific Thales RF windows, which had shown up already during preconditioning at the RF test stand in Hamburg. At the end of December 2014, tests started to study the long-term stability of the two-window gun setup.

3D ellipsoidal laser system

Compared to laser systems that deliver cylindrically shaped laser pulses, such as the Max Born Institute (MBI) laser system that has been in use at PITZ for many years, simulations show that the generation of electron bunches from 3D ellipsoidal laser pulses can further improve the overall brightness of a photoinjector thanks to the linearisation of space charge forces.

Such an advanced laser system was developed for PITZ at the Institute of Applied Physics in Nizhny Novgorod, Russia. Installation of the laser system at PITZ required a major rearrangement of the laser hutch, which was done during the summer shutdown. The installation of the new laser system took place from October to December 2014 (Fig. 2). The 3D ellipsoidal laser system is currently being commissioned and will be experimentally tested at PITZ starting in 2015.

Extensive beam dynamics simulations accompanied the development of the 3D ellipsoidal laser system and supported the shift of the booster cavity position realised during the summer shutdown.

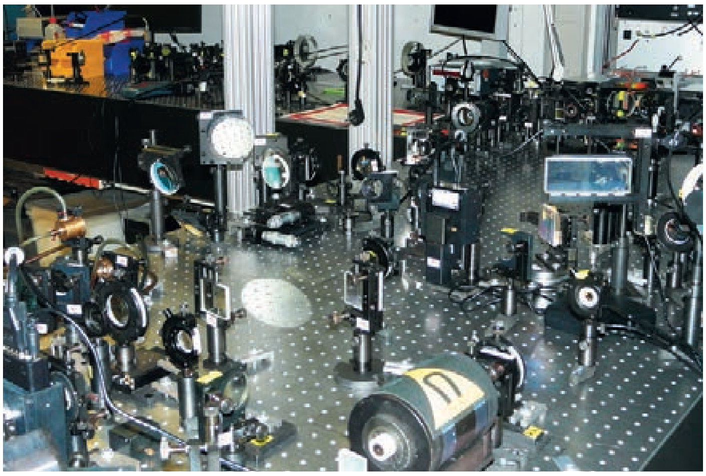

Figure 2

New 3D ellipsoidal laser system in the re-arranged laser hutch

Plasma cell integration

As a proof-of-principle experiment for the AWAKE experiment at CERN, a plasma cell will be installed in the PITZ beamline with the goal to measure the energy modulation of an electron beam passing through the plasma. In 2014, a plasma cell – basically a lithium heat pipe oven with helium buffers – was built (Fig. 3). Coupling of the ionisation laser is done through the side ports. The fabrication of the plasma cell was finished in January 2014, and lab tests were carried out throughout 2014. The plasma cell will be inserted into the PITZ beamline in spring 2015 for first experiments with electron bunches. At the same time, a transverse deflecting cavity (TDS), which is *the* basic diagnostics tool for plasma self-modulation studies, will be taken into operation: in 2014, a commercial provider for the modulator was chosen (ScandiNova), and the system passed the fabrication acceptance test at the company very successfully at the end of November 2014. The delivery of the system is expected in early January 2015.

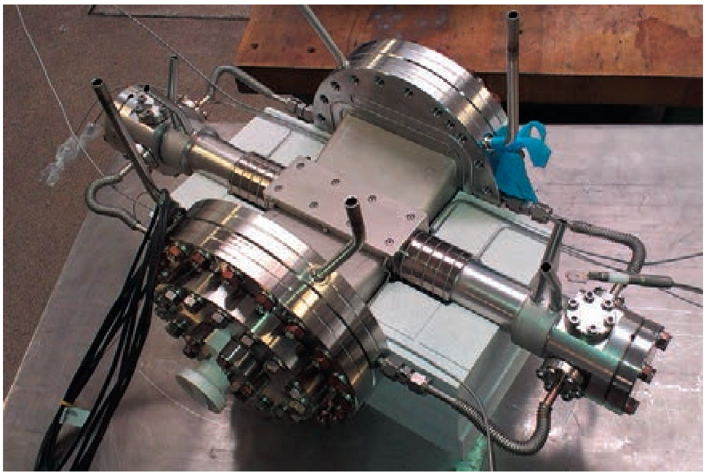

Figure 3

Completed plasma cell. The big side ports allow the coupling of the ionisation laser, which generates the plasma channel at the centre of the lithium column, and leave additional space for plasma diagnostics.

Contact: Anne Oppelt, anne.oppelt@desy.de

European XFEL.

Accelerator construction in full swing

The linear accelerator complex of the European XFEL X-ray free-electron laser and its comprehensive infrastructure are being constructed by an international Accelerator Consortium of 17 European research institutes under the leadership of DESY. In 2014, series production continued for many components, numerous others were delivered, accelerator module assembly was ramped up, and installation started. By the end of the year, the European XFEL injector had essentially been set up, with the exception of the accelerator sections, and installation of the main cold sections of the linear accelerator had begun.

Manufacturing accelerator components to specification

The production of accelerator components for the European XFEL started in 2013 and continued in 2014.

The production of more than 700 beamline magnets of altogether 24 types by Efremov Institute (NIIEFA) in St. Petersburg, Russia, is basically finished, marking the end of a very successful collaboration. Incoming inspection and final quality control including magnet field mapping will be soon done. The required magnetic field quality was reached with only a minimum number of iterations on very few magnets.

A very large number of beam diagnostic elements are under production, available for installation, or have already been integrated in the injector beamline sections. Others are being installed in the accelerator modules. Regular delivery of cold beam position monitors (BPMs) for accelerator module assembly was established. The fabrication of 228 warm BPMs needed in almost all sections of the accelerator complex is finished. The readout electronics development has reached and even exceeded specifications. So-called toroids are needed for beam current monitoring. A network of monitors is used to set up an interlock in case of transmission and bunch pattern failure. The achieved noise level corresponds to less than 1 pC. Dark-current monitors are used to probe the electron beam for a possible beam halo. The monitors are cavity-based and can reach a sensitivity of about 10 nC (direct current) or 100 fC (bunched beam). About 60 scintillator-based screen stations will be installed. They all consist of an on-axis screen, with some also including an off-axis screen and a calibration target.

Figure 1

European XFEL accelerator modules in the AMTF at DESY (October 2014)

Figure 2

View into the injector tunnel (November 2014)

Wire scanners are indispensable devices for measuring the electron beam profile. The externally triggered fast scanners move at 1 m/s, but slow scans can also be done. Further beam diagnostics elements used at the European XFEL include beam loss monitors based on scintillators, beam halo monitors using diamond and sapphire crystals used as ionisation chambers and 380 electronic dosimeters distributed in electronics racks along the accelerator complex.

Altogether, 3.2 km of warm beamline vacuum sections will be installed. Approximately 95% of all commercial products (pumps, valves, etc.) for these sections were delivered. Installation of vacuum girders started, including beam diagnostic elements and smaller beam transport magnets. At the injector, more than 90% of vacuum girders were installed in 2014, with the individual sections still to be connected to each other. For the bunch compressor sections BC1 and BC2, girder installation started; tunnel installation will happen as soon as the cryogenic transfer line, which is located above the electron beamline, is finished. Beam distribution systems in the sections downstream of the cold linear accelerator will be suspended from the ceiling. In the downstream undulator sections, installation is scheduled to begin in the first quarter of 2015; about half of the undulator chambers are ready for installation, and the vacuum chamber supports and intersection vacuum systems – both contributed by BINP in Novosibirsk, Russia – need to be delivered next.

Figure 3

Installation of vacuum components on girders in the DESY cleanroom (August 2014)

The cold linear accelerator of the European XFEL consists of several sections with a total of 101 accelerator modules. The production rate was scheduled at one finished module per week. In 2014, this challenging goal was achieved. In September, stable delivery from CEA in Saclay, France, to DESY was established. By the end of 2014, almost a quarter of the total number of modules had been produced.

Accelerator module production ramp-up

While the ramp-up of the industrial production of superconducting cavities was finished at the end of 2013, the assembly of the accelerator modules at IRFU of CEA in Saclay required a strong collaborative effort in 2014. All components needed to be delivered at a sufficient rate and quality so the assembly team could concentrate on the procedures and especially on the throughput of the different workstations.

The production of superconducting cavities became very stable and, by the end of 2014, approximately 500 of the 800 European XFEL cavities had been delivered. Many of them can be operated at accelerating gradients as high as 30 MV/m. In 2014, a clear improvement in production quality at the vendors was visible.

In 2014, coupler production ramp-up was still an issue. For the first six months, fabrication and assembly mistakes caused problems, and since then, the request for constant quality at a high production rate has dominated. As a consequence of the delayed ramp-up, only an insufficient buffer of couplers for module assembly was available during 2014. In total, 800 couplers are required for the European XFEL. The presently improved situation, together with the use of a second vendor, hopefully solved the problem.

The superconducting quadrupole packages are built in a collaboration between CIEMAT in Madrid, Spain, IRFU and DESY, with magnet tests performed by IFJ-PAN, Kraków, Poland. All 101 magnets were delivered and successfully tested; many of them were integrated in the quadrupole packages ready for module integration at IRFU.

Figure 4

Inserting a vertical cryogenic transfer line into the media shaft in the European XFEL entrance shaft (May 2014)

The cryostats were contracted, and production is supervised by DESY together with INFN in Milano, Italy. Cold vacuum components are provided by BINP. The supply chain requires a perfectly timed delivery, and the schedule needs to include quality assurance and subsequent improvement or cleaning when necessary.

IRFU has contracted a company to assemble all accelerator modules. Pre-series modules were used to train personnel and start the ramp-up of module production in 2013. At the beginning of 2014, a welding problem first halted and then delayed the assembly of further modules, but the definition of a repair procedure soon allowed the assembly schedule to be corrected. By the summer, the total assembly time had become shorter, and finally, a reorganisation of the contracted assembly team brought the required success. The specified assembly and thus delivery rate of one module per week was finally reached in mid-September.

All modules of the European XFEL are tested at the Accelerator Module Test Facility (AMTF) at DESY (Fig. 1). Taking advantage of the increasing number of delivered accelerator modules, module testing was also ramped up in 2014. By the end of the year, the testing time had been shortened sufficiently to match an output rate of one module per week. Seventeen modules were tested in 2014.

Preliminary conclusions are that the average usable accelerating gradient for the modules tested so far fulfills the European XFEL specification. But a major problem was revealed in 2014. While the first modules suffered mostly from a coupler assembly issue, all later modules show a gradient degradation in typically one to three cavities. The cause of this degradation, which leads to an operation well below the high value measured in the vertical test, was still unknown at the end of 2014. Expert review is ongoing, and assembly procedures are followed with even more care. Extensive tests of the used infrastructure were started. Fortunately, the gradient degradation can be compensated by a clever but sophisticated balancing of the RF power fed into the individual cavities.

Based on the resources assumed so far, the last module (XM100) will be assembled in late summer 2016. Therefore, an accelerated module assembly taking advantage of additional resources, which could reduce the delay by some months, is under discussion. For 2015, acceleration of the subsequent module testing at the AMTF and the module installation in the main linear accelerator tunnel is to be arranged.

Injector

Injector construction advanced well in 2014 (Fig. 2). In principle, the injector components resemble the complete European XFEL accelerator: the photocathode electron source is followed by a superconducting linear accelerator consisting of a standard 1.3 GHz and a special 3.9 GHz module and, after these, a warm electron beamline incorporating the laser heater system and advanced beam diagnostics, before the electrons are injected into the main linear accelerator or discarded in the electron dump.

The warm electron beamline is pre-assembled on reinforced concrete girders. All vacuum installations have to be done in cleanroom conditions to avoid later contamination of nearby superconducting modules. After mechanical pre-alignment of the magnets on the girders, the assembly of the vacuum parts and the integration of all subcomponents, such as diagnostics devices, therefore take place in a dedicated DESY cleanroom (Fig. 3). All components are aligned with respect to each other by means of a specially designed fixation system that avoids the need for mechanical alignment later on.

Figure 5

Another vertical cryogenic transfer line (February 2014)

The achieved precision is in the range of 300 µm peak-to-peak and well within specifications. All six completed girders are now installed in the injector tunnel and await final global alignment, vacuum connection and cabling.The cryogenic installation for the injector linear accelerator was completed with the installation of the accelerator feed and end cap and of the transfer lines (Figs. 4 and 5). The finalisation of the injector linear accelerator awaits the completion of the 3.9 GHz superconducting module. This module, which hosts eight 9-cell cavities and allows the manipulation of the longitudinal phase space, is crucial for the operation of the European XFEL.

The photocathode electron source, which was installed in 2013, was operated in between installation periods, allowing the operation crew to gain valuable experience with all involved subsystems. The ultimate beam quality that is required for the European XFEL can only be obtained with a large accelerating gradient of about 60 MV/m in the gun structure. This requires a peak power of about 6.5 MW over a time of about 1 ms. Both the peak power and the average power put stress on the waveguide subcomponents, in particular at the ceramic window that separates the waveguide system from the gun body vacuum.

The injector laser was set up and put into operation (Fig. 6). The laser will illuminate the photocathode with ultraviolet light and also serve as source for the laser heater. The laser was developed by MBI in Berlin, Germany, in a long-standing cooperation with DESY. The integration, future operation and development will be performed by DESY's recently established laser group.

Figure 6

Working on the injector laser (June 2014)

Figure 7

Modules for the first accelerator section installed in the European XFEL linear accelerator tunnel (November 2014)

Installation and infrastructure

The infrastructure and installation planning is nearing completion. With the southern beam fan, the last underground section got its planning approval in 2014. The corresponding tendering processes are under way. The installation work in the supply buildings is advancing well after a delayed start.

In the SASE1 section, the infrastructure is ready, the undulator and beamline supports are installed, and a large fraction of the racks are in place. After the final enclosures and the supports for the beamlines leading towards and away from the undulators are finished, the installation of the vacuum chambers and the roll-in of the undulators can begin. This is expected in the second quarter of 2015.

In the linear accelerator tunnel, the modules for the first accelerator section are installed and aligned (Fig. 7). Welding the connections between the modules and connecting the beam vacuum are expected in early February 2015. Installation of the corresponding RF station will follow immediately so RF commissioning with warm modules can start in the first quarter of 2015. Meanwhile, installation of the modules for the subsequent accelerator sections continues.

The main cryogenic transfer line is progressing well. The cold compressor box was preliminarily commissioned in the refrigerator hall and subsequently transferred to its final position in the injector building. The cryogenic transfer line for the injector was completed and tested. Parts for the main accelerator cryogenic supply system were delivered and installed; completion is expected in the second quarter of 2015.

Section reviews are continuing for the underground tunnels and beamline sections to conclude the detailed planning. The design for the beamline suspensions in the downstream end of the linear accelerator tunnel is complete; tendering is under way.

Contact: Hans Weise, hans.weise@desy.de
Winfried Decking, winfried.decking@desy.de

REGAE.

Improved operation

To reach the ultimate performance of REGAE, DESY's Relativistic Electron Gun for Atomic Exploration, continuous improvements of diagnostics techniques are required. In particular, measurements of the bunch length and the relative timing of laser and electron beam are difficult at the envisioned parameters and require specially designed solutions. The preparations of the plasma experiment at REGAE are progressing towards installation in 2015.

Bunch length measurement…

Optimising the bunch length at a facility such as REGAE is a challenging task, because bunch length measurement tools are not available in the envisaged parameter range. While in simulations, bunch lengths even below 1 fs can be reached, measurements of the bunch length have a typical resolution of 50 to 100 fs. In addition, some techniques are practically excluded at the small bunch charges and the low beam energy of ≤ 5 MeV available at REGAE.

Transverse deflecting RF structures are developing into standard tools for longitudinal phase space diagnostics at high-brightness beam facilities. Conceptually equal to an inline streak camera, a transverse deflecting structure introduces a correlation between longitudinal position in the bunch and transverse momentum, which can be used to image the longitudinal particle distribution. However, the beam dynamics in these structures is complex and poses special challenges at slightly non-relativistic particle energies. The energy or velocity spread that is unavoidably induced by the structure leads to a lengthening of the bunch at electron energies of a few MeV. If the structure is too long, this process starts already inside the structure, distorts the correlation between position and momentum and thus limits the achievable resolution. Short structures operating at high fields are hence requested. To limit the required RF power at high gradients, a high efficiency of the structure is desirable. However, it turns out that the structures with the highest RF efficiency lead to large emittance growth due to field non-linearities.

The new structure designed for REGAE (Fig. 1) avoids these problems by decoupling geometrical properties relevant for RF efficiency from those relevant for field linearity. It thus promises a resolution of 10 fs at an RF power of only a few kW.

… and arrival timing diagnostics

Pump–probe type experiments as they are performed at REGAE require a stable timing of the electron beam relative to the pump laser. Another focus of activity in 2014 was hence on the temporal stability of the arrival time of the electron and laser beams at the target position. A prerequisite for achieving the desired stability is to be able to measure it. A relatively simple technique makes use of a tiny plasma lens created by the pump laser. When the laser is tightly focused onto a metal grid, the power density is high enough to heat up the metal to high temperatures. Thus a plasma is formed, which acts like a lens onto the electron beam (Fig. 2). The electrons are affected by this lens, however only when the timing between laser and electron beam is correct.

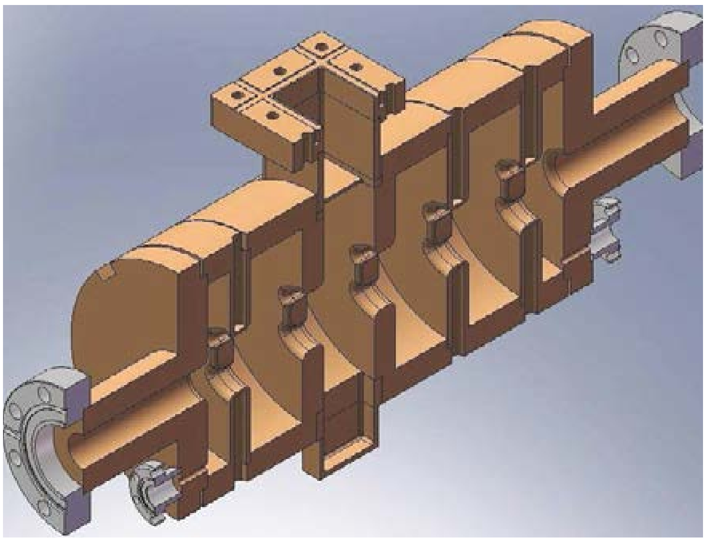

Figure 1

Transverse deflecting RF structure for bunch length measurements at REGAE

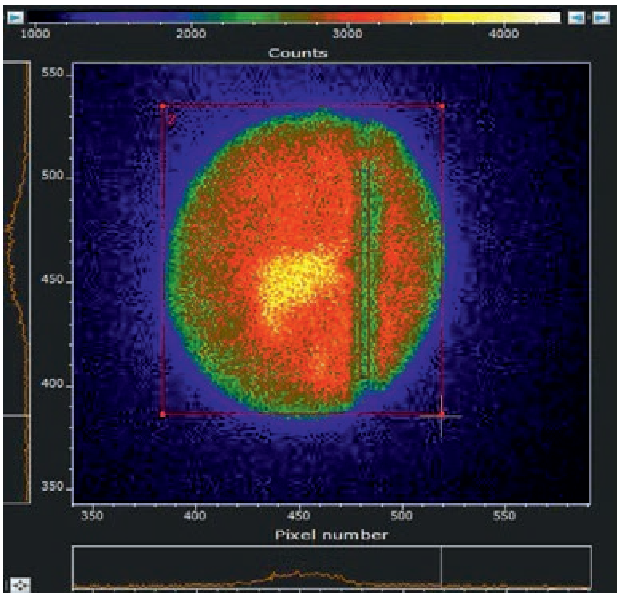

Figure 2

The image shows the electron beam on the diffraction detector. The laser is adjusted to form a line focus on the grid. Electrons are repelled by the plasma along the focus line.

Detailed experimental studies have been carried out at REGAE to optimise the process, i.e. to find the laser parameters at which the plasma lens is formed most quickly and the electron beam optics that yields the strongest signal. Most importantly, the technique has been used to improve the temporal stability of the facility, which now reaches a level of 50 fs at the target.

Preparing the plasma experiment

In parallel to the operation of REGAE, preparations of the planned plasma experiment are ongoing. Plasma acceleration employs electrical fields generated in plasmas, i.e. dilute gases, to reach accelerating gradients outranging those achieved in classical resonating cavities by many orders of magnitude. At REGAE, the fields will be generated by a high-power laser beam passing through a gas target. After passage of the short, high-power laser pulse, electrons swing around the inert ion cloud, thus forming a plasma wave that generates gradients of up to 500 MV/m. Significantly higher gradients can be generated in a plasma; however, the focus of the REGAE experiment is not on the highest gradient but on a controlled injection and extraction of the REGAE beam into and out of the plasma.

A well-defined and controlled acceleration of the electron bunch by the plasma wave requires a bunch length significantly shorter than the plasma wavelength of some 100 µm. Also, in the transverse direction, the bunch needs to be focused down to below 10 µm, so that it fits into the accelerating wave – a challenging task, which requires not only strong focusing magnets but also leads to very demanding beam stability requirements. Emittance conservation is another issue, because the combination of energy spread and large beam divergence as it appears in the extraction region of the plasma leads to a strong chromatic emittance growth.

The situation can be significantly improved by adding matching sections making use of the plasma fields directly to the plasma target. The strong focusing fields of the plasma can be adiabatically tapered and thus used to relax the requirements on the external focusing and the transverse stability. In addition, the chromatic emittance growth in the extraction section can be suppressed by keeping the beam divergence under control.

Significant improvements due to the additional matching sections were demonstrated in analytical and numerical beam dynamics studies. One goal of the REGAE experiment will be to verify these predictions and show that adiabatic matching sections can also be realised in practical applications.

Besides these and other theoretical studies, the layout and construction of the experiment reached important milestones in 2014. All basic design questions were worked out, and most parts of the laser beamline, the new electron beamline and the complex central experimental chamber are in house, so that the pre-assembly in a cleanroom can start soon.

One of the tasks to be mastered in the experiment is the precise alignment of electron beam, laser beam and plasma target. One of the central components inside the target chamber will hence be an alignment table allowing nanometre control of the positions and angles of the plasma target in all three dimensions (Fig. 3). The ultrahigh-vacuum compatible piezo-driven table developed for this purpose will not only carry the plasma target but also various diagnostics components to determine the size and position of both the electron beam and the laser beam.

Figure 2

Piezo-driven in-vacuum alignment table for the plasma target and diagnostics components

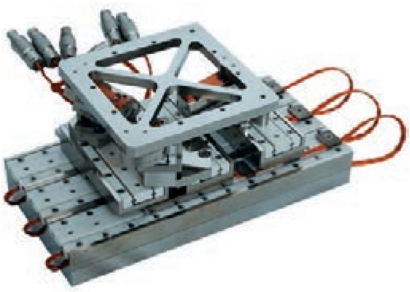

Contact: Klaus Flöttmann, klaus.floettmann@desy.de

Highlights · New technology · Developments.

FLASH2.

Simultaneous operation of two beamlines at FLASH

Simultaneous operation of FLASH1, the old undulator beamline of DESY's free-electron laser facility FLASH, and the new beamline FLASH2 was established in May 2014. This was a major step towards true parallel operation of user experiments in both experimental halls. Thanks to the superconducting accelerator technology, FLASH can accelerate two sub-trains of electron bunches within one RF pulse at a repetition rate of 10 Hz. The first sub-train is directed into FLASH1, the second one is kicked towards FLASH2. Both beamlines are served with beam at the same 10 Hz rate. Key parameters of both sub-trains can be adjusted independently to the needs of the experiments: bunch charge; compression factor and thus photon pulse duration; and intra-pulse repetition rate. The wavelength requested by FLASH1 experiments determines the electron beam energy. FLASH2 allows a wide range of wavelengths to be generated for a given electron beam energy by tuning the gap height of the new variable-gap undulators. This extraordinary flexibility will allow a large number of experiments to be operated truly in parallel.

Commissioning

The year 2014 was dedicated to putting FLASH2 into operation. First, beam time was used for standard commissioning tasks: directing the electron beam step by step through the new beamline and putting basic electron beam diagnostics, such as charge monitors, beam position monitors and loss monitors, into operation. A major step was the implementation of the new timing system, which is a prerequisite for parallel operation.

A major milestone was achieved at the end of May, when parallel operation with FLASH1 was established. Since then, whenever possible, FLASH2 has been run in parallel to user experiments at FLASH1, showing that this basic feature is indeed possible.

On 20 August, first lasing was achieved at a wavelength of 40 nm – the most important highlight in 2014. Later on, lasing at many other wavelengths was demonstrated as well (Fig. 1).

To make parallel operation possible, several changes were implemented in operation procedures and controls of the FLASH facility as a whole. New electron beam optics were designed and put into operation to match the beam into the new FLASH2 undulators while at the same time keeping the match into the old FLASH1 undulators. Another important novelty is the new timing system, which is derived from the system to be implemented at the European XFEL. Its most important feature is the ability to generate beam triggers for the two beamlines and injector lasers independently in the correct manner, taking veto signals from the machine protection system into account. A second injector laser was put into operation, generating beam for FLASH2. Using two laser systems allows an independent adjustment of the charge and the number of pulses in the sub-trains as well as the intra-train repetition rate.

The most visible change is the new bifurcating beamline after the FLASH accelerator. A kicker/septum system was installed to extract bunch trains from the FLASH accelerator into the FLASH2 extraction arc.

In 2012 already, before the septum was installed, several tests of the kicker magnets were performed with beam in FLASH1. The results were very promising; an excellent stability of the

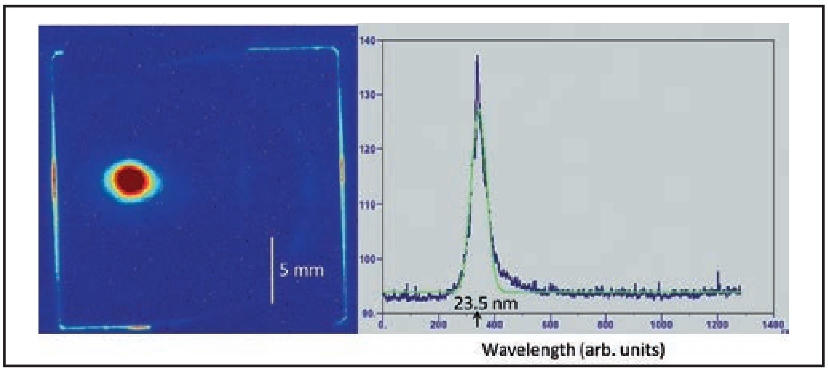

Figure 1

Lasing at FLASH2 on 24 August 2014 at a wavelength of 23.5 nm. Shown are the transverse image of the photon pulse taken with a scintillating Ce:YAG screen (left) and the corresponding wavelength spectrum (right).

current pulse was obtained. No increased fluctuation in SASE energy and flatness over the photon pulse train was observed. The kickers are fast magnets with a ramp-up time of the magnet current of 30 μs. The magnet current is then held stable and flat over the electron sub-train to be kicked by the septum magnet into the extraction arc. A precise measurement of the flatness and stability of the kickers has not yet been performed. A first look, however, showed a slight slope over the flat hat. The reason has been identified and will be fixed soon.

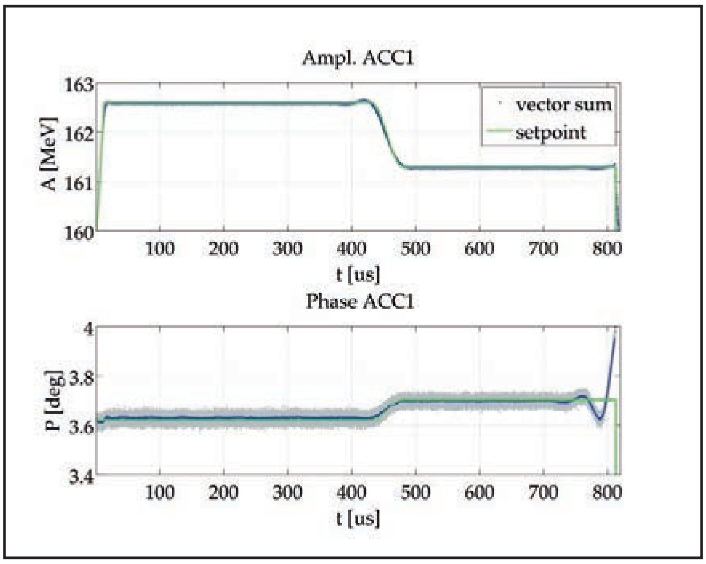

Figure 2

Example of steps in the RF amplitude and phase within an RF pulse. ACC1 is the first accelerating module. The first part of the RF amplitude (upper plot) and phase (lower plot) from 0 to 400 μs is tuned for FLASH1, the second part for FLASH2.

Providing different photon pulse lengths in both beamlines requires an independent adjustment of the bunch compression. For this, the RF pulse is divided into two parts, which can be adjusted independently to a certain extent. An example is shown in Fig. 2. In this case too, first successful tests were already performed in 2012 and 2013 at FLASH1. These were done with the old VME-based low-level RF (LLRF) system, however. The LLRF system controls the flatness and stability of the RF amplitude and phase for beam acceleration.

Simultaneous operation

Since August 2013, the accelerator modules of FLASH have been operated with a new LLRF system based on the MTCA.4 technology. The new system is already able to operate with the split RF pulse option, although the complete functionality of the old VME-based system has not yet been implemented. In extreme cases, for example when FLASH1 is lasing with strong compression and FLASH2 is running on-crest – in other words, when the amplitude and phase for the two parts differ too much – instabilities show up in the feedback algorithm of the new system. Work is ongoing to enlarge the tuning range and minimise the required transition time between the two parts of the RF pulse. Nevertheless, the split RF option is now being applied routinely, enabling parallel operation and independent tuning of RF parameters for both beamlines. Under normal conditions, the difference in settings is small, typically a few degrees in phase and a few MeV in amplitude. Figure 2 shows an example of small steps in amplitude and phase created over the flat top.

Two injector laser systems

To ensure maximum flexibility of operation for both beamlines, FLASH uses two injector lasers, one for FLASH1 and one for FLASH2. Each of them can have a different repetition rate and number of bunches, and can also generate a different charge. Furthermore, they can have a different start time and a different phase with respect to the RF pulse. The new timing system assures that all triggers supplied to the lasers to generate beam are communicated to all relevant subsystems, such as beam diagnostics, kickers, beam loss monitors and – most importantly – the LLRF system. This ensures that all sub-systems are aware of the beam pattern generated, that is, of which part of the beam goes into which beamline.

Contact: Bart Faatz, bart.faatz@desy.de

FLASH optics.

Operating two beamlines in parallel

DESY's FLASH facility is the world's first free-electron laser (FEL) operating two undulator beamlines in parallel, FLASH1 and FLASH2. Beam parameters like charge, pulse duration and intra-train repetition rate can be adjusted to a large extend independently for both beamlines. Since the beam is accelerated by the same superconducting accelerator before it is split in two, the beam optics has to be adjusted such that both beamlines are served with the best possible beam while maintaining beam parameter flexibility. While the wavelength of the FEL radiation in FLASH1 is determined by the beam energy, the FLASH2 wavelength is tuned by varying the undulator gap height. This opens up a large parameter space challenging the flexibility of the beam optics. In 2014, commissioning of the new optics started, and lasing at many wavelengths for many different beam energies was already achieved.

Optics modifications for simultaneous operation

FLASH is based on a superconducting linear accelerator with a usable RF pulse length of 800 µs at a repetition rate of 10 Hz. This makes it possible, for example, to accelerate trains of 800 electron bunches with a bunch spacing of 1 µs. This unique feature allows each train to be split into sub-trains serving multiple beamlines – all at a repetition frequency of 10 Hz. In this way, operating two beamlines essentially doubles the capacity for X-ray photon experiments.

In 2012 and 2013, the new undulator beamline FLASH2 was built and connected to the existing FLASH facility. The beam is first accelerated in the superconducting accelerator and then split into two parts. The first part of the beam goes straight ahead as before towards the old FLASH1 beamline; the part for FLASH2 is separated from the FLASH1 beam and bent towards the new undulators. To make the separation of these two sub-trains possible, the 12 m long section after the last accelerating module was redesigned. Fast magnetic kickers are now installed together with a Lambertson septum, a special dipole magnet with two beamlines separated vertically by 2 cm. The upper one bends the beam horizontally towards FLASH2, the lower one is shielded against the bending magnetic field by an iron plate. The task of the kickers is to vertically kick the sub-train designated for FLASH2 into the upper beamline of the septum magnet.

Electron beam optics has many similarities to light optics: the electron beam is transported through a series of focusing and defocusing elements, the quadrupole magnets. Correctly adjusted, the transverse beam size is perfectly matched to the requirements given by the FEL process in the undulator (Fig. 1). Since the electrons in the beam do have a small but non-negligible energy variation, the beam optics has to take care of dispersion effects as well.

The formerly used beam optics has been adapted to the new beamline and to the constraints defined by the beam separation itself. Furthermore, preserving the beam quality in both beamlines, which is absolutely essential for stable generation of high-brilliance photon beams, puts additional constraints on the electron beam optics.

In order to give the kicker system time to raise its high-voltage pulse, the two sub-trains are separated by 30 µs. While the first sub-train is unaltered, the second sub-train for FLASH2 is deflected vertically by 2.4 mrad. The kicker system has three fast-pulsed magnets. These magnets are optimised for supplying an extremely constant flat-top magnetic field with a flatness better than 10^{-4}. A perfect flatness guarantees that all electron bunches in the sub-train for FLASH2 are kicked with exactly the same angle. The focusing structure – in other words, the beam optics – is used to transform the vertical angle into a vertical offset perfectly suited to pass through the upper beamline of the Lambertson septum.

In order to achieve a sufficient separation of the two beams after the septum, the horizontal deflection angle is chosen to be rather large. The larger the bend angle, the more difficult it is to preserve excellent beam properties required for the FEL process to work. It turned out that a bend angle of 6.3° at the septum is sufficient to obtain a separation large enough to fit beamline elements like quadrupoles and corrector magnets into the limited space available between the bifurcating beamlines.

The extremely short bunches needed for the FEL process are prone to beam size degradation due to coherent synchrotron radiation (CSR) generated in the bending dipoles. This effect can be ameliorated by adapting the beam optics so as to

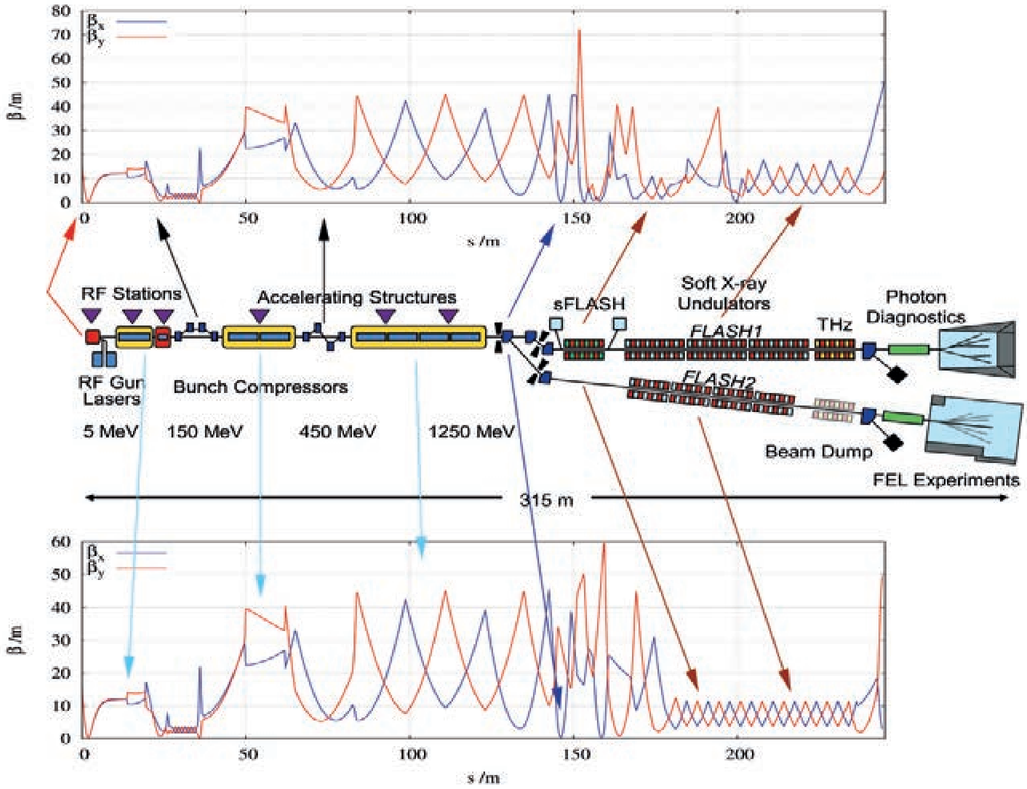

Figure 1

Schematic sketch of the FLASH facility showing the two FEL beamlines (middle) and the beta functions for FLASH1 (top) and FLASH2 (bottom). The beta function is proportional to the square root of the transverse beam size. In the undulators, the beam size is periodically focused and defocused, keeping the average envelope small. In the common part, the beta function is identical. The blue lines show the horizontal, the red lines the vertical beta function.

create a specifically tailored beam waist inside the septum dipole. Since this beam waist is prepared by the common part of the accelerator, measures have to be taken not only to prepare the beam for the extraction bend towards FLASH2, but also to ensure proper re-match into the FLASH1 beamline. In addition, the extraction arc has to be set up in such a way that the unavoidable energy deviations along a compressed FEL bunch do not destroy the transverse beam size outside of the bending arc. Moreover, the arc should not compress or decompress the electron bunches, as the bunch length is a crucial parameter in the dynamics of the FEL process.

Variable optics in the FLASH2 undulator section

The wavelength of the FEL radiation can be varied via the electron beam energy or the undulator parameter, which is proportional to the magnetic field of the undulator. While the FLASH1 undulators have a fixed gap, the new modern FLASH2 undulators provide the possibility to change the gap height between the undulator poles. A smaller gap results in a stronger magnetic undulator field and in fact a longer FEL wavelength. For example, for a beam energy of 1 GeV and a FLASH2 undulator gap of 10 mm, a wavelength of 18 nm is achieved. For this beam energy, the fixed-gap FLASH1 undulators produce a wavelength of 6.4 nm. A change in wavelength for FLASH1 always requires a change of the electron beam energy, while the wavelength for FLASH2 can be largely adjusted by varying only the undulator gap.

FLASH2 has 12 undulator segments with a length of 2.5 m each. Between each undulator segment, a quadrupole is installed. Transverse beam motion in planar undulators can be described as a free-space drift in the horizontal direction and as an extended constant focusing lens in the vertical direction. The vertical focusing depends on the electron beam momentum and the peak magnetic field, in other words, on the gap height. The need to provide optimal electron beam optics for the FEL process at varying energies and for varying wavelengths implies that a large variability and flexibility in the electron beam optics must be provided. Moreover, in order to optimally match into the photon beamline optics, the source point of the FEL radiation should not vary too much along the undulator. Ideally, it should be at the last undulator segment. Unfortunately, the undulator length required for optimal FEL radiation output varies with wavelength. Thus, it is beneficial to use only the most downstream undulator segments and leave the upstream segments inactive with open gaps. Only for very short wavelengths do all 12 undulator segments need to be used. Such variability is technically facilitated by the possibility to independently adjust the focusing strength of the quadrupoles between the undulators.

This flexibility also means that a large set of electron beam optics for the various operational requirements need to be prepared and commissioned. In 2014, many different wavelengths for different beam energies have already been realised. Many others are still to be explored. The optics commissioning is not yet completely finished, but no indications of unresolvable problems or non-conformities have been found so far. FLASH is now routinely being operated with beam simultaneously in FLASH1 and FLASH2.

Contact: Mathias Vogt, mathias.vogt@desy.de

Single-spike lasing at FLASH.

With ultrashort bunches to single SASE spikes

The generation of very short free-electron laser pulses in the soft X-ray regime in self-amplified spontaneous emission (SASE) mode at DESY's high-gain free-electron laser FLASH is of major interest for studying ultrafast processes in different areas of science. The most robust method to produce pulses of a few femtoseconds at free-electron lasers is to create a short electron bunch. In the most extreme case, the lasing part of the bunch is as short as one longitudinal optical mode. At FLASH, this so-called single-spike SASE operation requires bunches whose lasing parts have a duration of a few femtoseconds only. To mitigate space charge forces, this can only be achieved by reducing the bunch charge to the 20 pC level. Operating FLASH with such a small charge is a challenge, as most beam diagnostic devices require a factor of 10 more. To reduce RF tolerances during compression, much shorter bunches than usual have to be generated already at the RF gun. This is possible with a new injector laser system that provides laser pulses as short as 1 ps.

Short-pulse injector laser

To generate short and at the same time bandwidth-limited and longitudinally coherent single-spike SASE pulses, the lasing part of the bunch length (σ_b) has to fulfil the following condition: $\sigma_b \leq 2\pi\, L_{coop}$. The cooperation length L_{coop} is very short, on the order of 0.3 µm, which corresponds to 1 fs. In consequence, the electron bunches need to be much shorter than usually produced at FLASH. The goal is to achieve bunch durations of a few femtoseconds only.

The FLASH RF gun is optimised for operation with a bunch charge of around 500 pC and a bunch duration of about 6 ps. Thus, a very strong compression by a factor of 1000 would be required to achieve a 6 fs bunch. Such a strong compression would lead to strong instabilities in the accelerator caused by very small RF phase and amplitude fluctuations. The required tolerance of 0.0015° in phase cannot be achieved with the present low-level RF system.

A solution is to relax the compression factor by about a factor of 10. A phase stability of 0.01° is routinely achieved. However, the bunch length produced at the RF gun is limited by the fixed pulse length of 6.5 ps (rms) of the two injector laser systems presently installed. Therefore, a new laser system was set up and commissioned. The new laser has a reduced pulse duration that can be varied in the range from 0.7 to 1.7 ps (rms). The small pulse duration allows much shorter electron bunches to be generated already at the RF gun.

The new laser consists of a passively mode-locked laser oscillator synchronised to the RF, followed by a Yb:YAG amplifier. In the infrared, an average output power of up to 7 W has been achieved. This corresponds to a single-pulse energy of 7 µJ, enough for bunch charges up to 200 pC. The laser produces trains of pulses with an intra-train repetition rate of 1 MHz. Figure 1 shows a schematic layout of the laser.

Diagnostics

To monitor laser parameters and correlate them with electron beam properties, new diagnostic devices were installed. These include an ultraviolet spectrometer and a set of quadrant diodes to monitor the transverse laser pointing stability with single-pulse resolution.

To understand the beam dynamics of low-charge bunches, a few key diagnostic elements of FLASH need to be upgraded. As an example, different types of optics and cameras were studied to optimise the optical readout system of the transverse deflecting cavity LOLA. With LOLA, single-shot images of the longitudinal phase space are obtained with a time resolution of a few femtoseconds. In addition, the bunch arrival time monitor (femtosecond resolution in arrival time) and the THz spectrometer (femtosecond resolution in bunch duration) were redesigned for operation at low charge.

Short-pulse operation

A first success with the new laser system was achieved in January 2013, when SASE was produced for the first time using the new laser. The wavelength was 13 nm; the bunch charge could be reduced to 80 pC, with 35 pC also possible. After the FLASH shutdown in 2013, the laser system was recommissioned in early 2014 and prepared for standard operation as one of the three injector lasers at FLASH.

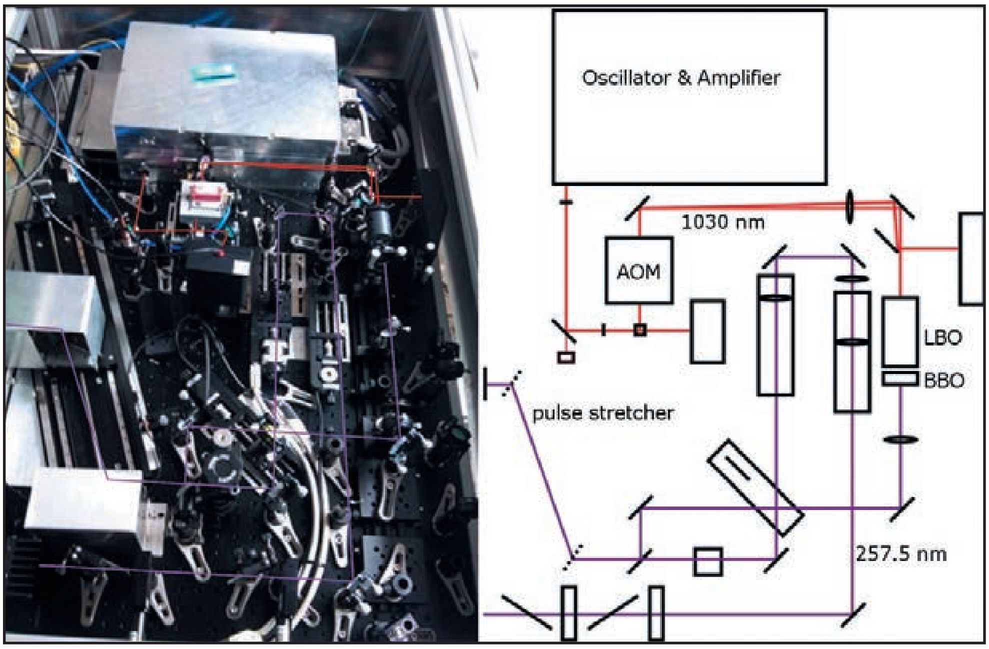

Figure 1

Top view of the new injector laser system with part of the beamline (left) and schematic layout (right)

Single-spike lasing

In May 2014, SASE was optimised at a wavelength of 6.9 nm for a bunch charge of 110 pC, which was then reduced step by step to 55 pC. The laser pulse duration was chosen to be 1 ps (rms), about six times shorter than in standard operation. The transverse distribution of the laser at the photocathode was a truncated Gaussian with a diameter of 1 mm. These parameters were chosen in such a way that the charge density at the photocathode was comparable to the charge density optimised for standard operation. The initial bunch duration was estimated to be 1 ps.

Finally, the spectral SASE distribution was measured using a high-resolution single-shot monochromator. Figure 2 shows six randomly chosen examples of single-shot SASE spectra. Only one or two spikes are strongly emphasised. An analysis of a set of spectra yields an average of 1.5 spikes within the FWHM of the spectrum. The small number of spikes in the frequency domain suggests a very small pulse duration. With some reasonable assumptions, a radiation pulse duration of 2.4 ± 0.2 fs (rms) is estimated. This agrees with previous measurements of the coherence time of 3 fs at a wavelength of 8 nm.

To conclude, the generation of ultrashort SASE pulses close to single-spike operation in the extreme ultraviolet and soft X-ray range was demonstrated at FLASH for the first time. The results were reproduced in September 2014. According to beam dynamics studies, a further reduction in bunch charge should allow the generation of a pure single spike.

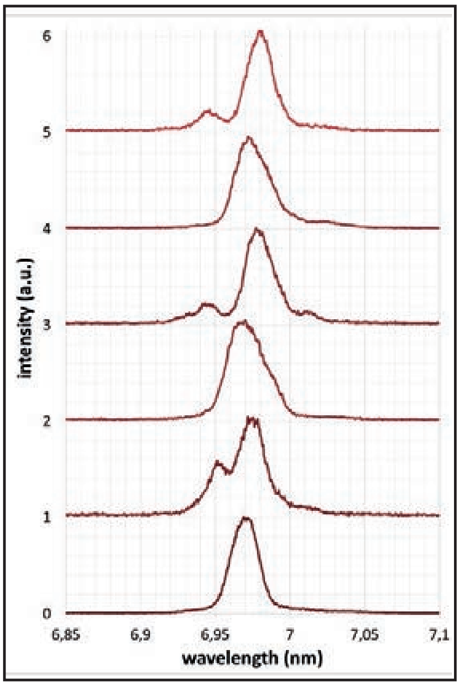

Figure 2

Six randomly chosen examples of single-shot SASE spectra measured at FLASH. The average number of spikes of a larger sample is 1.5.

Contact: Juliane Roensch-Schulenburg, juliane.roensch@desy.de

Tailored electron beams.

Seeding at FLASH

The temporal and spectral properties of highly intense radiation pulses of free-electron lasers (FELs) such as DESY's FLASH facility can be improved by giving the electron beam a defined density modulation prior to the FEL radiator. In order to generate this defined density modulation, the electron beam is manipulated using external laser fields. This process, called seeding, allows for the generation of fully coherent FEL radiation pulses. In combination with collective effects occurring in high peak current electron beams, external seeding gives control of the electron bunch structure and thus tailors the radiation properties of the FEL output.

Seeding of free-electron lasers

Accelerator-based light sources such as FELs use relativistic electron beams to generate ultraintense radiation pulses over a broad spectral range for the exploration of the structure and dynamics of matter. The high spectral brightness, in combination with a high degree of coherence, is one of the key features that scientists are interested in. These properties can only be achieved if the FEL amplification process is properly initiated either by an external fully coherent radiation pulse (direct seeding) or by well-controlled electron bunches comprising defined microstructures that lead to fully coherent FEL pulses. In the latter case, the microstructures can be created by manipulating the ultrarelativistic electron beam with external laser fields in combination with special magnet arrangements. Figure 1 exemplarily shows the so-called high-gain harmonic generation (HGHG) operation mode. Such techniques have already proven to reliably generate FEL pulses in the soft X-ray wavelength range. At FLASH, an experimental setup for seeding development was installed in 2010 and intially used for the investigation of direct seeding. Since 2013, the focus has shifted to the research and development of seeding techniques for manipulating the electron microstructure that should pave the way to fully coherent FEL radiation towards shorter wavelengths. For this purpose, the setup was upgraded with new laser beamlines and diagnostics to overlap ultraviolet laser pulses with the electron bunches from the FLASH accelerator.

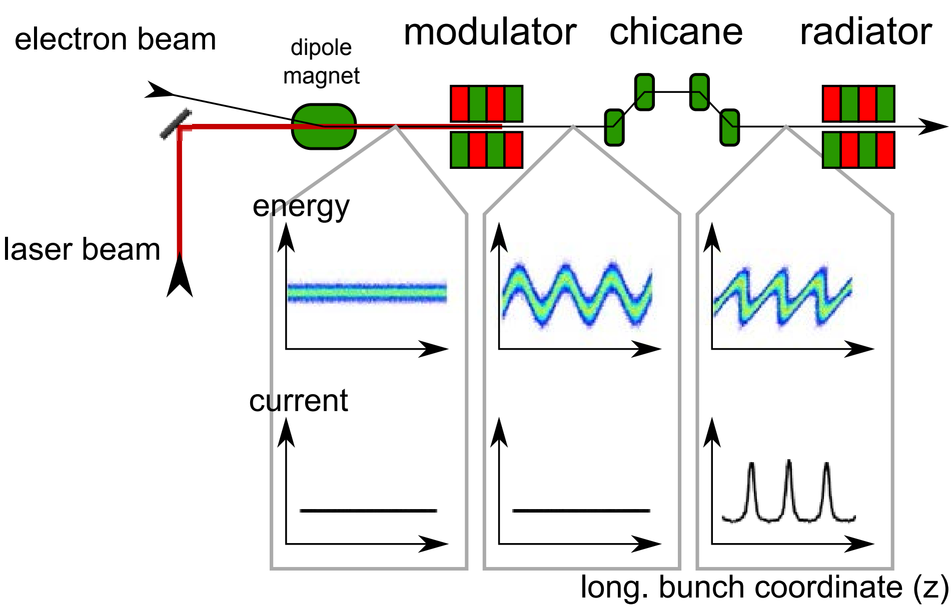

Figure 1

Schematic of the HGHG seeding principle. Starting with a flat energy distribution along the electron bunch, the interaction of the electrons with the laser inside the modulator leads to a sinusoidal energy modulation. At the exit of the magnetic chicane, the electrons are longitudinally redistributed, which results in a modulated current profile. These electron bunches then pass the second undulator (radiator) where the FEL process takes place.

Laser-induced energy modulation

One of milestones towards the well-controlled manipulation of the electron bunch microstructure is to imprint a sinusoidal energy modulation with the period of the laser wavelength, in this case 267 nm. To this end, the electron bunches are overlapped with a strong laser pulse inside a short undulator magnet, usually called a modulator (see Fig. 1). The undulator field forces the electrons to travel along a wiggling trajectory. The corresponding transverse velocity components lead to an interaction with the laser pulses, hence enabling an energy exchange between light and electrons. To characterise this energy transfer, the bunches are streaked using a transverse deflecting structure (TDS) mapping out the longitudinal energy profile of the electrons, also known as the longitudinal phase space distribution. Figure 2a shows a measurement of an uncompressed electron bunch exhibiting a modulated region visible as an increase in the local energy spread. The comparison with simulation allows the characterisation of the actually generated modulation amplitude. Figure 2b shows the simulation result for a modulation amplitude of 350 keV.

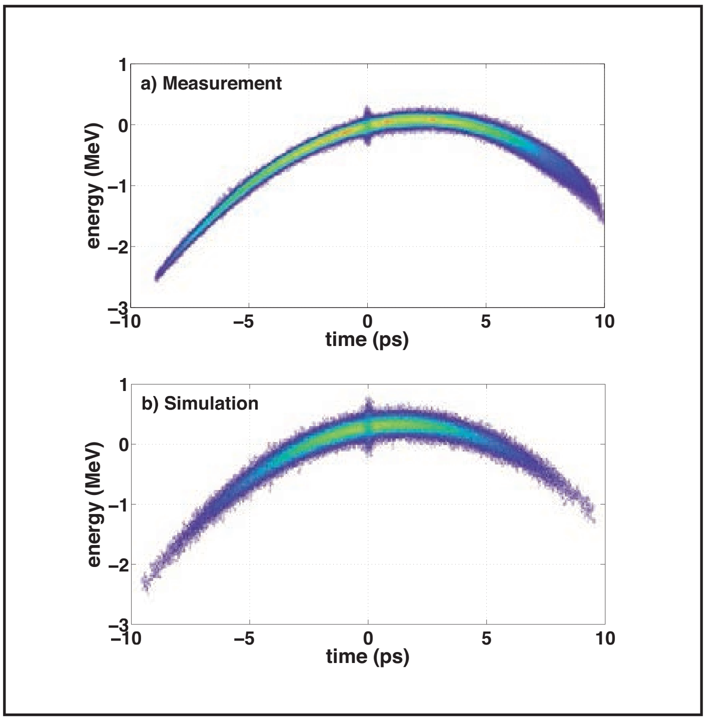

Figure 2

a) Measurement of the mapped longitudinal phase space distribution of the electron bunches using the TDS. The region with the enhanced local energy spread at time zero of the plot is the part where the energy modulation was induced by the seed laser.
b) Simulation of the observable longitudinal phase space distribution mapping for an initial modulation amplitude of 350 keV.

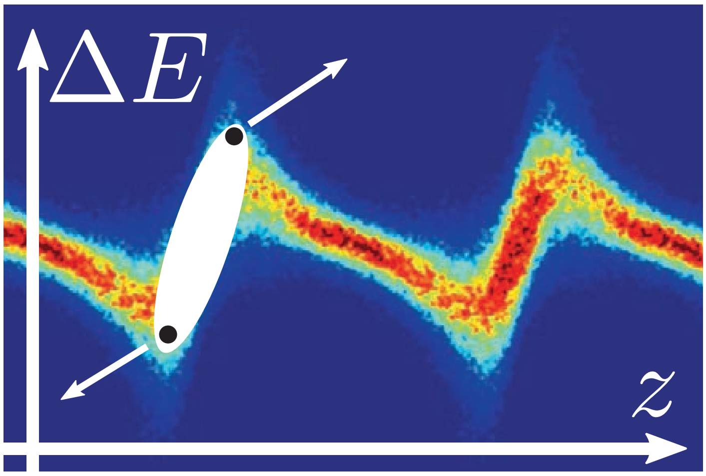

Figure 3

Simulated longitudinal phase space distribution of the electron bunch (bunch head to the right). Two test particles (black) in the high-current region (white) are indicated.

Studies of laser-induced microbunching instability

The high-quality electron bunches driving soft X-ray FELs are susceptible to microbunching instabilities driven by collective effects, such as longitudinal space charge (LSC) or coherent synchrotron radiation (CSR). Besides seeded FEL operation, external laser pulses also enable the investigation of these collective effects at the laser wavelength (here 800 nm) by imprinting a defined current modulation into mildly compressed electron bunches (peak current 0.3 kA). While the electron bunch is passing through the beamline, LSC effects locally modify its properties. This leads, for example, to a growth in energy spread as seen in Fig. 3 (white arrows). At the TDS, the longitudinal phase space distribution of the electron bunches were characterised for different initial parameters (dispersive strength of the chicane and laser modulation amplitude). Such electron bunches were also used to drive the FLASH1 SASE FEL. In this case, a significant decrease in FEL pulse energy was observed in coincidence with the density modulation induced approximately 40 m upstream.

Contact: Jörn Bödewadt, joern.boedewadt@desy.de,
Christoph Lechner, christoph.lechner@desy.de

Cavity beam position monitors in FLASH2.

Excellent resolution of beam offset measurements with European XFEL components

The commissioning of FLASH2 – a new soft X-ray free-electron laser (FEL) undulator line at DESY's FLASH facility – started in 2014. The beam positions in the FLASH2 undulator intersections are measured using 17 cavity beam position monitor (CBPM) pickups and electronics developed for the European XFEL X-ray laser. The new CBPM system enables an unprecedented position and charge resolution at FLASH2, thus allowing further analysis and optimisation of the FLASH2 beam quality and overall accelerator performance. This article describes the results of first beam measurements as well as correlations with other FLASH2 diagnostics systems.

The new CBPM system gives the possibility to measure beam positions with resolutions below 1 µm, which would allow fine-tuning of the FEL performance. In FLASH2, new CBPMs from a European XFEL pre-series are installed between the undulators (Fig. 1).

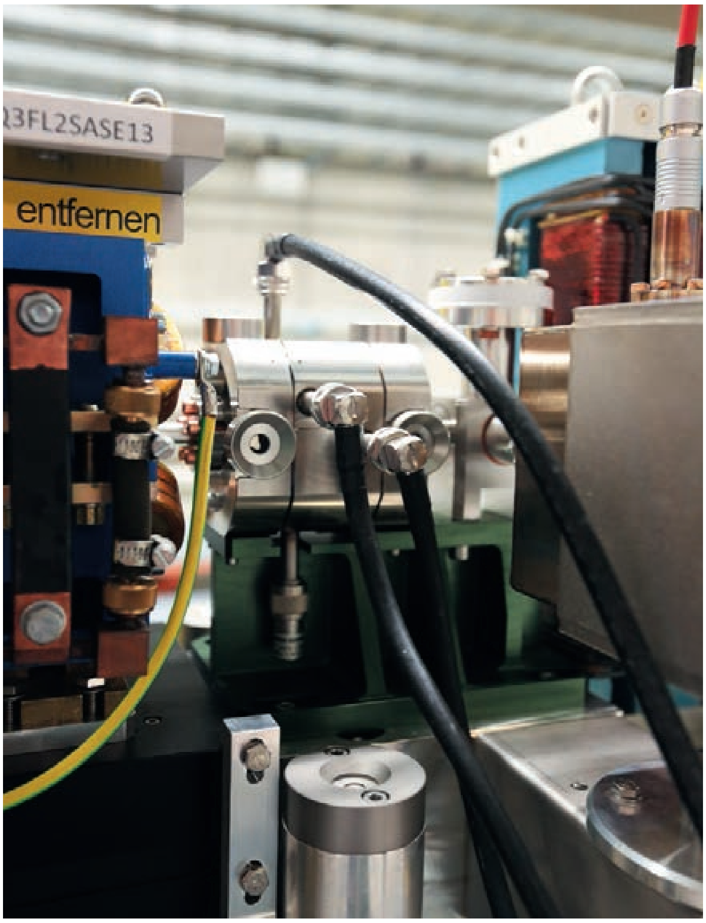

Figure 1

CBPM in an intersection of FLASH2

In addition to supporting the FLASH2 user operation, this provides the opportunity to gain experience with the operation and beam-based calibration of a CBPM system in a working accelerator before the European XFEL is commissioned. The electronics for the CBPMs was provided by Paul Scherrer Institut (PSI) in Villigen, Switzerland. Before first beam operation, the CBPMs were already pre-calibrated, using measured RF properties of the pickups and cables as well as signal generators for the electronics. Only the suitable trigger delay needed to be adjusted to get first beam position and charge readings. The electronics also has a self-triggered mode using the reference cavity signal, but since the signal threshold may not always be reached during first commissioning (e.g. when the beam is lost somewhere), the external trigger was used.

The CBPMs were already integrated into the DOOCS control system for the commissioning of FLASH2, together with a parallel network system from PSI for test and verification. CBPM measurements can be compared with other FLASH diagnostics and subsystems.

In addition to the measurement of the beam position, the CBPM system also provides a measurement of the beam charge. For the absolute calibration of the CBPM charge measurement, the standard FLASH toroid charge monitor was used, requiring a correction of only 2.9%.

To get a first impression of the resolution of the BPM system at FLASH2, the charge reading values were compared with the toroid system. A mean charge value for each bunch was calculated such that the deviation due to noise from each single monitor was negligible, except for the monitor under test. This results in a difference between expected and measured charge for the monitor under test. The standard deviation from the Gaussian fit shows the sum of systematical and statistical measurement errors, defined here as *sum error*. The values for all charge monitors at FLASH2 generated by this method are shown in Fig. 2. All values above 0.6 pC are delivered by the toroids; the CBPMs deliver resolution values between 0.1 and 0.17 pC for a bunch charge of 100 pC.

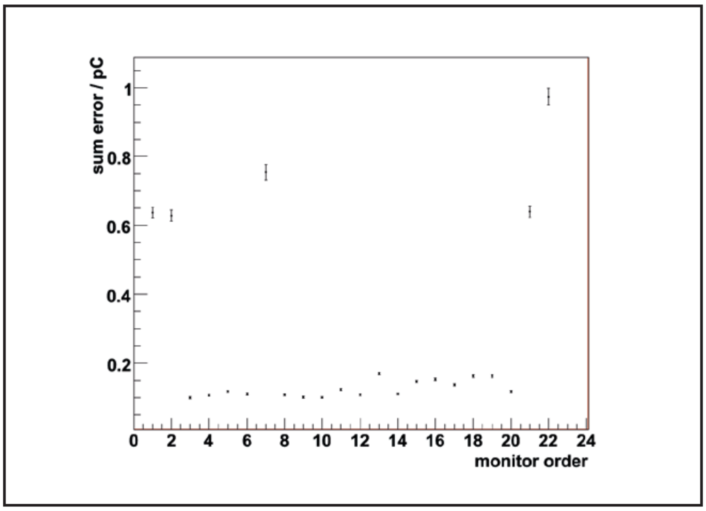

Figure 2

Sum error of charge readings at FLASH2 with a charge of 100 pC, ordered according to the beam direction. Values above 0.6 pC are from toroids, values below from CBPMs.

To obtain the position sum error (including statistical and systematical errors), two button BPMs after the acceleration modules and all CBPMs at FLASH2 were used. A correlation between each BPM and the BPM under test was calculated, and the difference between expected and measured position value was obtained. The position sum errors of all considered BPMs are shown in Fig. 3.

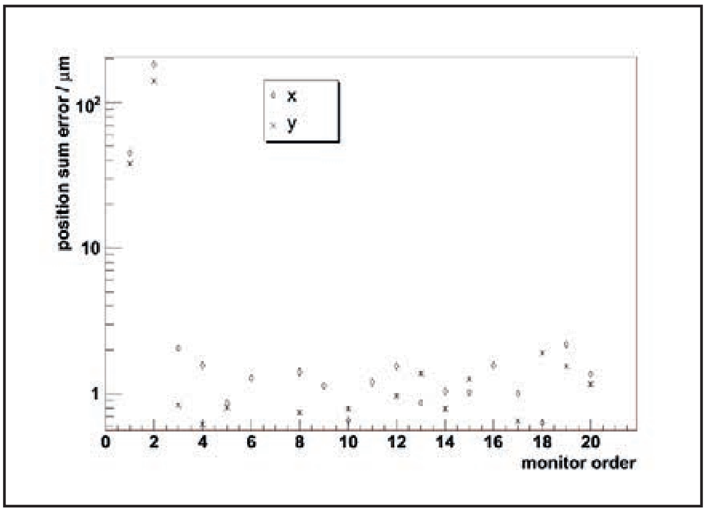

Figure 3

Sum error of BPM correlation at FLASH in both transverse planes for a charge of 100 pC. The first two monitors are button BPMs.

The resolution values of the CBPMs were between 0.6 and 2 µm, depending on the individual beam position (Fig. 4).

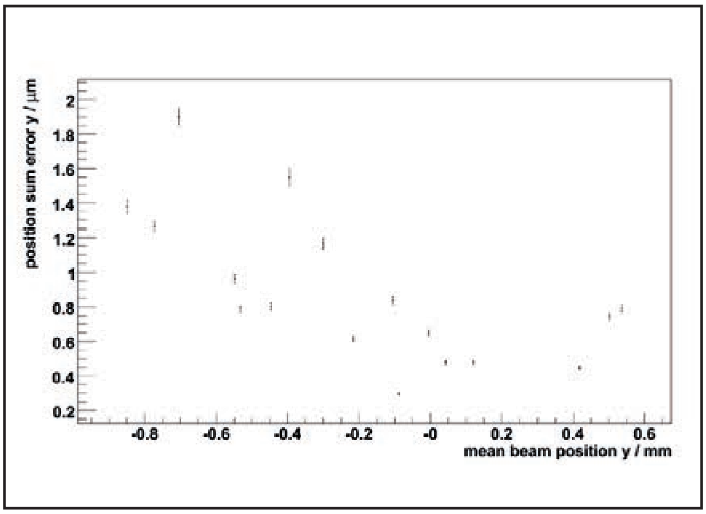

Figure 4

Sum error of CBPMs correlation measurement at FLASH2 at the vertical plane with a charge of 100 pC as a function of mean beam position

As expected, the sum error of the correlation is much better for the CBPMs compared to the button BPMs (Fig. 3). The sum error obtained for the CBPMs has several systematic contributions:

1) The CBPMs in FLASH2 were operated in a preliminary commissioning mode where a feedback loop permanently adapted the internal attenuators of the RF front-end (RFFE) channels to the varying beam charge and positions. This enlarges the dynamic range of the system. Since the attenuators of the CBPMs were calibrated only approximately so far, the frequent changes of the attenuators caused systematic measurement errors in the position and charge readings.

2) In case of large beam position changes, the analogue-to-digital converters (ADCs) of the BPMs may saturate, which is indicated by the BPMs by a valid flag, but this is not yet recorded by the control system.

3) Further systematic contributions to the sum error include mechanical vibrations of the CBPM pickups and systematic errors of the measurement method itself (e.g. due to dispersive effects or *X*/*Y* rotation of the pickups).

A CBPM test stand at FLASH1 (with three successive CBPMS) with similar settings but less systematic error contributions already showed resolution values below 1 µm within the required charge range of 0.1 to 1 nC.

The development of the CBPM system for the European XFEL is in an advanced state. The European XFEL pre-series version of the CBPM pickups and electronics was installed and tested in FLASH1 and FLASH2. It already fulfils the requirements for the European XFEL. Future activities will focus on improvement of laboratory and beam-based calibration techniques, as well as on enhanced automated range control and digital signal processing to further improve the CBPM system performance.

Contact: Dirk Lipka, dirk.lipka@desy.de

FLASH2 extraction.

Enabling independent beam operation for the two FLASH beamlines

The new FLASH2 beamline is an extension of FLASH, DESY's free-electron laser in the vacuum-ultraviolet and soft X-ray range. FLASH2 uses the linear accelerator of the existing facility, with the new extraction system placed directly behind the last accelerating module. Three kicker magnets – two operational, one spare – and a Lambertson septum were installed.

As beam operation should be independent for the FLASH1 and FLASH2 beamlines, FLASH uses two lasers. Two bunch trains with individual bunch numbers and bunch frequencies are generated. The kicker pulse length varies with the bunch train. The gap for kicker rise time and RF pulse change originates from the laser timing and needs to be as short as possible. The pulsers are designed to work with identical currents and waveforms with an amplitude stability of 0.3‰.

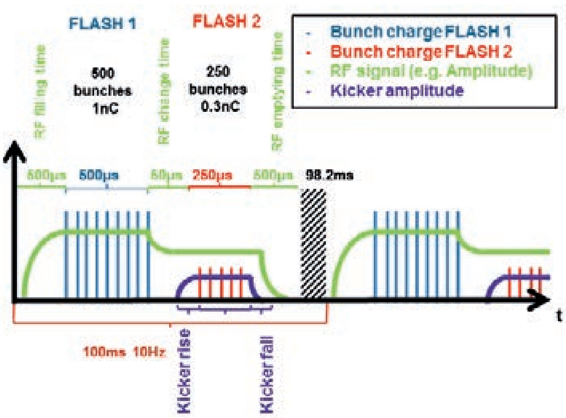

Figure 1
Extraction timing example

Concept of the kicker magnet

The kicker magnets were realised as air coils outside the beam vacuum system. They use strip lines that form a single vertical conductor loop around a ceramic beam chamber, which is sputtered (metallically covered) at the inside. The kicker mounting structure needs to be non-metallic, as eddy currents strongly distort the magnetic field of the current pulses. The thermoplastic PEI was chosen for its radiation and heat resistance and mechanical properties. To suppress electromagnetic interference (EMI), a separate large aluminium housing covers the magnets.

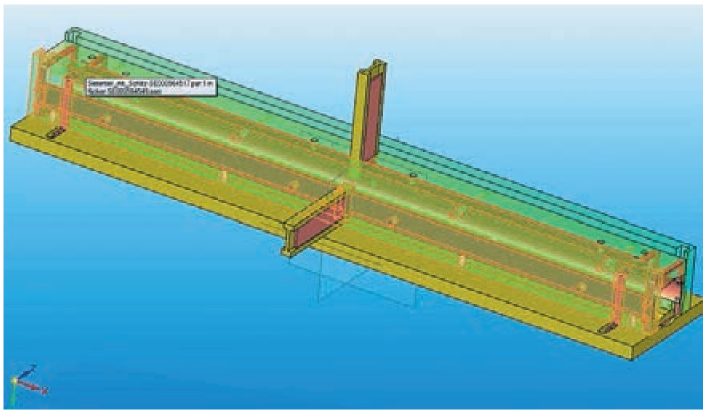

Figure 2
Sketch of the kicker magnet

The kicker design requires a metal-coated ceramic chamber. Sputtering of the chamber is necessary in order to keep the high-frequency components of the beam inside the chamber while the magnetic field of the kicker (at lower frequency) penetrates the chamber's wall. Questions are:

- How big is the reduction of the magnetic field due to the sputtered chamber?
- Which coating material can be used for sputtering?
- How big is the reduction of the magnetic field by a shorted turn?
- How thick can the material be to dissipate the heat generated by the beam?

The coating material is stainless steel 4.4541 (titan stabilised). The reduction of the magnetic field is determined by the electrical conduction and the coating thickness. The reduction of the magnetic field by a shorted turn is given by the electrical conduction. The heat dissipation is defined by the layer thickness.

Presently, we use chambers with 1 µm (i.e. PETRA III injection kicker, FLASH LOLA kicker) and 700 nm (some feedback kicker) coating thickness. For the FLASH2 extraction, we decided to use a 1 µm design because the field attenuation is tolerable (<3%), it is a proven and reliable process, and no other, more demanding constraints had to be met.

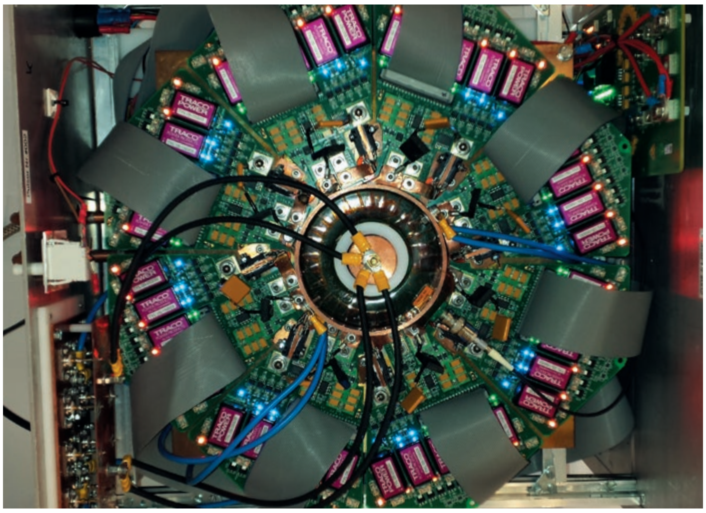

Figure 3

Pulser

Concept of the pulser

For the new FLASH2 extraction, pulse rise and fall times of less than 50 µs and a nearly rectangular current pulse with a very stable flat top are important. Therefore, a pulse-regulated current source with MOSFET technology is used (Fig. 4).

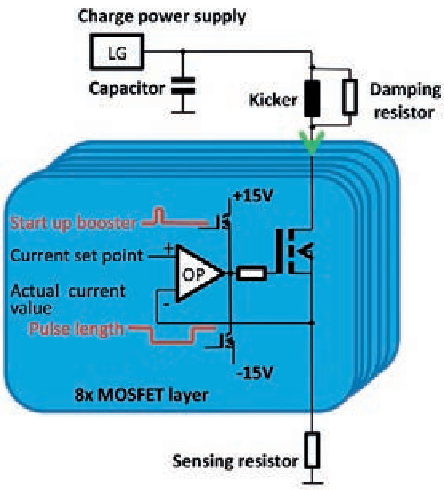

Figure 4

Layout principle of the pulser

The main MOSFET is switched by a push–pull driver providing a fast rise time. While turned on, the current through the kicker magnet is sensed and fed back to the main MOSFET through an op-amp circuit, providing a very stable flat top. Eight MOSFETs are operated in parallel, generating a pulse current of up to 800 A. Data communications, internal timings, power-up and power-down sequences and some service modes are realised with an FPGA board. The pulser is triggered with a 5 V TTL signal from the MTCA-based main timing system, with the pulse length and trigger start time being controlled by the bunch pattern.

Energy	1.2 GeV
Deflection	2 mrad
Pulse current (max.)	800 A
Pulse voltage (max.)	150 V
Pulse waveform	Rectangle
Rise time	10 µs
Fall time	14 µs
Pulse length	10 µs – 1 ms (variable)
Pulse frequency (max.)	10 Hz
Free aperture	44 mm
Conductor length	549 mm
Kicker length	628 mm
Impedance	0.54 Ω
Inductance	~1.2 µH
Number of windings	1
Number of kickers	3

Table 1

Data of extraction pulser and kicker magnet

Beam for FLASH2 was first extracted on 4 March 2014. Operation since then has been performed with energies up to 1200 GeV. Some further testing is needed, especially with longer pulse trains, to investigate flat top stability.

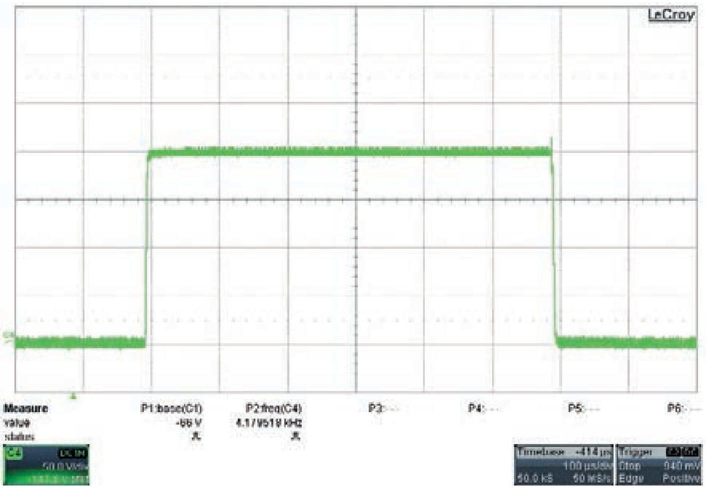

Figure 5

Example of current pulse

Contact: Frank Obier, frank.obier@desy.de, Joachim Kahl, joachim.kahl@desy.de

Particle beams with fine structure.

Space charge simulations with very high resolution

Particle distributions with fine structure are created intentionally (such as microbunching in free-electron lasers, seeding, or seeding with echo-enabled harmonic generation) or through side effects (such as plasma oscillations and microbunch instability). Such fine structures are typically some orders of magnitude (100 – 10 000 times) shorter than the bunch dimension. High-resolution computations of space charge effects need very fine meshes and high particle (or macroparticle) numbers, meaning that they are numerically very expensive. This effort can be dramatically reduced if periodicity can be assumed. Then a newly developed periodical Poisson solver can be applied, which is orders of magnitude more efficient regarding computation time and memory.

Method

The Poisson approach assumes that all particles are in uniform motion with identical velocity vector. Therefore, the problem is equivalent to an electrostatic problem and can be solved through the convolution of the charge density of the complete distribution with the field of only one particle. This is usually done on a three-dimensional mesh with a fast Fourier transform (FFT) convolution. Supposing the distribution is periodic, then the periodicity of the distribution can be interchanged with a periodicity of the field, now caused by one particle and its periodic repetitions. The complete distribution can then be replaced by only one single period. This reduces the volume of the discretisation and the number of particles to be tracked.

Example

The current profile in Fig. 1 is calculated for typical FLASH parameters with an energy of 585 MeV, a bunch charge of 0.3 nC, a normalised emittance of 1.5 µm and a peak current (without modulation) of 1.5 kA. The beam is energy-modulated in an undulator by a laser pulse with a wavelength of 800 nm. After a short section with longitudinal dispersion, the laser modulation causes a high-frequency density modulation, as can be seen in Fig. 1 in the middle of the bunch. This bunch travels through a lattice of about 20 m, experiences high-frequency space charge forces and passes a second section with longitudinal dispersion to evolve the phase space pattern displayed in Fig. 3.

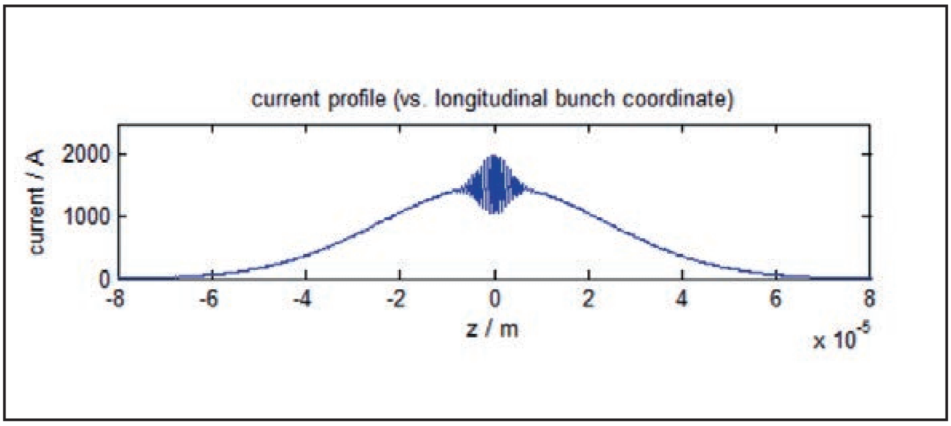

Figure 1

Density-modulated bunch current

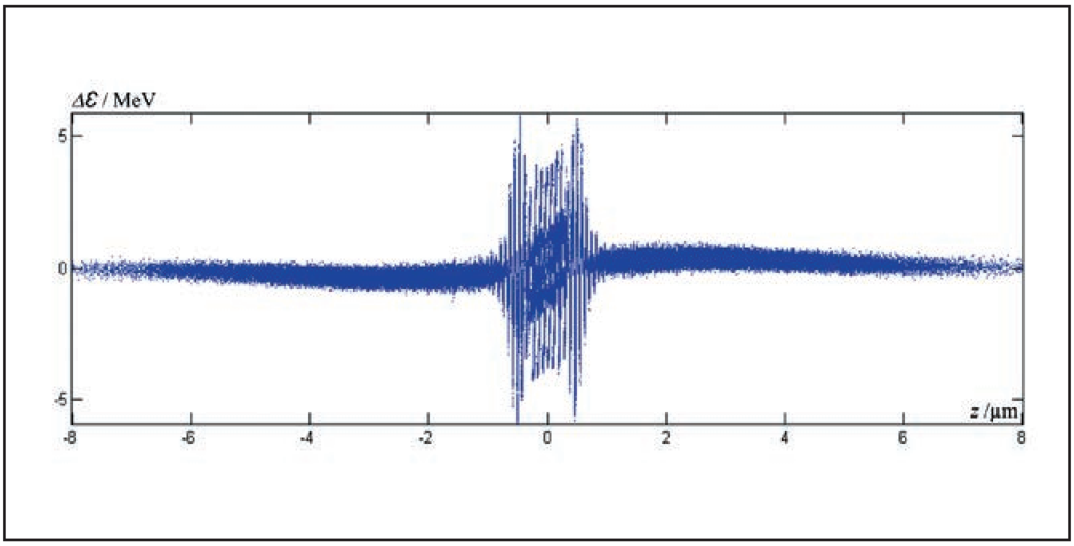

Figure 2

Longitudinal phase space with fast modulation

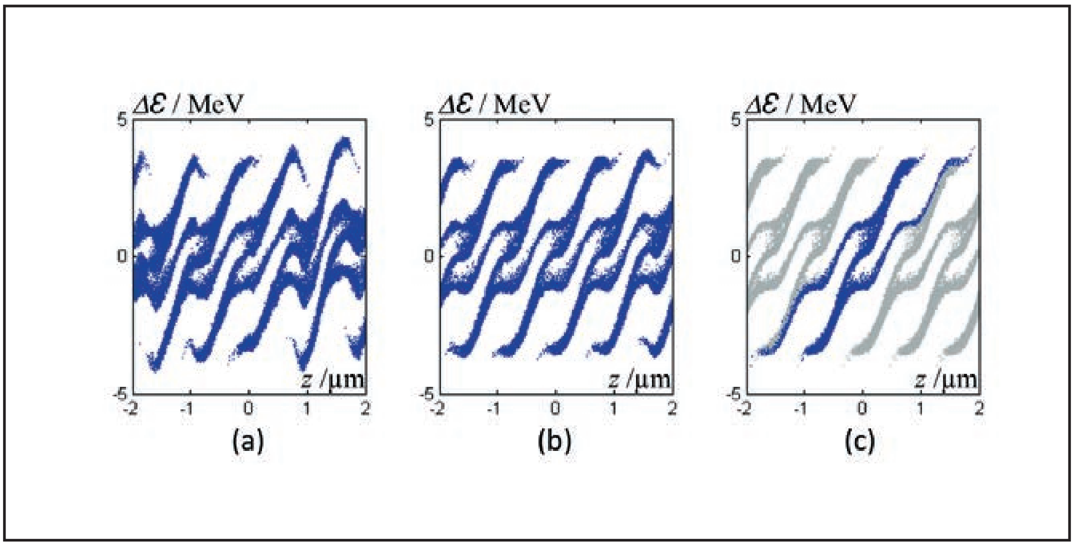

Figure 3

Detail of longitudinal phase space distribution

The quasi-periodic distribution in panel (a) is computed for the complete bunch without periodic approach. Panel (b) shows the result of a similar computation, but for a long laser excitation. It is obvious that a regular periodic pattern appears in the centre of the Gaussian distribution, which can be calculated by the periodic approach, as shown in panel (c). The full-bunch simulation needs about 100 times more particles and a 1000 times larger mesh volume than the periodic simulation. The periodic approach allows problems to be investigated efficiently on a single CPU, where otherwise large-scale computation would be required.

Contact: Martin Dohlus, martin.dohlus@desy.de

Ultrashort bunches in accelerator R&D.

Aiming for femtosecond bunches using conventional accelerator technology

Ultrashort electron bunches with an rms length below 1 fs are of great interest for various applications. First of all, they can be used for ultrafast science, for example to generate ultrashort radiation pulses or to run electron diffraction experiments. Moreover, they are expected to allow superior performance when injected into novel compact accelerating structures (e.g. based on plasma wakefield acceleration) [1]. Besides studying novel acceleration techniques aiming to produce high-brightness short bunches, the Accelerator Research and Development (ARD) group at DESY is working on the design of a conventional RF accelerator that will be hosted at the new SINBAD facility for Short Innovative Bunches and Accelerators at DESY. The Accelerator Research Experiment at SINBAD (ARES) will allow the production of such ultrashort bunches and the direct experimental comparison of the performance achievable by using different bunch compression techniques. At a later stage, ARES will be used to inject ultrashort electron bunches into a laser-driven plasma wakefield accelerator.

Limits of bunch length compression

The factors limiting the minimum bunch length in linear accelerators are well known. The main limitation is the space charge repulsion among the electrons in the bunch. As the effect scales as γ^{-2} (with γ being the relativistic factor of the beam), it limits the maximum electron densities especially at low energies. The next limitation is set by the uncorrelated energy spread of the beam, which is given by the minimum achievable spot size of the laser at the photocathode. Indeed, the compression of an electron bunch is equivalent to a rotation of the particle distribution in the longitudinal phase space. Moreover, the sinusoidal shape of the RF fields or the non-linear space charge force causes non-linear distortions of the distribution of the electrons in the longitudinal phase space [2]. Also, a magnetic chicane or a dogleg, when present, contains non-linear dispersion terms that increase the longitudinal emittance of the beam. In addition, when the magnetic compression is considered, coherent synchrotron radiation (CSR) further spoils the longitudinal emittance of the beam.

At ARES, we plan to accelerate electron bunches with very low charge (0.5–20 pC) to moderate energy levels (100–200 MeV) and to compress them to fs and sub-fs bunch durations. The chosen energy range allows the space charge limitation that characterises low-energy accelerators (3–5 MeV) to be relaxed, while dealing with a considerably more compact and relatively simple accelerator than the high-energy (>1 GeV) user facilities.

Moreover, the ARES layout (Fig. 1) will allow the experimental comparison of different types of bunch compression techniques (RF compression, hybrid RF compression and pure magnetic compression with the slit method), thus constituting a valuable tool for beam dynamics studies aimed at maximising beam brightness and stability.

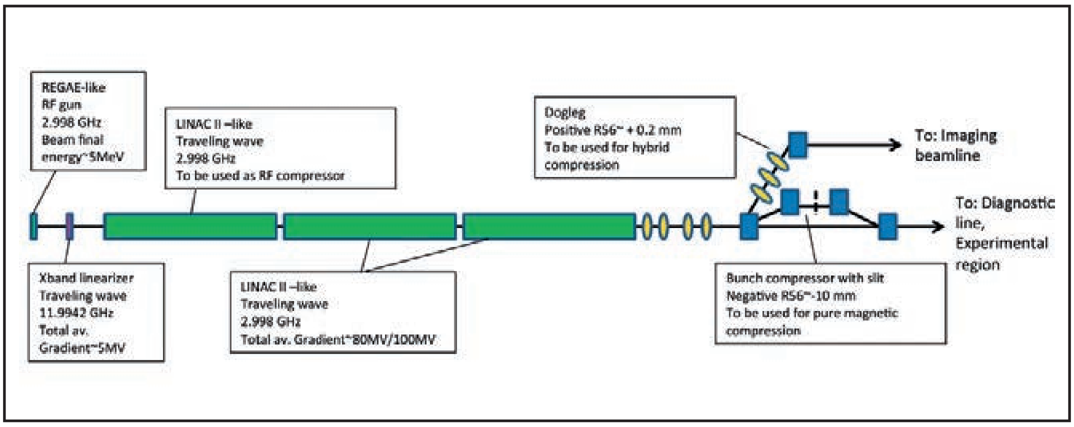

Figure 1

Sketch of the ARES accelerator. The electron beam is accelerated to 100–200 MeV by three travelling-wave RF cavities. The main linear accelerator is followed by two magnetic lattices with opposite linear momentum compaction (R_{56}) sign.

ARES layout and strategy

The electron bunches are produced in an RF gun of the type used at DESY's REGAE facility, where they are created by photoemission from a photocathode and accelerated to an energy of about 5 MeV. These bunches are subsequently accelerated and compressed in three LINAC II-type RF cavities. The layout allows three different compression schemes to be compared.

When using the RF compression technique, also referred to as velocity bunching, the low-energy electron bunch is injected into the first travelling-wave cavity close to the zero phase of the electric field. In this configuration, the head of the bunch experiences lower field amplitude than the tail. In this way, the bunch is compressed and accelerated at the same time. In fact, due to the different propagation velocities of the RF field and the electrons, the tail slips on the higher electric field amplitude region while travelling inside the cavity. At the exit of the first RF module, the longitudinal phase space of the electron bunch is rotated [3]. The following two RF structures are then operated on crest in order to maximise the acceleration. An example of the phase space distribution of an electron bunch after compression is shown in Fig. 2.

In the second compression scheme, we use the magnetic compression with the slit method. The three travelling-wave RF cavities are all operated off crest, establishing a linear correlation between the particle energy and its longitudinal coordinate along the bunch. A slit, placed at the centre of the chicane, where the transverse beam dimension is dominated by the particle momentum dispersion, selects a longitudinal slice of the bunch [5]. An example of the phase space distribution of an electron bunch after compression is shown in Fig. 3.

Finally, we can run a hybrid RF–magnetic compression scheme. The velocity bunching scheme is used once again, but the beam travels through the dogleg with positive linear momentum compaction R_{56}. This compensates for the elongation caused by the space charge force during the transport from the exit of the linear accelerator up to the experimental station.

Contact: Barbara Marchetti, barbara.marchetti@desy.de

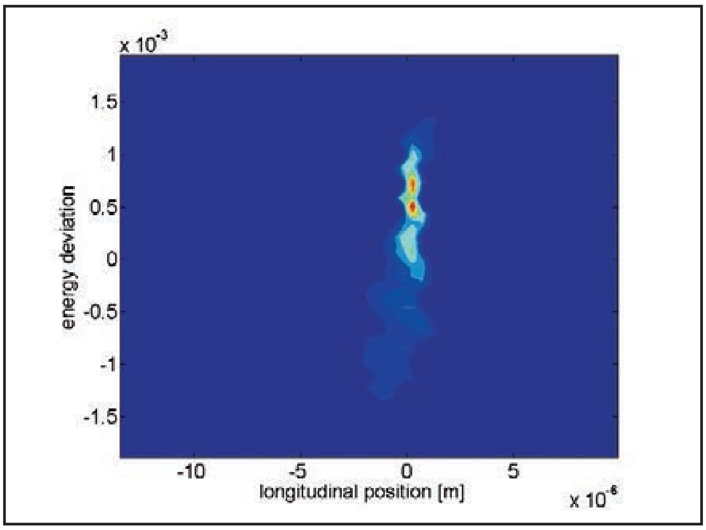

Figure 2

Longitudinal phase space of an electron beam compressed by velocity bunching at the exit of the second travelling-wave structure (simulation) [4]. The colour encoding indicates the local density of the particles. The final charge of the bunch is 0.5 pC, its FWHM duration is 2.8 fs.

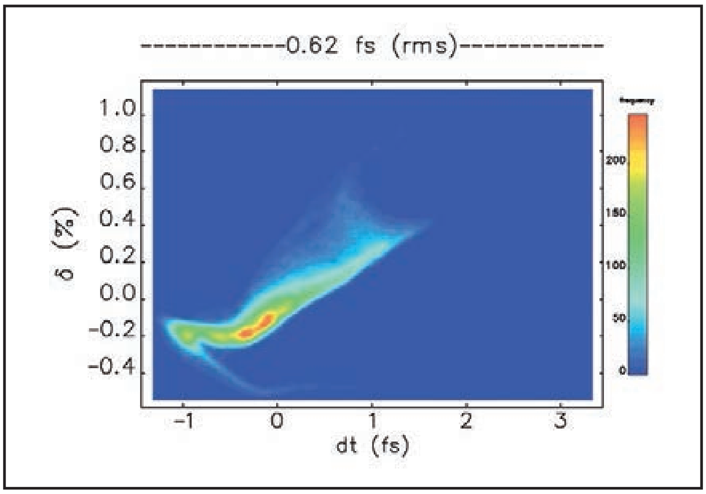

Figure 3

Longitudinal phase space of an electron beam compressed with the slit method at the exit of the magnetic compressor (simulation) [6]. The final charge of the bunch is 2.8 pC.

References:

[1] R. Assmann, J. Grabenyuk TUOBB01, Proceedings of IPAC 2014
[2] K. Flöttmann, NIM A 740 (2014) 34–38
[3] M. Ferrario et al. PRL 104 054801 (2010)
[4] B. Marchetti et al., to be submitted to proceedings IPAC 2015
[5] S. Di Mitri et al., PRSTAB 16 042801 (2013)
[6] J. Zhu et al., to be submitted to proceedings IPAC 2015

Plasma-based dechirper.

Energy chirp compensation scheme for plasma wakefield accelerators

Recent years have brought rapid progress in plasma wakefield acceleration. Although different injection schemes have been proposed, they all have in common a significant time–energy correlation. This energy chirp impedes beam quality preservation and eventually prevents any kind of X-ray light source application. A promising scheme for compensating such energy chirps is under investigation in the FLASHForward collaboration at DESY. It provides the basis for efficient post-plasma beam transport and thus paves the way for plasma-acceleration-based free-electron lasers (FELs).

Plasma wakefield acceleration

Plasma wakefield acceleration (PWFA) is a novel acceleration technique supporting electric fields in excess of 10 GV/m. The wakes generating these field gradients are excited by propagating a charged particle beam through a plasma. In order for the drive beam to resonantly excite the plasma wake, its bunch length has to be on the order of the plasma wavelength, which is a function of the density. Compared to conventional radio-frequency cavities, the accelerating gradients are orders of magnitude higher. A witness beam placed in the correct phase of the wake can be accelerated to 1 GeV within only 1 cm of propagation distance. Hence, PWFA might offer the possibility for compact, affordable, next-generation X-ray light sources.

Since the witness beam quality strongly depends on the injection process, different techniques are being studied. Although the recently proposed injection schemes produce low emittance and high peak current, they generate a significant time–energy correlation within the beam. This energy chirp leads to energy bandwidths of up to 10%. Such energy bandwidths cause severe emittance growth in drift spaces and focusing optics. Efficient beam transport with beam quality preservation is therefore impeded. Eventually, this beam degradation will prevent compact X-ray light source applications, since the performance of such sources is determined by electron beam parameters such as energy bandwidth and beam emittance.

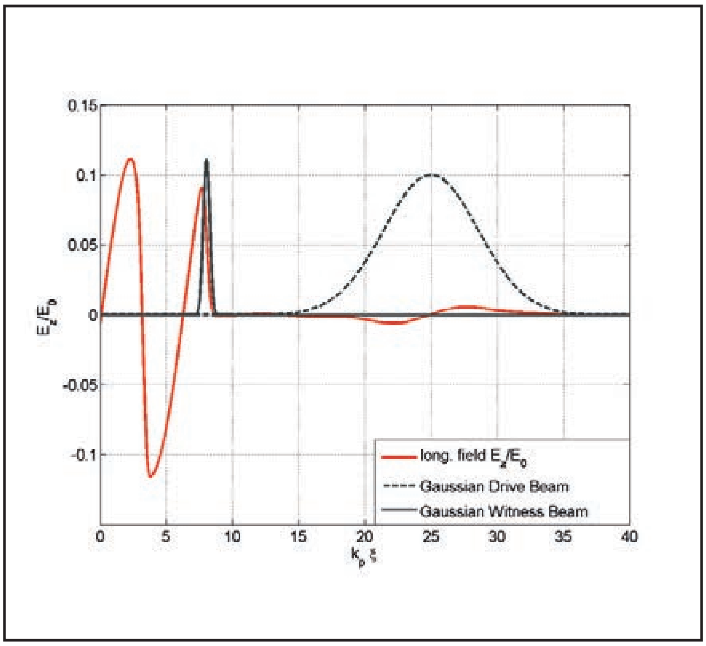

Figure 1

Longitudinal fields generated by a Gaussian drive beam and a Gaussian witness beam within plasma. The witness beam is resonantly driving a plasma wake, while the drive beam is too large to efficiently excite the plasma wake.

Energy chirp compensation

Energy-chirped beams do not solely occur in plasma-based acceleration schemes, but also in classical accelerators owing to the bunch compressing process. Thus, much effort has been made in the FEL community to reduce these correlated energy spreads. Recently, corrugated pipes [1] or dielectric structures [2] were proposed as a technique for compensating energy chirps. These schemes exploit the wakefields generated within the structure to cancel energy chirps of a few 10 MeV per millimetre bunch length within metres of propagation distance [1, 2]. However, these techniques are not applicable to electron beams from PWFA, because the energy chirps produced are orders of magnitude higher. Therefore, we suggest an analogous scheme to compensate the initially imposed energy chirp using the strong wakefields generated by the witness electron beam itself in the plasma.

The first half period of the longitudinal wakefield is decelerating, offering the possibility to cancel the negative energy chirp. In order for the witness to be dechirped by its own wakefield, it should not be affected by the fields generated by the drive beam. Therefore, the drive beam must be either dumped or brought out of resonance with the plasma density. Since the witness beam is longitudinally and transversely much smaller than the drive beam, the plasma density can be adjusted accordingly. Figure 1 shows the longitudinal fields generated by a large drive beam and a short witness beam, calculated using the three-dimensional particle-in-cell code HiPACE [3]. The plasma density is matching the resonance condition for the short witness beam. Thus, the wakefields generated by the drive beam are negligible.

In order for the energy chirp of the witness beam to be cancelled linearly, the decelerating field must act on the majority of the beam. This requirement imposes a criterion for the ratio of the plasma density and the witness beam bunch length.

Simulations for FLASHForward

The proposed dechirping scheme is not capable of removing density modulations from the longitudinal phase space distribution. Therefore, injection schemes producing linear time–energy correlations, such as field-ionisation-based schemes, are expected to produce the best results. According to simulations for wakefield-induced ionisation injection [4], a FLASH drive beam is capable of producing 2.5 GeV energy electron beams with a peak current of 5 kA, an rms bunch length of 0.2 µm and a normalised emittance of 0.3 mm mrad. The energy spread is typically on the order of 5% FWHM. Figure 2(a) shows the longitudinal phase space distribution of a Gaussian beam with these beam parameters. Three-dimensional simulations with the HiPACE code show an energy spread reduction down to 0.52% within a propagation distance of less than 1 mm in a plasma density of 3×10^{19} cm^{-3} (Fig. 2(a)). Due to the shape of the wakefields, the energy chirp is compensated best within the core of the beam. The dechirping technique leads to an emittance growth on the order of a factor of 2 (Fig. 2(b)). This increase is significantly smaller than the emittance growth due to chromaticity effects, which the beam would suffer without energy chirp compensation. Since the witness beams generated by PWFA have intrinsically small emittances, we can accept this growth without suffering a relevant FEL performance degradation.

Mono-energetic electron beams

The simulation results show a significant energy bandwidth reduction. The combination of controlled injection schemes such as wakefield-induced ionisation injection with the wakefield-based dechirping scheme brings mono-energetic electron beams within reach and thus paves the way towards PWFA-based FELs.

First experiments showing energy bandwidth reduction are planned for 2015 at the FACET facility at SLAC National Accelerator Laboratory in California.

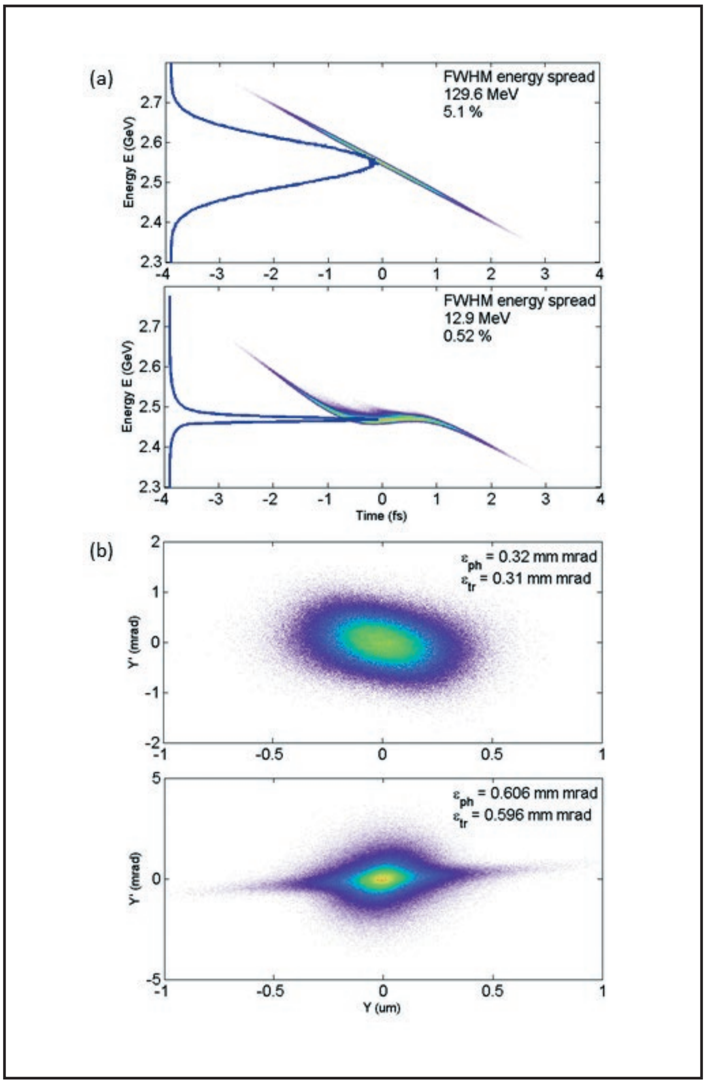

Figure 2

The upper figures (a) show the witness beam phase space distribution, the lower figures (b) the phase space emittance, both before and after propagating a distance of 0.95 mm in a plasma with density $n_0 = 3 \times 10^{19}$ cm^{-3}. The FWHM energy spread is reduced to 0.5% FWHM, corresponding to a 90% reduction. The emittance increases by a factor of about 2 to 0.6 mm mrad.

Contact: Violetta Wacker, violetta.wacker@desy.de
Christopher Behrens, christopher.behrens@desy.de

References:

[1] K. L. F. Bane, G. Stupakov, NIM A 690, 106 (2012)
[2] S. Antipov et al., PRL 112, 114801 (2014)
[3] T. Mehrling et al., Plasma Phys. Control. Fusion 56 084012 (2014)
[4] A. M. de la Ossa et al., Phys. Rev. Lett. 111, 245003 (2013)

RF distribution for the European XFEL Accelerator Module Test Facility.

New type of flexible high-power RF waveguide distribution for the AMTF

In order to test, within two years, the 100 superconducting accelerator modules required for the European XFEL X-ray free-electron laser, three test benches were set up in the Accelerator Module Test Facility (AMTF) at DESY. This will allow for a test rate of one accelerator module per week. Each RF station of the test facility provides up to 5 MW RF power at 1.3 GHz frequency, 1.37 ms pulse width and 10 Hz repetition rate via a waveguide distribution system. Each waveguide distribution supplies eight cavities, i.e. four times a pair of cavities. The distribution allows for a maximum power of 1 MW per cavity when switched to a mode supplying power to only four cavities. A new type of 1 MW isolator and a new compact 5 MW power divider were developed to achieve that goal. Several accelerator modules were already successfully tested with this setup.

The AMTF waveguide distribution meets several specific, sometimes conflicting, requirements. On one side, the distribution has a compact size, since only limited space in the AMTF shielding tunnel is available. On the other side, it supplies high pulsed RF power to the individual cavities in the cryogenic module with high flexibility using only one high-power klystron. In addition, the waveguide distribution protects the klystron against reflected power from the superconducting cavities.

The basic RF power requirements are 1 MW maximum pulse power per cavity and 2.2 kW maximum average power per cavity generated by one 5 MW klystron. The pulse width has to be adjustable between 50 µs and 1.37 ms, and the repetition rate between 2 Hz and 10 Hz. The waveguide elements are of size WR650.The waveguide distribution layout must allow for free access to the cavity input couplers for local cleanroom installation. In order to satisfy these conditions, two new specific waveguide components, a 1 MW isolator and a 5 MW power divider, were developed and integrated in the waveguide distribution. A 3D view of the AMTF RF waveguide distribution is shown in Fig. 1.

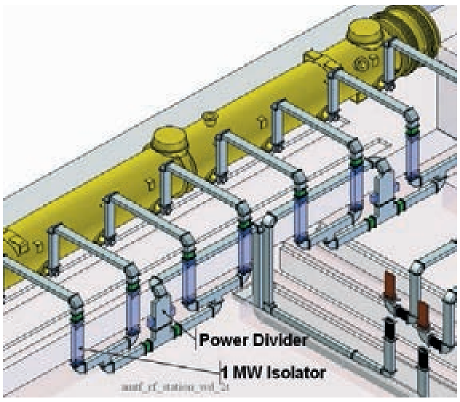

Figure 1
3D view of the RF waveguide distribution at the AMTF

During maintenance of the RF station, the klystron has to be connected to two dummy loads. To this end, a mechanical waveguide switch is installed, which allows for quick connection of the klystron and the RF loads.

To protect the klystrons against reflected power, Y-junction circulators or four-port phase shift circulators with matched load are usually used. For the AMTF waveguide distribution, these components could not be used since the Y-junction circulators are limited in power and phase shift circulators are too large. Therefore, a new type of 1 MW isolator was developed by the company FERRITE in St. Petersburg, Russia. The new FWHI3-27A-type isolator uses non-reciprocal energy absorption in ferrite elements through ferromagnetic resonance for waves with circular polarisation. An overview of the device (without magnetic system) is shown in Fig. 2. The ferrite elements are shown in grey.

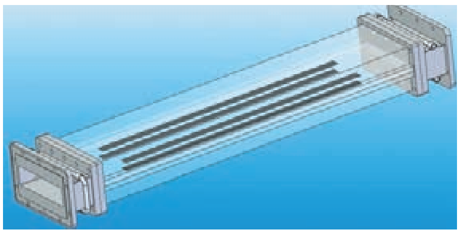

Figure 2
Schematic view of 1 MW isolator. The ferrite elements are shown in grey.

A 5 MW power divider was developed in cooperation with MicroPlus in Sofia, Bulgaria. The device is designed in accordance with a classical scheme: shunt tee, two phase shifters and hybrid with integrated H-bends. Each waveguide component was designed especially for this power divider. Simulation results of the device with CST Microwave Studio (MWS) are shown in Fig. 3. Depending on the phase shifter position, the RF power is distributed between the two outputs ports.

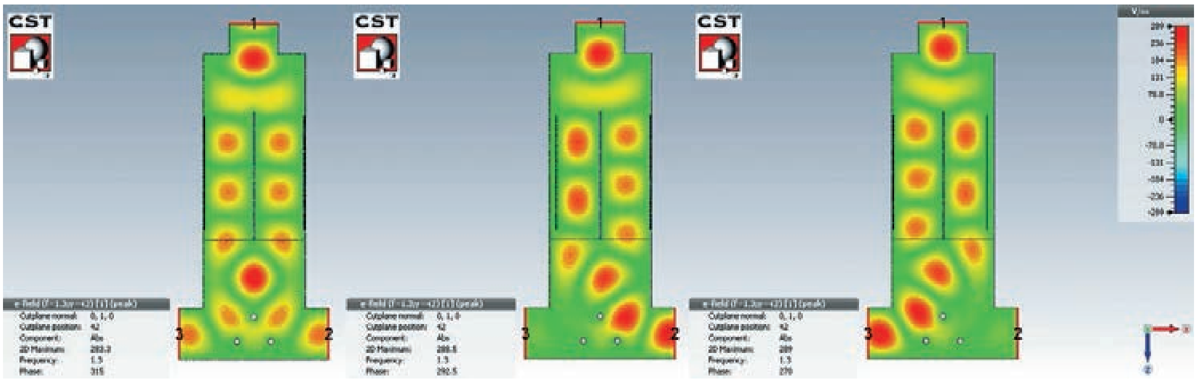

Figure 3

5 MW power divider

The AMTF comprises three RF test stands to test cryogenic modules for the European XFEL. This allows for a test rate of one cryogenic module per week. Each RF station consists of a 5 MW RF station and the specific waveguide distribution, which supplies one cryogenic module with eight superconducting cavities. A schematic of the waveguide distribution system is shown in Fig. 4. Each pair of cavities is supplied through a shunt tee, which divides the RF power equally between the two cavities. For two pairs of cavities, one 5 MW power divider is installed, which allows for flexible adjustment of the RF power between the two pairs. Another 5 MW power divider is installed after the klystron and distributes the RF power between the two halves of the cryogenic module.

Figure 5

Installation of the RF waveguide distribution at the AMTF

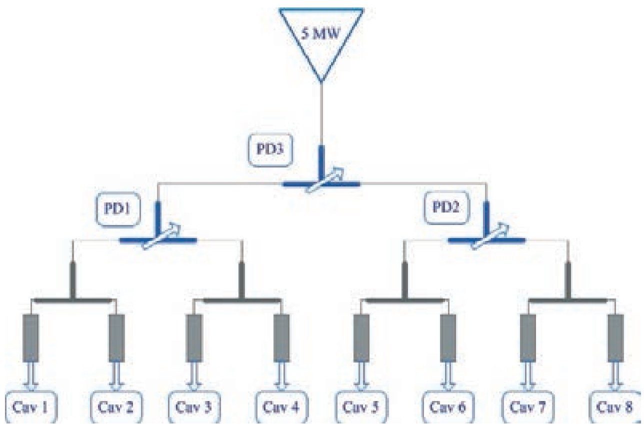

Figure 4

Schematic layout of an AMRF RF station

Three RF stations were successfully installed at the AMTF. The waveguide distribution system for each station was tuned and tested up to full power. Until the end of 2014, about 15 accelerator modules for the European XFEL had been tested at the AMTF and prepared for installation in the European XFEL tunnel.

Contact: Stefan Choroba, stefan.choroba@desy.de,
Valery Katalev, valery.katalev@desy.de

European XFEL superconducting cavity performance.

RF results for more than 500 European XFEL superconducting cavities

The main linear accelerator of the European XFEL X-ray free-electron laser will consist of 100 superconducting accelerator modules with 800 superconducting cavities operated at an average design gradient of 23.6 MV/m. Cavity fabrication in industry (which includes chemical surface preparation) is now in full swing, with approximately 540 cavities delivered by the end of 2014. After its arrival, each cavity undergoes a vertical acceptance cold test at 2 K in the Accelerator Module Test Facility (AMTF) at DESY. For more than 80% of the cavities, this acceptance test was successful, with the cavities fulfilling the European XFEL specifications. In those cases where the specification was not achieved, an in-house surface retreatment is performed and the cavity has to be retested. The success rate of this retreatment procedure is about 80%.

The 17.5 GeV superconducting linear accelerator for the European XFEL is currently under construction at DESY. An accelerator module production rate of one eight-cavity module per week requires an average cavity production and vertical acceptance testing rate of at least eight cavities per week. Testing is performed in the AMTF, a dedicated facility at DESY. By the end of 2014, more than 500 of the 800 series 1.3 GHz superconducting cavities had been produced, each having undergone at least one vertical acceptance test at the AMTF. Vertical and module testing is performed by a team from Henryk Niewodniczánski Institute of Nuclear Physics (IFJ-PAN) in Kraków, Poland, in close collaboration with several DESY groups.

Figure 1

Vertical test stand with bath cryostat, concrete shielding and cryogenic installation at the AMTF. A cryogenic insert with four superconducting accelerating cavities is under installation.

Industrial production of superconducting accelerator cavities for the European XFEL includes mechanical fabrication using niobium and niobium–titanium material provided by DESY, followed by surface preparation consisting of a well-proven procedure including surface removal, annealing and ultra-clean assembly steps. Series production is divided equally between E. Zanon Spa. (EZ), Italy, and Research Instruments (RI), Germany. Both vendors must exactly follow well-defined specifications for the mechanical fabrication and surface treatments, but no RF performance guarantee is required. The cavities are delivered complete with a helium tank, ready for testing. All cavities are fully equipped with their higher-order mode (HOM) antennas, pick-up probe and a high-*Q* input coupler antenna with fixed coupling. The cavities arrive under ultraclean UHV conditions.

After their arrival at DESY, the cavities are visually checked for damage during transportation and obvious assembly errors as well as for conformity with electrical and vacuum specifications.

In order to achieve the required testing rate of at least eight cavities per week, the vertical acceptance tests are made using two independent test systems, each consisting of an independent bath cryostat (Fig. 1) and RF test stand. Each test cryostat accepts a “cryogenic insert” that supports up to four cavities, greatly increasing the efficiency of the cool-down / warm-up cycles. The test infrastructure has been in full operation since October 2013 and has achieved an average greater than nine vertical cavity tests per week (Fig. 2).

The vertical acceptance tests follow a standardised procedure, which includes the measurement of the unloaded *Q*-value (Q_0) versus the accelerating gradient E_{acc} at 2 K, as well as the frequencies of the fundamental modes. For each point of the

$Q_0(E_{acc})$ curve, X-rays – indicating the limiting effect of field emission – are measured inside the concrete shielding above and below the cryostat. After a successfully completed test, selected key data are transferred to the European XFEL cavity data base, which forms the basis of the analyses reported here. All cavities are tested to their maximum achievable gradient ($E_{acc,max}$). Of greater importance for accelerator operation, however, is the usable gradient ($E_{acc,us}$), which takes design values for Q_0 as well as field emission performance into account. Cavities with $E_{acc,us}$ < 20 MV/m are considered for further processing or retreatment. The exact nature of the handling of low-performance cavities is judged on a case-by-case basis. As there are no vendor performance guarantees, retreatments are in general the responsibility of DESY.

Figures 3 and 4 show histograms and yield curves for the vertical test performance for both maximum and usable gradient, as received from the vendors. The average usable gradients for both vendors (EZ: 25.5 MV/m; RI: 28.9 MV/m) are above the required operational gradient for the European XFEL. The usable gradient is reduced from the maximum performance by ~4 MV/m on average, predominantly due to field emission. The effect can be seen in Fig. 3 and 4 as an increase in the numbers of cavities with performance less than ~28 MV/m. For both vendors, ~20% of the cavities require a retreatment due to field emission. There is also a statistically significant difference in the average performance of the two vendors (~6 MV/m and ~4 MV/m for the maximum and usable gradients, respectively), and gradients above 40 MV/m have only been observed with RI cavities. The better performance is attributed to the use by RI of electropolishing as the final surface preparation scheme, but also to the fact that RI cavities show less thermal breakdowns at low gradients. The percentage (yield) of cavities with a usable gradient above 26 MV/m (20 MV/m) is 54% (79%) for EZ and 73% (88%) for RI, with a total yield of 62% (83%). As described above, cavities with usable gradients below 20 MV/m undergo retreatment to increase their performance.

In general, high-pressure ultrapure water rinsing (HPR) is applied as a first retreatment. This is particularly effective since most low-performance cavities are dominated by field emission, which is likely associated with a removable surface emitter (e.g. particles). Figure 5 shows the distributions of 82 test results before and after retreatment (this also includes cavities whose initial performance was above 20 MV/m, but which still underwent a retreatment). The average usable gradient before and after retreatment for cavities with initial (before) performance < 20 MV/m (51 test results) is 14.6 MV/m and 26.3 MV/m respectively, an average gain of nearly 12 MV/m, with 78% of those cavities achieving ≥ 20 MV/m. The remaining ~22% in general undergo a second retreatment with HPR or possibly chemical polishing.

Contact: Detlef Reschke, detlef.reschke@desy.de,
Nicholas Walker, nicholas.walker@desy.de

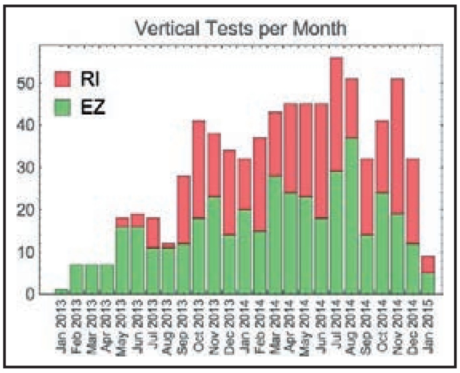

Figure 2
The trend of the vertical test rate after October 2013 is greater than nine vertical tests per week.

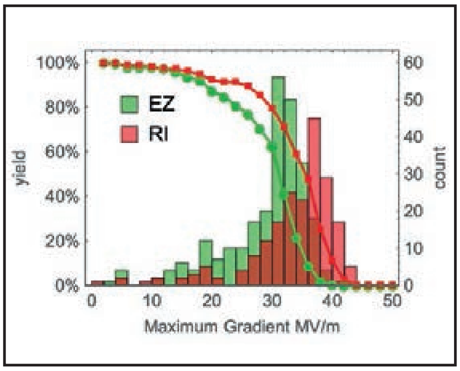

Figure 3
Comparison of performance distribution and yield for maximum gradient “as received” from RI (red) and EZ (green) (the darker colour is the overlap of both companies).

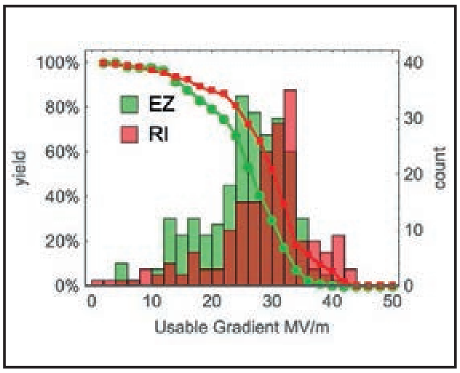

Figure 4
Comparison of performance distribution and yield for usable gradient “as received” from RI (red) and EZ (green) (the darker colour is the overlap of both companies).

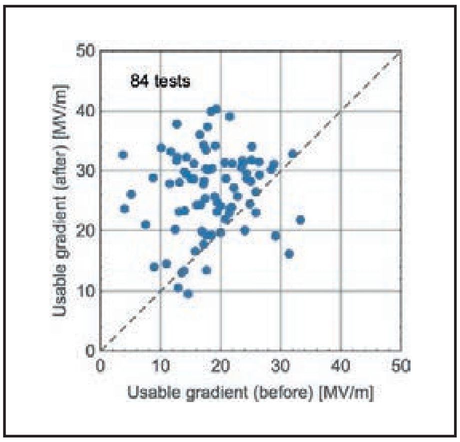

Figure 5
Comparison of usable gradient performance for cavities undergoing retreatment at DESY (82 retreatments)

Superconducting cavity material for the European XFEL.

Sophisticated material inspection process established at DESY

Work on the superconducting cavity material for the European XFEL X-ray free-electron laser was finished in 2014. In a period of approximately three years, four companies produced about 25 000 semi-finished parts (SFPs) of high-purity niobium and niobium–titanium alloy. DESY took care of the procurement of the material, quality control (QC), documentation and shipment to the cavity producers. Working out precise specifications for the material fabrication and keeping close contact with the manufacturers contributed to successful production. This report presents statistics on eddy current scanning (ECS) of niobium sheets for the QC of cavity half-cells. The main imperfections and defects in rejected sheets were analysed. Some samples containing foreign material inclusions were extracted from the sheets and investigated more precisely. Some inclusions persisted even after removal of a 140 µm surface layer by electrochemical polishing (EP).

Material (as SFPs) for the series cavities was ordered in 2011 from four companies qualified for the European XFEL, with delivery completed in 2014. Material foreseen for the production of the first 32 cavities (dummy, reference and pre-series cavities) had been purchased previously. The main order for the material was distributed between the companies as follows:

- 95% of SFPs for end groups from Heraeus
- 52% of sheets for half-cells from Tokyo Denkai
- 30% of sheets for half-cells, the rest of SFPs and 100% of niobium–titanium from Ningxia OTIC
- 18% of sheets for half-cells from PLANSEE

Besides all the commercial activities, the material procurement process also included an incoming QC, ECS inspection of the sheets, material analysis to check the conformity with specifications (analysis of residual resistivity ratio (RRR), interstitial and metallic impurities, metallography, tensile test, hardness test, dimensional and surface roughness check), documentation using an engineering data management system (EDMS) at DESY, definition of numbering system and marking, and delivery of the material to the companies producing the cavities.

A demanding QC infrastructure and appropriate logistics for guiding-through of SFPs were created at DESY, and the details of the workflow were organised. An example of the most critical procedure, the workflow for the niobium sheets required for half-cell fabrication, is shown in Fig. 1. Three workstations were created:

- “Labelling” for incoming inspection, certificate examination and sheet labelling
- “Scanning” for visual examination and ECS
- “Stamping” for marking of the sheets and preparation of their delivery to the cavity producers

Finally, the RF surface on each sheet accepted for cavity fabrication was determined and mechanically engraved.

A visual control of the delivered sheets allowed the selection of sheets in need of reconditioning by the suppliers. Sheets that passed the visual inspection were EC-scanned. Two new EC devices were developed and built in conjunction with industrial partners for scanning of the European XFEL niobium sheets. All sheets, including those replaced and reprocessed by the suppliers, were scanned.

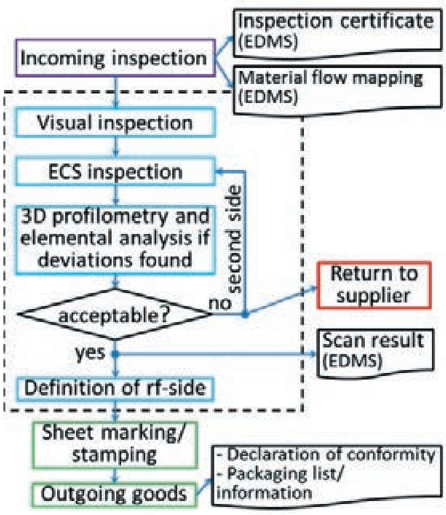

Figure 1
Simplified workflow of the incoming inspection and QC procedure at DESY for the niobium sheets for half-cell fabrication

The operators judged whether a sheet was qualified by means of the following criteria:

- First side good: sheet is qualified
- First side bad, second side good: sheet is qualified
- First and second sides bad: sheet is not qualified and belongs to non-usable sheets

Subsequent non-destructive investigation of non-usable sheets included visual surface inspection, optical microscopy and 3D profilometry, surface roughness measurement and X-ray fluorescence element analysis. The aim of these

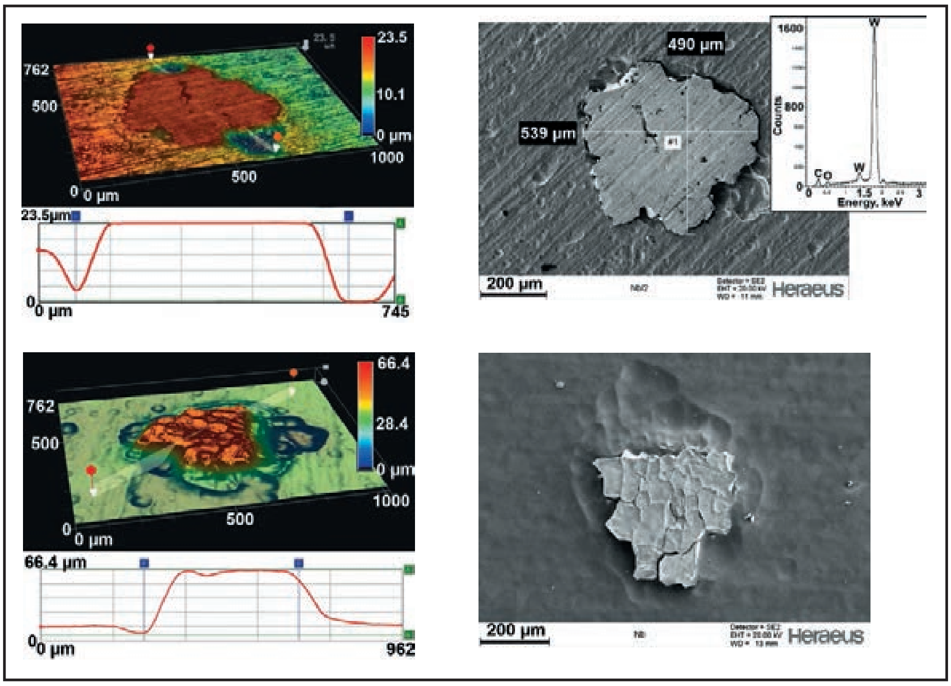

Figure 2

Optical (left) and SEM (right) microscopy image of a tungsten inclusion, as identified by EDX (see part of the EDX spectra in the inset), found in the area indicated by ECS. Comparison of the inclusion before (top row) and after (bottom row) 150 µm EP. Note the different orientation of the images.

additional analyses was to separate the sheets that had to be rejected from the sheets suitable for reconditioning.

Non-qualified sheets were returned to the vendors. Detailed analysis of these sheets allowed two main categories of defects to be defined: foreign material inclusions and topographical defects (scratches, holes, pits, marks and delamination). All sheets with foreign material inclusions were replaced. The sheets with topographical defects were mostly reconditioned (re-grinded) by the vendors and accepted after repeated QC. Delaminations were revealed on several sheets at the beginning of the production. Their cause was understood by the companies, and the number of sheets with delaminations was radically reduced.

Approximately 26% of the sheets were scanned on both sides. About 2% (310 out of 15 612) of all scanned sheets were classified as non-usable.

In the sheets from all three suppliers, inclusions of iron, nickel, chromium and titanium were detected. Inclusions of tantalum were found in the sheets from companies A and B, zirconium from company A, and tungsten, molybdenum and zinc from company C. Topographical deviations were found on sheets from all three companies.

The main treatment procedure of the inside surface of the European XFEL cavities is electrochemical polishing (EP), which removes a layer 110 to 140 µm thick. In connection with this surface treatment, the question arose whether the foreign material inclusion would disappear during EP or remain and possibly cause a quench in the cavity. This was checked on some rejected sheets. Samples of round shape with defects in the middle area were extracted from the sheets and EP-treated with EP parameters similar to those used for the European XFEL cavities. The evolution of the surface and influence of the EP process on the inclusions were analysed using optical microscopy with a Keyence digital microscope, scanning electron microscopy (SEM) and energy-dispersive X-ray spectroscopy (EDX).

One example illustrating the effect of EP on defects can be seen in Fig. 2. The investigations showed that some foreign material inclusions remained almost unaffected by EP, whereas others disappeared completely. The effect clearly depended on the inclusions' size and location depth, as well as on the material type and its concentration, since the EP removal rate is different for different elements.

More than 70% of the superconducting cavities for the European XFEL were produced by the end of 2014. The relatively low number of cavities (about 7%) with hard quenches below 20 MV/m allows us to conclude that a high quality of the procured material has been achieved.

Material inspection based on ECS of 100% of the delivered material and supplemented by a detailed non-destructive investigation is a reasonable inspection method to avoid diminished RF performance of cavities caused by the material. First of all, it allows a better choice of the side of the sheet to be exposed to the RF. Moreover, not utilising such material inspection would mean that, in the worst case mentioned, the 2% of sheets that were rejected would affect the performance of approximately every third cavity, supposing that the non-usable sheets are homogeneously distributed throughout the production lots.

Contact: Waldemar Singer, waldemar.singer@desy.de
Jens Iversen, jens.iversen@desy.de

LINAC II.

Reliable beams for PETRA III and DESY II

In 2014, the shutdown of the PETRA III accelerator chain was used to install a second injector in the LINAC II pre-accelerator. In addition to increasing reliability thanks to redundancy, the installation is expected to bring some qualitative improvements for the operation of the linear accelerator.

As the first element in the PETRA III accelerator chain, the linear accelerator LINAC II is designed to deliver electron and positron beams for injection into the synchrotron DESY II. Therefore, it actually consists of two accelerators: one primary linac to produce high-power beams for the positron converter and a secondary linac to re-accelerate the positrons. In positron mode, to produce sufficient power in the primary beam, a peak beam current of 2 A is required at the converter. Due to the low capture efficiency of the old injector, a gun current of 6 A is necessary to meet this requirement. The gun is a 120 kV pulsed DC diode gun, which produces beam pulses of up to 6 A and 4 µs duration. The cathode is made of a thoriated tungsten plug, heated by a 3 kV, 1.2 kW bombarder. For best performance, the cathode plug has to be carburised. An electrostatic chopper forms beam pulses of 2 ns to 30 ns duration, depending on the operation conditions. In electron mode, the primary beam is used directly, which reduces the required average beam current. A 2.998 GHz pre-buncher cavity is fed by a portion of the first structure's forward RF power drawn from a directional coupler. The beam then enters the first accelerator section, which is not tapered.

One problem connected with the current gun is the ceramic high-voltage isolator that is at the same time sealing the vacuum against the oil of the modulator. If this ceramic should break, the leak would cause irreparable damage to probably the whole linac. Secondly, it is becoming increasingly hard to find suppliers for the carburised cathode plugs. Thirdly, due to the bunching scheme, a substantial portion of the primary beam is lost at high energies along the linac.

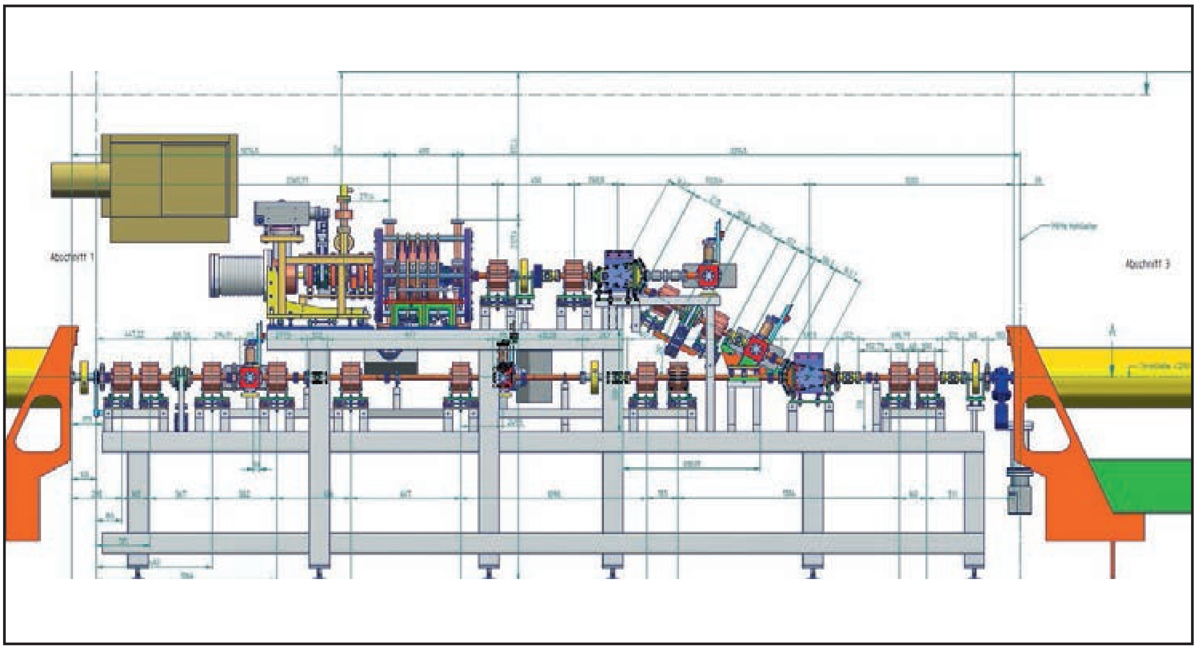

Figure 1
CAD model of the new injector with its surroundings at the position of the old acceleration section #2. The arrow "a" indicates the direction of the beam from the old gun, the arrow "b" the beam from the new gun.

To remedy these problems, a new injector was designed that avoids all the problems described above (Fig. 1). The cathode is commercially available, and the isolator in air provides ample reserve for the operation voltage of 100 kV. Like the old gun, the new one does not produce electron bunches fitting into the 3 GHz RF buckets of the linac from the beginning. The bunches are rather formed by a combination of a pre-buncher cavity and buncher structure.

The buncher structure is equipped with a capture cell adapted for a particle velocity of approximately half the speed of light (Fig. 2). To achieve this, the capture cell is coupled in standing-wave mode to the input cell of the otherwise travelling-wave structure. In this way, the phase difference between the first and second cell is increased from 120° to 180° and, at the same time, the RF properties of the other cells are disturbed the least. The structure is therefore a hybrid between a standing-wave cavity and a travelling-wave structure. The capture cell should improve the capture efficiency by 50–100%. This has yet to be proved in the commissioning of the new injector.

The gun and buncher are shifted from the beam axis of the main accelerator (Fig. 3). The beam is guided onto the axis by a magnetic chicane. This configuration allows for fast switching between the old and new gun. At the same time, it comprises an energy filter for the injected beam. This filter ensures that electrons that were not captured correctly are lost at low energy so that the damage resulting from such electrons is minimised.

While it is foreseen to operate the linac with the new gun exclusively, the old gun will be held in stand-by, sealed off from the linac by a vacuum valve. In the long run, the old gun may be replaced entirely. The gun that will be installed then might be optimised for a different mode of operation, however.

Contact: Markus Hünning, markus.huenning@desy.de

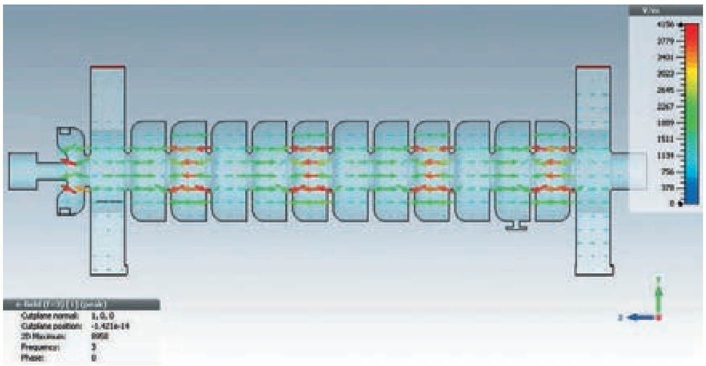

Figure 2

RF field distribution in the hybrid buncher structure as simulated using CST Microwave Studio. The leftmost cell is the capture cell. It has a reentrant shape with a beam pipe of reduced diameter. In this way, it could be adjusted to approximately $\beta = 0.5$.

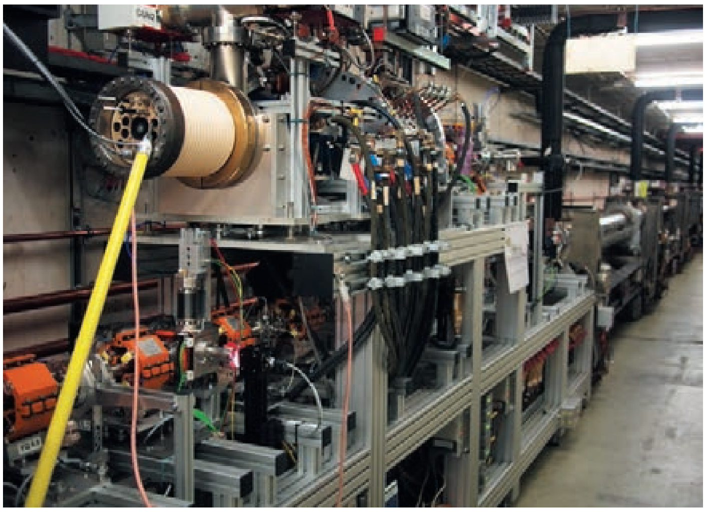

Figure 3

The new injector in the linac tunnel: The high-voltage isolator of the new gun can be seen in the foreground. The buncher structure, which captures and accelerates the beam, is located closely behind the gun. In the picture, it is hidden behind the solenoid surrounding it. The chain of quadrupoles beneath the gun belong to the beam transport from the old injector.

References

Committees.

DESY Board of Directors

R. Brinkmann
(Accelerator division)

H. Dosch
(Chairman of the DESY Board of Directors)

J. Mnich
(High-energy physics and astroparticle physics)

C. Scherf
(Administrative division)

E. Weckert
(Photon science division)

C. Stegmann
(Representative of the directorate in Zeuthen)

Machine Advisory Committee (MAC)

Michael Borland (ANL, USA)
Hans Braun (PSI, CH)
Massimo Ferraio (INFN, I)
Zhirong Huang (SLAC, USA)
Andreas Jankowiak (HZB, Chair)
Katsunobu Oide (KEK, JP)
Pantaleo Raimondi (ESRF, F)
Rüdiger Schmidt (CERN, CH)

DESY Scientific Board

R. Aßmann (DESY)
F. Beckmann (HZG)
T. Behnke (DESY)
M. Bieler (DESY)
I. Bloch (DESY)
I. Brock (KET)
W. Buchmüller (DESY)
K. Büßer (DESY)
H. Chapman (DESY)
M. Diehl (DESY)
R. Döhrmann (DESY)
W. Drube (DESY)
G. Eckerlin (DESY)
H.-J. Eckoldt (DESY)
A. Ehnes (DESY)
E. Elsen (DESY)
S. Fiedler (EMBL)
T. Finnern (DESY)
B. Foster (DESY)
E. Gallo (DESY)
H. Graafsma (DESY)
I.M. Gregor (DESY)
C. Grojean (DESY)
G. Grübel (DESY)
W. Gülzow (DESY)
J. Haller (Univ. Hamburg)
M. Hempel (DESY)
K. Honkavaara (DESY)
K. Jansen (DESY)
F. Kärtner (DESY)
M. Kasemann (DESY)
C. Kluth (DESY)
M. Kowalski (DESY)
T. Laarmann (DESY)
A. Maier (KfB)
N. Meyners (DESY)
W.-D. Möller (DESY)
K. Mönig (DESY)
B. Murphy (KfS)
A. Mußgiller (DESY)
T. Naumann (DESY)
C. Niebuhr (DESY)
D. Nölle (DESY)
B. Petersen (DESY)
E. Plönjes-Palm (DESY)
M. Pohl (DESY)
B. Racky (DESY)
A. Ringwald (DESY)
R. Röhlsberger (DESY)
W. Sandner (DESY)
R. Santra (DESY)
V. Schomerus (DESY)
T. Schörner-Sadenius (DESY)
S. Schreiber (DESY)
C. Schroer (DESY)
H. Schulte-Schrepping (DESY)
C. Schwanenberger (DESY)
U. Schwanke (HU Berlin)
A. Schwarz (DESY)
O. Seek (DESY)
G. Servant (DESY)
J. Spengler (DESY)
A. Stierle (DESY)
K. Tackmann (DESY)
S. Techert (DESY)
M. Tischer (DESY)
T. Tschentscher (EuropeanXFEL)
J. Viefhaus (DESY)
M. Vogt (DESY)
P. Wegner (DESY)
G. Weiglein (DESY)
H. Weise (DESY)
M. v. Zimmermann (DESY)

Memberships.

ANKA Machine Advisory Committee
Klaus Balewski

APAC ESRF
Reinhard Brinkmann

AREAL Project, Armenia, International Technical Advisory Committee
Klaus Flöttmann

Apollon/CILEX Technical Advisory Committee
Ralph Aßmann

Accelerator Test Facility (ATF) Programme Advisory Committee
Ralph Aßmann

AWAKE Experiment CERN Collaboration Board
Ralph Aßmann

BerlinPro Machine Advisory Committee
Holger Schlarb, Siegfried Schreiber

BESSY Machine Advisory Committee
Winfried Decking

BMBF Gutachterausschuss Hadronen- u. Kernphysik (HKP)
Hans Weise

CERN Accelerator School on Plasma Acceleration (CAS 2014)
Ralph Aßmann

CERN Machine Advisory Committee
Reinhard Brinkmann

CTA Data and Controls Review
Kay Rehlich

European Advanced Accelerator Concepts Workshop (EAAC2015) Organising Committee
Ralph Aßmann

European Advanced Accelerator Concepts Workshop (EAAC2015) Co-Chairman
Ralph Aßmann

European Physical Society Accelerator Group (EPS-AG)
Ralph Aßmann, Kay Wittenburg

ESS Review Follow-up
Wilhelm Bialowons

European Coordination for Accelerator R&D (EuCARD2) Deputy Coordinator
Ralph Aßmann

European Coordination for Accelerator R&D (EuCARD2) Steering Board
Ralph Aßmann

European Coordination for Accelerator R&D (EuCARD2) Governing Board
Ralph Aßmann

European Strategy Group for Accelerator R&D (ESGARD)
Eckhard Elsen, Ralph Aßmann

FAIR Machine Advisory Committee
Kay Wittenburg

FEL 2015 Scientific Programme Committee
Frank Stephan, Siegfried Schreiber

FLAC, Machine Advisory Committee SwissFEL
Holger Schlarb

Future Circular Collider (FCC) Collaboration Board
Ralph Aßmann

Helmholtz Virtual Institute 2012
"Plasma Wakefield Acceleration of Highly Relativistic Electrons with FLASH"
Brian Foster (Coordinator)

High-Luminosity LHC Collaboration Board
Rainer Wanzenberg

ICALEPCS International Scientific Advisory Committee (ISAC)
Reinhard Bacher

ICFA Beam Dynamics Panel
Rainer Wanzenberg

ILC Accelerator Advisory Panel (AAP) and International Detector Advisory Group (IDAG)
Eckhard Elsen

ILC and High-Gradient Superconducting RF Cavities (ILC-HiGrade)
Eckhard Elsen (Project Coordinator)

ILC Technical Board
Nicholas Walker

International Conference on RF Superconductivity (SRF2014) International Programme Committee
Wolf-Dietrich Möller

IPAC 2014 Scientific Advisory Committee
Ralph Aßmann

IPAC 2015 Scientific Advisory Committee
Ralph Aßmann

Joint University Accelerator School Advisory Board
Winfried Decking

Komitee für Beschleunigerphysik
Hans Weise

LINAC 2014 International Organising Committee
Hans Weise

LINAC 2014 Scientific Programme Committee
Stefan Choroba

LCLS-II Director's Review
Winfried Decking

LCLS-II DOE Review
Stefan Choroba

LCLS-II Facility Advisory Committee
Jacek Sekutowicz

MAX IV Machine Advisory Committee
Klaus Balewski

PCaPAC Programme Committee
Philip Duval, Reinhard Bacher

PHIL Scientific Committee
Frank Stephan

Physical Review Special Topics – Accelerator and Beams – Editor
Klaus Flöttmann

QRC-KAERI World-Class Institute, International Advisory Committee
Klaus Flöttmann

Real-Time Conference Scientific Advisory committee
Kay Rehlich

SESAME Council Meeting
Wilhelm Bialowons

SPIE Advances in X-ray Free-Electron Laser Instrumentation Scientific Programme Committee
Siegfried Schreiber

STFC Accelerator Strategy Board
Reinhard Brinkmann

TIARA Governing Board
Reinhard Brinkmann

TTC Executive Committee
Hans Weise

TTC Technical Board
Wolf-Dietrich Möller, Detlef Reschke

US LHC Accelerator Research Programme Advisory Committee
Kay Wittenburg

European XFEL Council Appointed Member – Advisor to the German Delegation
Reinhard Brinkmann

Publications.

Publications

R. Assmann et al.
Proton-driven plasma wakefield acceleration: a path to the future of high-energy particle physics.
Plasma physics and controlled fusion, 56(8):084013, and PUBDB-2014-04590, arXiv:1401.4823.
doi: 10.1088/0741-3335/56/8/084013.

N.-I. Baboi and R. M. Jones.
Statistical Methods for Transverse Beam Position Diagnostics with Higher Order Modes in Third Harmonic 3.9GHz Superconducting Accelerating Cavities at FLASH.
Nuclear instruments & methods in physics research / A, 734(Part A):84, and DESY-2013-00598.
doi: 10.1016/j.nima.2012.11.057.

V. Balandin et al.
First non-intercepting emittance measurement by means of optical diffraction radiation interference.
New journal of physics, 16(11):113029, and PUBDB-2014-04102.
doi: 10.1088/1367-2630/16/11/113029.

R. Brinkmann et al.
Prospects for CW and LP Operation of the European XFEL in Hard X-ray Regime.
Nuclear instruments & methods in physics research / A, 768:20, and PUBDB-2014-03854, DESY 14-025.
doi: 10.1016/j.nima.2014.09.039.

H. Brueck et al.
First Results of the Magnetic Measurements of the Superconducting Magnets for the European XFEL.
IEEE transactions on applied superconductivity, 24(3):1, and PUBDB-2015-01319.
doi: 10.1109/TASC.2013.2284197.

A. Cianchi and J. Osterhoff.
Summary of the Working Group 5: Plasma sources and instrumentation.
1st European Advanced Accelerator Concepts Workshop, La Biodola, Isola d'Elba (Italy), 06/02/2013 - 06/07/2013.
North-Holland Publ. Co., Amsterdam, June 2014.
doi: 10.1016/j.nima.2014.01.036.

S. Duesterer et al.
Development of experimental techniques for the characterization of ultrashort photon pulses of extreme ultraviolet free-electron lasers.
Physical review / Special topics / Accelerators and beams, 17(12):120702, and PUBDB-2014-04594.
doi: 10.1103/PhysRevSTAB.17.120702.

M. Ferrario et al.
IRIDE: Interdisciplinary Research Infrastructure Based on Dual Electron Linacs and Lasers.
Nuclear instruments & methods in physics research / A, 740:138, and PUBDB-2015-01259.
doi: 10.1016/j.nima.2013.11.040.

K. Floettmann.
Adiabatic Matching Section for Plasma Accelerated Beams.
Physical review / Special topics / Accelerators and beams, 17(5):11, and PUBDB-2015-00549.
doi: 10.1103/PhysRevSTAB.17.054402.

K. Floettmann.
Generation of sub-fs Electron Beams at few-MeV Energies.
Nuclear instruments & methods in physics research / A, 740:34, and PUBDB-2015-00538.
doi: 10.1016/j.nima.2013.12.031.

K. Floettmann and V. V. Paramonov.
Beam Dynamics in Transverse Deflecting RF Structures.
Physical review / Special topics / Accelerators and beams, 17(2):024001, and PUBDB-2015-00536.
doi: 10.1103/PhysRevSTAB.17.024001.

G. Geloni et al.
Interference effects in super-radiant THz sources.
Infrared physics & technology, 64:26, and DESY-2014-01914.
doi: 10.1016/j.infrared.2014.01.009.

H.-W. Glock et al.
Scattering parameters of the 3.9 GHz accelerating module in a free-electron laser linac: a rigorous comparison between simulations and measurements.
Physical review / Special topics / Accelerators and beams, 17(2):022003, and PUBDB-2014-04145.
doi: 10.1103/PhysRevSTAB.17.022003.

S. Hillenbrand et al.
Study of Laser Wakefield Accelerators as injectors for Synchrotron light sources.
Nuclear instruments & methods in physics research / A, 740:153, and PUBDB-2015-00711.
doi: 10.1016/j.nima.2013.10.081.

K. M. Hock et al.
Beam tomography research at Daresbury Laboratory.
Nuclear instruments & methods in physics research / A, 753:38, and PUBDB-2014-04589.
doi: 10.1016/j.nima.2014.03.050.

P. N. Juranić et al.
A Scheme for a Shot-to-Shot, Femtosecond-Resolved Pulse Length and Arrival Time Measurement of Free Electron Laser X-Ray Pulses that Overcomes the Time Jitter Problem between the FEL and the Laser.
Journal of Instrumentation, 9(03):P03006, and PUBDB-2015-01096.
doi: 10.1088/1748-0221/9/03/P03006.

P. Kneisel et al.
Review of Ingot Niobium as a Material for Superconducting Radiofrequency Accelerating Cavities.
Nuclear instruments & methods in physics research / A, 774:133, and PUBDB-2015-00668.
doi: 10.1016/j.nima.2014.11.083.

J. Lorkiewicz et al.
Deposition and Optimization of Thin Lead Layers for Superconducting Accelerator Photocathodes.
Physica scripta, T161:014071, and PUBDB-2015-01095.
doi: 10.1088/0031-8949/2014/T161/014071.

S. Manz et al.
Mapping Atomic Motions with Ultrabright Electrons: Towards Fundamental Limits in Space-Time Resolution.
Faraday discussions, 1:25, and PUBDB-2014-04597.
doi: 10.1039/C4FD00204K.

Y. C. Nie et al.
Tuning of 2.998GHz S-band Hybrid Buncher for Injector Upgrade of LINACII at DESY.
Nuclear Instruments and Methods in Physics Research A, 761:69, and PUBDB-2014-03884.
doi: 10.1016/j.nima.2014.05.043.

S. Roling et al.
Time-Dependent Wave Front Propagation Simulation of a Hard X-Ray Split-and-Delay unit: Towards a Measurement of the Temporal Coherence Properties of X-Ray Free Electron Lasers.
Physical review / Special topics / Accelerators and beams, 17(11):110705, and PUBDB-2015-00039.
doi: 10.1103/PhysRevSTAB.17.110705.

L. G. Sukhikh et al.
Backward Transition Radiation in the Extreme Ultraviolet Regionas a Tool for the Transverse Beam Profile Diagnostic.
Physical review / Special topics / Accelerators and beams, 17:112805, and PUBDB-2014-04101.
doi: 10.1103/PhysRevSTAB.17.112805.

G. Valentino et al.
Simulator for Beam-Based LHC Collimator Alignment.
Physical review / Special topics / Accelerators and beams, 17(2):021003, and PUBDB-2015-00999.
doi: 10.1103/PhysRevSTAB.17.021003.

V. V. Zelenogorskii et al.
Scanning cross-correlator for monitoring uniform 3D ellipsoidal laser beams.
Quantum electronics, 44(1):76, and PUBDB-2014-04591, BMBF 05K10CHE; HRJG-400.
doi: 10.1070/QE2014v044n01ABEH015224.

Preprints and Internal Reports

I. Agapov et al.
Laser Wire Scanner Compton Scattering Techniques for the Measurement of the Transverse Beam Size of Particle Beams at Future Linear Colliders.
PUBDB-2014-04579, arXiv:1412.3004.

V. Balandin, W. Decking and N. Golubeva.
Possibilities for reduction of transverse projected emittancesby partial removal of transverse to longitudinal beam correlations.
PUBDB-2014-03910, DESY 14-167; arXiv:1409.6164v1.

R. Brinkmann et al.
Prospects for CW and LP Operation of the European XFEL in Hard X-ray Regime.
DESY-2014-03285, DESY 14-025.

V. Gharibyan.
Accelerator Experiments Contradicting General Relativity.
DESY-2014-03175, DESY 14-003; arXiv:1401.3720.

K. Heinemann et al.
A New and Unifying Approach to Spin Dynamics and Beam Polarization in Storage Rings.
PUBDB-2014-03992, arXiv:1409.4373; DESY 14-163.

Y. Kot, T. Limberg and I. Zagorodnov.
Different Charges in the Same Bunch Train at the European XFEL.
DESY-2014-03192.

V. Paramonov et al.
Deflecting RF Structures with reduced level of aberrations for transformation of particle distributions in the bunch.
Physics of particles and nuclei letters, 11(5):636, and PUBDB-2015-00533.
doi: 10.1134/S1547477114050239.

E. A. Schneidmiller and M. Yurkov.
Optimization of a High Efficiency FEL amplifier.
PUBDB-2015-00034, DESY 14-161; arXiv:1410.5957.

E. A. Schneidmiller and M. Yurkov.
Statistical Properties of the Radiation from SASE FEL Operating in a post-saturation Regime with and without Undulator Tapering.
PUBDB-2015-00035, DESY 14-239.

Books

P. Schmüser et al.
Free-Electron Lasers in the Ultraviolet and X-Ray Regime : Physical Principles, Experimental Results, Technical Realization; 2. erw. Auflage.
Vol. 229. *Springer Tracts in Modern Physics*.
Springer International Publishing, Cham, 2009.

Contributions to a book

M. Krasilnikov et al.
Development of a photo cathode laser system for quasi ellipsoidal bunches at a high brightness photo injector.
Structure of matter.
Helmholtz Geschäftsstelle, Berlin, 2014.

S. Schreiber.
An Engineering Guide To Photoinjectors, Ch. 11: Diagnostics.
An Engineering Guide To Photoinjectors.
arXiv.org, Cornell, 2014.

S. Schreiber.
x-Ray Free-Electron Lasers.
Comprehensive Biomedical Physics.
Elsevier, Amsterdam, 2014.
doi: 10.1016/B978-0-444-53632-7.00609-2.

Conference Contributions

PCaPAC 2014

S. Aytac.
Redesign of Alarm Monitoring System Application "BeamlineAlarminfoClient" at DESY.
10th International Workshop on Personal Computers and Particle Accelerator Controls, Karlsruhe (Germany), 10/14/2014 - 10/17/2014.
Oct. 2014.

R. Bacher.
Renovating and Upgrading the Web2cToolkit Suite: A Status Report.
10th International Workshop on Personal Computers and Particle Accelerator Controls, Karlsruhe (Germany), 10/14/2014 - 10/17/2014.
Oct. 2014.

P. Duval, H. G. Wu and J. Bobnar.
Common Device Interface 2.0.
10th International Workshop on Personal Computers and Particle Accelerator Controls, Karlsruhe (Germany), 10/14/2014 - 10/17/2014.
Oct. 2014.

M. Killenberg et al.
Drivers and Software for MicroTCA.4.
10th International Workshop on Personal Computers and Particle Accelerator Controls, Karlsruhe (Germany), 10/14/2014 - 10/17/2014.
Oct. 2014.

J. Wilgen and S. Meykopff.
A Unified Matlab API for TINE and DOOCS Control Systems at DESY.
10th International Workshop on Personal Computers and Particle Accelerator Controls, Karlsruhe (Germany), 10/14/2014 - 10/17/2014.
Oct. 2014.

SRF 2013

A. Matheisen et al.
Strategy of Technology Transfer of EXFEL Preparation Technology to Industry.
16th International Conference on RF Superconductivity, Paris (France), 09/23/2013 - 09/27/2013.
JACoW, Geneva, Sept. 2014.

P. Michelato et al.
An x-ray fluorescence probe for defect detection in superconducting 1.3 GHz cavities.
16th International Conference on RF Superconductivity, Paris (France), 09/23/2013 - 09/27/2013.
JACoW, Geneva, Sept. 2014.

A. Navitski et al.
ILC-HIGRADE Cavities as a Tool of the Quality Control for European XFEL.
16th International Conference on RF Superconductivity, Paris (France), 09/23/2013 - 09/27/2013.
JACoW, Geneva, Sept. 2014.

A. Navitski et al.
***R&D* on Cavity Treatments at DESY Towards the ILC Performance Goal**.
16th International Conference on RF Superconductivity, Paris (France), 09/23/2013 - 09/27/2013.
JACoW, Geneva, Sept. 2014.

A. Navitski et al.
ILC HiGrade cavities as a tool of quality control for European XFEL.
16th International Conference on RF Superconductivity, Paris (France), 09/23/2013 - 09/27/2013.
JACOW, Geneva, Sept. 2014.

A. D. Palczewski et al.
Quench Studies and Preheating Analysis of Seamless Hydroformed Cavities Processed at Jefferson Laboratories.
16th International Conference on RF Superconductivity, Paris (France), 09/23/2013 - 09/27/2013.
JACoW, Geneva, Sept. 2014.

A. Schmidt et al.
PED Requirements Applied to the Cavity and Helium Tank Manufacturing.
16th International Conference on RF Superconductivity, Paris (France), 09/23/2013 - 09/27/2013.
JACoW, Geneva, Sept. 2014.

W. Singer et al.
The Challenge and Realization of the Cavity Production and Treatment in Industry for the European XFEL.
16th International Conference on RF Superconductivity, Paris (France), 09/23/2013 - 09/27/2013.
JACoW, Geneva, Sept. 2014.

RT2014

S. Bou Habib, H. Schlarb and K. Czuba.
Performance Evaluation of MicroTCA.4 Multichannel Fast Digitizer for Direct Sampling Applications.
19th Real-Time conference, Nara (Japan), 05/26/2014 - 05/30/2014.
May 2014.

W. Cichalewski et al.
The Superconducting Cryo-Modules Characterization for European XFEL - LLRF Tests in AMTF.
19th Real-Time conference, Nara (Japan), 05/26/2014 - 05/30/2014.
May 2014.

K. Czuba et al.
RTM RF Backplane for MicroTCA.4 Crates.
19th Real-Time conference, Nara (Japan), 05/26/2014 - 05/30/2014.
May 2014.

M. Fenner et al.
Using Industrial Standard FMC Carrier for Measurement Applications.
19th Real-Time conference, Nara (Japan), 05/26/2014 - 05/30/2014.
May 2014.

S. Jablonski et al.
2pi Low Drift Phase Detector for High Precision Measurements.
19th Real-Time conference, Nara (Japan), 05/26/2014 - 05/30/2014.
May 2014.

M. Killenberg et al.
Drivers and Software for MicroTCA.4.
19th Real-Time conference, Nara (Japan), 05/26/2014 - 05/30/2014.
May 2014.

F. Ludwig, D. Makowski and H. Schlarb.
Zone 3 Classifications for MicroTCA.4.
19th Real-Time conference, Nara (Japan), 05/26/2014 - 05/30/2014.
May 2014.

D. Makowski et al.
High-Speed Data Processing Module for LLRF.
19th Real-Time conference, Nara (Japan), 05/26/2014 - 05/30/2014.
May 2014.

D. Makowski et al.
Standardized Solution of Management Controller for MicroTCA.4.
19th Real-Time conference, Nara (Japan), 05/26/2014 - 05/30/2014.
May 2014.

U. Mavric et al.
Multi-Channel down-Conversion for MicroTCA.4 Based Control Systems.
19th Real-Time conference, Nara (Japan), 05/26/2014 - 05/30/2014.
May 2014.

M. Omet et al.
Development and Test of Klystron Linearization Packages for FPGA-Based Low Level RF Control Systems of ILC-like Electron Accelerators.
19th Real-Time conference, Nara (Japan), 05/26/2014 - 05/30/2014.
May 2014.

P. Predki et al.
Rapid FPGA Development Framework Using a Custom Simulink Library for MTCA.4 Modules.
19th Real-Time conference, Nara (Japan), 05/26/2014 - 05/30/2014.
May 2014.

A. Rosner et al.
RF-Backplane Management for the MicroTCA.4 Control System.
19th Real-Time conference, Nara (Japan), 05/26/2014 - 05/30/2014.
May 2014.

I. Rutkowski et al.
MTCA.4-Based Digital LLRF Control System for CW SRF Linacs.
19th Real-Time conference, Nara (Japan), 05/26/2014 - 05/30/2014.
May 2014.

C. Schmidt et al.
Real Time Control of RF Fields Using a MicroTCA.4 Based LLRF System at FLASH.
19th Real-Time conference, Nara (Japan), 05/26/2014 - 05/30/2014.
May 2014.

MT-23

P. Abramian et al.
Final Design and Prototyping of the Superconducting Magnet Package for the Linear Accelerator of the European XFEL.
23rd International Conference on Magnet Technology, Boston (USA), 07/14/2013 - 07/19/2013.
July 2014.

P. Abramian et al.
Experience on Series Production of the Superconducting Magnet Package for the Linear Accelerator of the European XFEL.
23rd International Conference on Magnet Technology, Boston (USA), 07/14/2013 - 07/19/2013.
July 2014.

LINAC 14

S. Barbanotti et al.
XFEL Cryomodule Transport: from the Assembly Laboratory in CEA-Saclay (France) to the Test-Hall in DESY-HAMBURG (GERMANY).
27th Linear Accelerator Conference, Geneva (Switzerland), 08/31/2014 - 09/05/2014.
Aug. 2014.

H. Hintz et al.
Qualification of the Titanium Welds in the E-XFEL Cryomodule and the CE Certification.
27th Linear Accelerator Conference, Geneva (Switzerland), 08/31/2014 - 09/05/2014.
Aug. 2014.

V. Vogel et al.
Testing of the First Part of Series Production 10MW MBKs for the XFEL Project.
27th Linear Accelerator Conference, Geneva (Switzerland), 08/31/2014 - 09/05/2014.
Aug. 2014.

FEL 2014

B. Beutner.
Beam Energy Management and RF Failure Compensation Scenarios for the European XFEL.
36th International Free Electron Laser Conference, Basel (Switzerland), 08/25/2014 - 08/29/2014.
Aug. 2014.

P. Boonpornprasert et al.
Start-to-End Simulations for IR/THz Undulator Radiation at PITZ.
36th International Free Electron Laser Conference, Basel (Switzerland), 08/25/2014 - 08/29/2014.
Aug. 2014.

R. Brinkmann et al.
Prospects for CW Operation of the European XFEL in Hard X-ray Regime.
36th International Free Electron Laser Conference, Basel (Switzerland), 08/25/2014 - 08/29/2014.
Aug. 2014.

M. K. Czwalinna et al.
Performance Study of High Bandwidth Pickups Installed at FLASH and ELBE for Femtosecond-Precision Arrival Time Monitors.
36th International Free Electron Laser Conference, Basel (Switzerland), 08/25/2014 - 08/29/2014.
Aug. 2014.

N. Ekanayake et al.
Indirect Measurements of NIR and UV Ultrashort Seed Laser Pulses Using a Transverse Deflecting RF-structure.
36th International Free Electron Laser Conference, Basel (Switzerland), 08/25/2014 - 08/29/2014.
Aug. 2014.

K. Honkavaara et al.
FLASH: First Soft X-Ray FEL Operating Two Undulator Beamlines Simultaneously.
36th International Free Electron Laser Conference, Basel (Switzerland), 08/25/2014 - 08/29/2014.
Aug. 2014.

P. N. Juranic et al.
THz Streak Camera for FELTemporal Diagnostics: Concepts and Considerations.
36th International Free Electron Laser Conference, Basel (Switzerland), 08/25/2014 - 08/29/2014.
Aug. 2014.

C. Lechner et al.
Demonstration of SASE Suppression Through a Seeded Microbunching Instability.
36th International Free Electron Laser Conference, Basel (Switzerland), 08/25/2014 - 08/29/2014.
Aug. 2014.

C. Lechner et al.
Measurements of the Timing Stability at the FLASH1 Seeding Experiment.
36th International Free Electron Laser Conference, Basel (Switzerland), 08/25/2014 - 08/29/2014.
Aug. 2014.

G. Marcus et al.
FEL Code Comparison for the Production of Harmonics via Harmonic Lasing.
36th International Free Electron Laser Conference, Basel (Switzerland), 08/25/2014 - 08/29/2014.
Aug. 2014.

P. Peier, H. Dinter and C. Gerth.
Coherent Radiation Diagnostics for Longitudinal Bunch Characterization at European XFEL.
36th International Free Electron Laser Conference, Basel (Switzerland), 08/25/2014 - 08/29/2014.
Aug. 2014.

J. Roensch-Schulenburg et al.
Operation of FLASH with Short SASE-FEL Radiation Pulses.
36th International Free Electron Laser Conference, Basel (Switzerland), 08/25/2014 - 08/29/2014.
Aug. 2014.

E. A. Schneidmiller and M. Yurkov.
An Overview of the Radiation Properties of the European XFEL.
36th International Free Electron Laser Conference, Basel (Switzerland), 08/25/2014 - 08/29/2014.
Aug. 2014.

E. A. Schneidmiller and M. Yurkov.
Circular Polarization Control by Reverse Undulator Tapering.
36th International Free Electron Laser Conference, Basel (Switzerland), 08/25/2014 - 08/29/2014.
Aug. 2014.

E. A. Schneidmiller and M. Yurkov.
Optimization of a High Efficiency FEL Amplifier.
36th International Free Electron Laser Conference, Basel (Switzerland), 08/25/2014 - 08/29/2014.
Aug. 2014.

E. A. Schneidmiller and M. Yurkov.
Statistical Properties of the Radiation from SASE FEL Operating in a Post-saturation Regime with and without Undulator Tapering.
36th International Free Electron Laser Conference, Basel (Switzerland), 08/25/2014 - 08/29/2014.
Aug. 2014.

E. A. Schneidmiller and M. Yurkov.
Suppression of the Fundamental Frequency for a Successful Harmonic Lasing in SASE FELs.
36th International Free Electron Laser Conference, Basel (Switzerland), 08/25/2014 - 08/29/2014.
Aug. 2014.

M. Scholz, M. Vogt and J. Zemella.
Optics measurements at Flash2.
36th International Free Electron Laser Conference, Basel (Switzerland), 08/25/2014 - 08/29/2014.
Aug. 2014.

S. Schreiber and B. Faatz.
First Lasing at FLASH2.
36th International Free Electron Laser Conference, Basel (Switzerland), 08/25/2014 - 08/29/2014.
Aug. 2014.

C. Sydlo et al.
Femtosecond timing distribution for the European XFEL.
36th International Free Electron Laser Conference, Basel (Switzerland), 08/25/2014 - 08/29/2014.
Aug. 2014.

J. Wychowaniak, C. Gerth and M. Yan.
Design of TDS-based Multi-screen Electron Beam Diagnostics for the European XFEL.
36th International Free Electron Laser Conference, Basel (Switzerland), 08/25/2014 - 08/29/2014.
Aug. 2014.

J. Wychowaniak, C. Gerth and M. Yan.
Design of TDS-based Multi-screen Electron Beam Diagnostics for the European XFEL.
36th International Free Electron Laser Conference, Basel (Switzerland).
2014.

M. Yan et al.
Comparison of Quadrupole Scan and Multi-screen Method for the Measurement of Projected and Slice Emittance at the SwissFEL Injector Test Facility.
36th International Free Electron Laser Conference, Basel (Switzerland), 08/25/2014 - 08/29/2014.
Aug. 2014.

IBIC 2014

N.-I. Baboi et al.
Commissioning of the Electronics for HOM-based Beam Diagnostics at the 3.9 GHz Accelerating Module at FLASH.
JACoW conferences. 3rd International Beam Instrumentation Conference, Monterey (USA).
JACoW, 2014.

M. Felber et al.
New MTCA.4-based Hardware Developments for the Control of the Optical Synchronization Systems at DESY.
3rd International Beam Instrumentation Conference, Monterey, California (USA), 09/14/2014 - 09/18/2014.
Sept. 2014.

M. Heuer et al.
Comparison of feedback controller for link stabilizing units of the laser based synchronization system used at the European XFEL.
3rd International Beam Instrumentation Conference, Monterey, California (USA), 09/14/2014 - 09/18/2014.
Sept. 2014.

B. Keil et al.
Beam-Based Calibration and Performance Optimization of Cavity BPMs for SwissFEL, E-XFEL and FLASH2.
JACoW conferences. 3rd International Beam Instrumentation Conference, Monterey (USA), 09/14/2014 - 09/18/2014.
JACoW, Geneva, Sept. 2014.

G. Kube.
Radiation Sources and Their Application for Beam Profile Diagnostics.
JACoW conferences. 3rd International Beam Instrumentation Conference, Monterey (USA), 09/14/2014 - 09/18/2014.
JACoW, Sept. 2014.

T.-J. Lensch et al.
Wire Scanner Installation into the MicroTCA Environment for the European XFEL.
JACoW conferences. 3rd International Beam Instrumentation Conference, Monterey (USA), 09/14/2014 - 09/18/2014.
JACoW, Geneva, Sept. 2014.

D. Lipka et al.
FLASH Undulator BPM Commissioning and Beam Characterization Results.
JACoW conferences. 3rd International Beam Instrumentation Conference, Monterey (USA).
JACoW, Geneva, 2014.

B. Lorbeer et al.
Design, Development and Commissioning of a MTCA-Based Button and Strip-Line BPM System for FLASH2.
JACoW conferences. 3rd International Beam Instrumentation Conference, Monterey (USA).
JACoW, Geneva, 2014.

D. Noelle.
Status of the Standard Diagnostic Systems of the European XFEL.
JACoW conferences. 3rd International Beam Instrumentation Conference, Monterey (USA), 09/14/2014 - 09/19/2014.
JACoW, Geneva, Sept. 2014.

U. Schneekloth et al.
Calibration of OLYMPUS/DORIS Beam Position Monitors.
JACoW conferences. 3rd International Beam Instrumentation Conference, Monterey (USA).
JACoW, Geneva, 2014.

L. Shi, N.-I. Baboi and R. M. Jones.
Stability Study of the Higher Order Mode Beam Position Monitors at the Accelerating Cavities at FLASH.
JACoW conferences. 3rd International Beam Instrumentation Conference, Monterey (USA).
JACoW, Geneva, 2014.

C. Simon et al.
Production Process for the European XFEL Re-Entrant Cavity BPM.
JACoW conferences. 3rd International Beam Instrumentation Conference, Monterey (USA), 09/14/2014 - 09/18/2014.
JACoW, Sept. 2014.

M. Stadler et al.
Low-Q Cavity BPM Electronics for E-XFEL, FLASH-II and SwissFEL.
JACoW conferences. 3rd International Beam Instrumentation Conference, Monterey (USA), 09/14/2014 - 09/18/2014.
JACoW, Sept. 2014.

M. Titberidze et al.
Novel Femtosecond Level Synchronization of Titanium Sapphire Laser and Relativistic Electron Beams.
3rd International Beam Instrumentation Conference, Monterey, California (USA), 09/14/2014 - 09/18/2014.
Sept. 2014.

S. Vilcins-Czvitkovits and D. Lipka.
Mechanical Design of Cryogenic Vacuum Feedthroughs for X-FEL Button BPMs.
JACoW conferences. 3rd International Beam Instrumentation Conference, Monterey (USA).
JACoW, Geneva, 2014.

T. Wamsat and N.-I. Baboi.
First Tests of a Micro-TCA-Based Downconverter Electronic for 5GHz Higher Order Modes in Third Harmonic Accelerating Cavities at the XFEL.
JACoW conferences. 3rd International Beam Instrumentation Conference, Monterey (USA).
JACoW, Geneva, 2014.

M. Werner et al.
A Toroid Based Bunch Charge Monitor System with Machine Protection Features for FLASH and XFEL.
JACoW conferences. 3rd International Beam Instrumentation Conference, Monterey (USA).
JACoW, Geneva, 2014.

S. Wunderlich et al.
A Double-Prism Spectrometer for the Longitudinal Diagnosis of Femtosecond Electron Bunches with Mid-Infrared Transition Radiation.
3rd International Beam Instrumentation Conference, Monterey (USA), 09/14/2014 - 09/18/2014.
JACoW, Geneva, Sept. 2014.

MicroTCA 2014

M. Fenner.
DESY Board Development Stage and Licensing.
3rd MicroTCA workshop for industry and research, Hamburg (Germany), 12/10/2014 - 12/11/2014.
Dec. 2014.

M. Fenner and D. Makowski.
Standardized Solution of Management Controller for MTCA.4.
3rd MicroTCA workshop for industry and research, Hamburg (Germany), 12/10/2014 - 12/11/2014.
Dec. 2014.

M. Grzegrzolka et al.
MTCA.4 Based LLRF System Using Direct Sampling Method.
3rd MicroTCA workshop for industry and research, Hamburg (Germany), 12/10/2014 - 12/11/2014.
Dec. 2014.

M. Killenberg et al.
Update on the MicroTCA.4 User Tool Kit (MTCA4U).
3rd MicroTCA workshop for industry and research, Hamburg (Germany), 12/10/2014 - 12/11/2014.
Dec. 2014.

F. Ludwig.
Ratified ZONE 3 Classes to Achieve Enhanced AMC-RTM Modularity.
3rd MicroTCA workshop for industry and research, Hamburg (Germany), 12/10/2014 - 12/11/2014.
Dec. 2014.

K. Przygoda.
High Voltage Piezo Driver RTM and its Application.
3rd MicroTCA workshop for industry and research, Hamburg (Germany), 12/10/2014 - 12/12/2014.
Dec. 2014.

I. Rutkowski et al.
Precision Regulation for SRF Cavities Using MTCA.4.
3rd MicroTCA workshop for industry and research, Hamburg (Germany), 12/10/2014 - 12/11/2014.
Dec. 2014.

IPAC 2014

S. M. Alzubaidi et al.
A Control System for the FRANZ Accelerator.
5th International Particle Accelerator Conference, Dresden (Germany), 06/15/2014 - 06/20/2014.
June 2014.

R. Aßmann and J. Grebenyuk.
Accelerator Physics Challenges towards a Plasma Accelerator with Usable Beam Quality.
5th International Particle Accelerator Conference, Dresden (Germany), 06/16/2014 - 06/20/2014.
June 2014.

R. Assmann et al.
SINBAD - a proposal for a dedicated accelerator research facility at DESY.
5th International Particle Accelerator Conference, Dresden (Germany), 06/15/2014 - 06/20/2014.
June 2014.

V. Balandin, W. Decking and N. Golubeva.
Beamlines With Two Deflecting Cavities Fortransverse-To-Longitudinal Phase Space Eschange.
5th International Particle Accelerator Conference, Dresden (Germany), 06/15/2014 - 06/20/2014.
June 2014.

V. Balandin, W. Decking and N. Golubeva.
Betatron Oscillations In Planar Dipole Field.
5th International Particle Accelerator Conference, Dresden (Germany), 06/15/2014 - 06/20/2014.
June 2014.

V. Balandin and N. Golubeva.
Dynamics of Twiss Parameters from the Geometrical Viewpoint.
5th International Particle Accelerator Conference, Dresden (Germany), 06/15/2014 - 06/20/2014.
June 2014.

A. Borysenko et al.
Electro-optical Bunch Length Monitor for FLUTE: Layout and Simulations.
5th International Particle Accelerator Conference, Dresden (Germany), 06/15/2014 - 06/20/2014.
June 2014.

J. Branlard et al.
European XFEL RF Gun Commissioning and LLRF Linac Installation.
5th International Particle Accelerator Conference, Dresden (Germany), 06/15/2014 - 06/20/2014.
June 2014.

R. Brinkmann.
Long-term Accelerator *R&D* as an Independent Research Field.
5th International Particle Accelerator Conference, Dresden (Germany), 06/15/2014 - 06/20/2014.
June 2014.

H. Delsim-Hashemi and K. Flöttmann.
Dark Current Studies at Relativistic Electron Gun for Atomic Exploration – REGAE.
5th International Particle Accelerator Conference, Dresden (Germany), 06/15/2014 - 06/20/2014.
June 2014.

M. Fakhari et al.
Design of New Buncher Cavity for Relativistic Electron Gun for Atomic Exploration – REGAE.
5th International Particle Accelerator Conference, Dresden (germany), 06/16/2014 - 06/20/2014.
June 2014.

M. Felber et al.
Compact MTCA.4 Based Laser Synchronization.
5th International Particle Accelerator Conference, Dresden (Germany), 06/15/2014 - 06/20/2014.
June 2014.

M. Gensch et al.
THz Facility at ELBE: A Versatile Test Facility for Electron Bunch Diagnostics on Quasi-CW Electron Beams.
JACoW conferences. 5th International Particle Accelerator Conference, Dresden (Germany).
JACoW, Geneva, 2014.

N. Golubeva, V. Balandin and W. Decking.
Layout and Optics of the Dump Line at the European XFEL.
5th International Particle Accelerator Conference, Dresden (Germany), 06/15/2014 - 06/20/2014.
June 2014.

J. Good et al.
Report on Gun Conditioning Activities at PITZ in 2013.
5th International Particle Accelerator Conference, Dresden (Germany), 06/15/2014 - 06/20/2014.
JACoW, June 2014.

M. Groß et al.
First Experiences with the PITZ Plasma Cell for Electronbeam Self-Modulation Studies.
5th International Particle Accelerator Conference, Dresden (Germany), 06/15/2014 - 06/20/2014.
JACoW, June 2014.

M. Hansli et al.
A Beam Arrival Time Cavity for REGAE at DESY.
JACoW conferences. 5th International Particle Accelerator Conference, Dresden (Germany).
Geneva, 2014.

H. Hassanzadegan et al.
Design, Implementation and Preliminary Test Results of the ESS Beam Current Monitor System.
JACoW conferences. 5th International Particle Accelerator Conference, Dresden (Germany).
JACoW, Geneva, 2014.

H. Hassanzadegan et al.
System Overview and Current Status of the ESS Beam Position Monitors.
JACoW conferences. 5th International Particle Accelerator Conference, Dresden (Germany), 06/16/2014 - 06/20/2014.
Geneva, June 2014.

Heinemann et al.
New and Unifying Formalism for Study of Particle-Spin Dynamics Using Tools Distilled from Theory of Bundles of Particle-Spin Dynamics Using Tools Distilled from Theory of Bundles.
5th International Particle Accelerator Conference, Dresden (Germany), 06/15/2014 - 06/20/2014.
June 2014.

N. Hiller et al.
Status of Single-shot EOSD Measurement at ANKA.
5th International Particle Accelerator Conference, Dresden (Germany), 06/15/2014 - 06/20/2014.
June 2014.

M. Hoffmann et al.
High Speed Digitial LLRF Feedbacks for Normal Conducting Cavity Operation.
5th International Particle Accelerator Conference, Dresden (Germany), 06/15/2014 - 06/20/2014.
June 2014.

E. Janas et al.
Design and Integration of the Optical Reference Module at 1.3 GHz for FLASH and the European XFEL.
5th International Particle Accelerator Conference, Dresden (Germany), 06/15/2014 - 06/20/2014.
June 2014.

M. Khojoyan, M. Krasilnikov and F. Stephan.
Studies on the Application of the 3D Ellipsoidal Cathodelaser pulses at PITZ.
5th International Particle Accelerator Conference, Dresden (Germany), 06/15/2014 - 06/20/2014.
JACoW, June 2014.

M. Killenberg et al.
Drivers and Software for MTCA.4.
5th International Particle Accelerator Conference, Dresden (Germany), 06/15/2014 - 06/20/2014.
June 2014.

G. Kourkafas et al.
Emittance Increase and Matching along the Tomography Module at PITZ.
5th International Particle Accelerator Conference, Dresden (Germany), 06/15/2014 - 06/20/2014.
JACoW, June 2014.

M. Krasilnikov et al.
Possibility of Application of THz Wiggler in Low Energy FEL for Measurements of Electron Bunch Longitudinal Structure.
5th International Particle Accelerator Conference, Dresden (Germany), 06/15/2014 - 06/20/2014.
June 2014.

A. Kuramoto, N.-I. Baboi and H. Hayano.
Simulations and Measurements of Beam Pipe Modes excited in 9-cell Superconducting Cavities.
JACoW conferences. 5th International Particle Accelerator Conference, Dresden (Germany).
JACoW, Geneva, 2014.

D. Lipka and S. Vilcins-Czvitkovits.
BPMs From Design to Real Measurement.
5th International Particle Accelerator Conference, Dresden (Germany), 06/15/2014 - 06/20/2014.
June 2014.

U. Mavric et al.
Mitigating Noise Sources in MTCA.4 Electronics for High Precision Measurements.
5th International Particle Accelerator Conference, Dresden (germany), 06/15/2014 - 06/20/2014.
June 2014.

U. Mavrič et al.
Performance of a Compact LLRF System using Analog RF Backplane in MTCA.4 Crates.
5th International Particle Accelerator Conference, Dresden (Germany), 06/15/2014 - 06/20/2014.
June 2014.

F. Mayet et al.
Studies on a Diagnostic Pulse for FLASH.
5th International Particle Accelerator Conference, Dresden (Germany), 06/16/2014 - 06/20/2014.
June 2014.

K. Przygoda et al.
MTCA.4 Module for Cavity and Laser Piezo Operation.
5th International Particle Accelerator Conference, Dresden (Germany), 06/15/2014 - 06/20/2014.
June 2014.

T. Rublack et al.
Development of a Quasi 3-D Ellipsoidal Photo Cathode Laser System for PITZ.
5th International Particle Accelerator Conference, Dresden (Germany), 06/15/2014 - 06/20/2014.
JACoW, June 2014.

R. Rybaniec et al.
Real-time Estimation of Superconducting Cavities Parameters.
5th International Particle Accelerator Conference, Dresden (Germany), 06/15/2014 - 06/20/2014.
June 2014.

C. Schmidt et al.
Performance of the MTCA.4 Based LLRF System at FLASH.
5th International Particle Accelerator Conference, Dresden (Germany), 06/15/2014 - 06/20/2014.
June 2014.

F. Schmidt-Föhre et al.
First Tests with the Self-triggered Mode of the New MicroTCA-based Low-charge Electronics for Button and Stripline BPMs at FLASH.
JACoW conferences. 5th International Particle Accelerator Conference, Dresden (Germany).
JACoW, Geneva, 2014.

P. P. Schneider et al.
Beam Dynamics in the LEBT for FRANZ.
5th International Particle Accelerator Conference, Dresden (Germany), 06/15/2014 - 06/20/2014.
June 2014.

E. A. Schneidmiller and M. Yurkov.
Analysis of Operation of Harmonic Lasing Self-seeded FEL.
5th International Particle Accelerator Conference, Dresden (Germany), 06/15/2014 - 06/20/2014.
June 2014.

E. A. Schneidmiller and M. Yurkov.
Harmonic Lasing in X-ray FELs.
5th International Particle Accelerator Conference, Dresden (Germany), 06/15/2014 - 06/20/2014.
June 2014.

E. A. Schneidmiller and M. Yurkov.
Investigation of the Coherence Properties of the Radiation at FLASH.
5th International Particle Accelerator Conference, Dresden (Germany), 06/15/2014 - 06/20/2014.
June 2014.

E. A. Schneidmiller and M. Yurkov.
Obtaining High Degree of Circular Polarization at X-ray FELs via a Reverse Undulator Taper.
5th International Particle Accelerator Conference, Dresden (Germany), 06/15/2014 - 06/20/2014.
June 2014.

M. Schuh et al.
Status of FLUTE.
5th International Particle Accelerator Conference, Dresden (Germany), 06/15/2014 - 06/20/2014.
June 2014.

M. Vogt et al.
Status of the Free Electron Laser User Facility FLASH.
5th International Particle Accelerator Conference, Dresden (Germany), 06/15/2014 - 06/20/2014.
June 2014.

C. Wiesner et al.
Experimental Performance of an $E\times B$ Chopper System.
5th International Particle Accelerator Conference, Dresden (Germany), 06/15/2014 - 06/20/2014.
June 2014.

L. Zembala et al.
Master Oscillator for the European XFEL.
5th International Particle Accelerator Conference, Dresden (Germany), 06/15/2014 - 06/20/2014.
June 2014.

J. Zemella et al.
Measurements of the Optical Functions at FLASH.
5th International Particle Accelerator Conference, Dresden (Germany), 06/15/2014 - 06/20/2014.
June 2014.

Other Conference Contributions

M. Heuer et al.
Modeling of the Master Laser Oscillator Phase Noise for the European XFEL Using Fractional Order Systems.
19th World Congress of the International Federation of Automatic Control, Cape Town (South Africa), 08/24/2014 - 08/29/2014.
Aug. 2014.

S. Roling et al.
A Hard x-Ray Split-and-Delay Unit for the HED Experiment at the European XFEL.
SPIE Optical Engineering + Applications, San Diego (United States), 08/09/2014 - 08/13/2014.
Aug. 2014.
doi: 10.1117/12.2061879.

J. Schaffran et al.
Design parameters and commissioning of vertical inserts used for testing the XFEL superconducting cavities.
AIP Conference Proceedings. Cryogenic Engineering Conference & International Cryogenic Materials Conference, Anchorage (USA), 06/17/2013 - 06/21/2013.
June 2014.
doi: 10.1063/1.4860705.

S. R. Uglov et al.
Investigation Of The Characteristics of EUV Backward Transition Radiation Generated by 5.7 MeV Electrons in Mono- and Multilayer Targets.
X International Symposium on ”Radiation from Relativistic Electrons in Periodic Structures”, Lake Sevan (Armenia), 09/23/2013 - 09/28/2013.
IOP Publ., Bristol, Sept. 2014.
doi: 10.1088/1742-6596/517/1/012009.

Conference Presentations

EuCARD2

R. Assmann et al.
European Network for Novel Accelerators (EuroNNAc2), WP7.
1st Enhanced European Coordination for Accelerator *R&D* Annual Meeting, Hamburg (Germany), 05/19/2014 - 05/23/2014.
May 2014.

H. Weise.
The European XFEL - Challenges and Status.
1st Enhanced European Coordination for Accelerator *R&D* Annual Meeting, Hamburg (Germany), 05/19/2014 - 05/23/2014.
May 2014.

ICEC2014

J. Schaffran et al.
Test sequence for superconducting XFEL Cavities in the Accelerator Module Test Facility (AMTF) at DESY.
25th International Cryogenic Engineering Conference & International Cryogenic Materials Conference, Enschede (The Netherlands), 07/07/2014 - 07/11/2014.
July 2014.

H. Wilhelm, B. Petersen and T. Schnautz.
Current status of the Modifications of the former HERA cryogenic plant for the XFEL facility.
25th International Cryogenic Engineering Conference & International Cryogenic Materials Conference, Enschede (The Netherlands), 07/07/2014 - 07/11/2014.
July 2014.

LINAC 14

J. Branlard.
Low Level RF for SRF Accelerators.
27th Linear Accelerator Conference, Geneva (Switzerland), 08/31/2014 - 09/05/2014.
Aug. 2014.

V. Katalev et al.
A new type of waveguide distribution for the accelerator module test facility of the European XFEL.
27th Linear Accelerator Conference, Geneva (Switzerland), 08/31/2014 - 09/05/2014.
Aug. 2014.

M. Krasilnikov and F. Stephan.
RF guns for FELs.
27th Linear Accelerator Conference, Geneva (Switzerland), 08/31/2014 - 09/05/2014.
Aug. 2014.

D. Reschke et al.
Analysis of the RF Test Results from the On-Going Cavity Production for the European XFEL.
27th Linear Accelerator Conference, Geneva (Switzerland), 08/31/2014 - 09/05/2014.
Aug. 2014.

A. Sulimov et al.
Efficiency of High Order Modes Extraction in the European XFEL Linac.
27th Linear Accelerator Conference, Geneva (Switzerland), 08/31/2014 - 09/05/2014.
Aug. 2014.

V. Vogel et al.
Testing of the First Part of Series Production 10 MW MBKS for the XFEL Project.
27th Linear Accelerator Conference, Geneva (Italy), 08/31/2014 - 09/05/2014.
Aug. 2014.

FEL 2014

S. Ackermann et al.
Indirect Measurements of NIR and UV Ultrashort Seed Laser Pulses Using a Transverse Deflecting RF-Structure.
36th International Free Electron Laser Conference, Basel (Switzerland), 08/25/2014 - 08/29/2014.
Aug. 2014.

P. Boonpornprasert et al.
Start-to-end simulations for IR/THZ undulator radiation at PITZ.
36th International Free Electron Laser Conference, Basel (Switzerland), 08/25/2014 - 08/29/2014.
Aug. 2014.

W. Decking and F. Le Pimpec.
European XFEL construction status.
36th International Free Electron Laser Conference, Basel (Switzerland), 08/24/2014 - 08/29/2014.
Aug. 2014.

G. Feng et al.
Start-to-End Simulation for FLASH2 HGHG Option.
36th International Free Electron Laser Conference, Basel (Switzerland), 08/25/2014 - 08/29/2014.
Aug. 2014.

K. Honkavaara.
FLASH at DESY - The First Soft X-ray FEL Operating Two Undulator Beamlines Simultaneously.
36th International Free Electron Laser Conference, basel (Switzerland), 08/24/2014 - 08/29/2014.
Aug. 2014.

M. Khojoyan et al.
Optimization of the PITZ photo injector towards the beste achievable beam quality.
36th International Free Electron Laser Conference, Basel (Switzerland), 08/25/2014 - 08/29/2014.
Aug. 2014.

T. Rublack et al.
Design of a spatio-temporal 3-D ellipsoidal photocathode laser system for the high brightness photoinjector PITZ.
36th International Free Electron Laser Conference, Basel (Switzerland), 08/25/2014 - 08/29/2014.
Aug. 2014.

S. Schreiber and B. Faatz.
First Lasing at FLASH2.
36th International Free Electron Laser Conference, Basel (Switzerland), 08/24/2014 - 08/29/2014.
Aug. 2014.

G. Vashchenko et al.
Recent electron beam optimization at PITZ.
36th International Free Electron Laser Conference, Basel (Switzerland), 08/25/2014 - 08/29/2014.
Aug. 2014.

IBIC 2014

N.-I. Baboi.
Commissioning of the FLASH2 Electron Beam Diagnostics in Respect to its use at the European XFEL.
3rd International Beam Instrumentation Conference, Monterey (USA), 09/14/2014 - 09/18/2014.
Sept. 2014.

D. Malyutin et al.
Longitudinal Phase Space Tomography Using a Booster Cavity at the Photo Injector Test Facility at DESY, Zeuthen site (PITZ).
3rd International Beam Instrumentation Conference, Monterey (United States), 09/14/2014 - 09/18/2014.
Sept. 2014.

S. Wunderlich et al.
A double-prism spectrometer for the longitudinal diagnosis of femtosecond electron bunches with mid-infrared transition radiation.
3rd International Beam Instrumentation Conference, Monterey (USA), 09/14/2014 - 09/18/2014.
Sept. 2014.

3rd oPAC Topical Workshop on Beam Diagnostics

D. Lipka et al.
DaMon: A Resonator to Observe Bunch Charge/Length And Dark Current.
3rd oPAC Topical Workshop on Beam Diagnostics, Vienna (Austria), 05/08/2014 - 05/09/2014.
May 2014.

K. Wittenburg.
Overview of BLM Technology.
3rd oPAC Topical Workshop on Beam Diagnostics, Vienna (Austria), 05/08/2014 - 05/09/2014.
May 2014.

IPAC2014

R. Aßmann and J. Grebenyuk.
Accelerator Physics Challenges towards a Plasma Accelerator with Usable Beam Quality.
5th International Particle Accelerator Conference, Dreden (Germany), 06/15/2014 - 06/20/2014.
June 2014.

S. Bayesteh, H. Delsim-Hashemi and K. Flöttmann.
Transverse Emittance Measurement at REGAE.
5th International Particle Accelerator Conference, Dresden (Germany), 06/15/2014 - 06/20/2014.
June 2014.

H. Delsim-Hashemi and K. Flöttmann.
Dark Current Studies at Relativistic Electron Gun for Atomic Exploration – REGAE.
5th International Particle Accelerator Conference, Dresden (Germany), 06/15/2014 - 06/20/2014.
June 2014.

M. Fakhari et al.
Design of New Buncher Cavity for Relativistic Electron Gun for Atomic Exploration – REGAE.
5th International Particle Accelerator Conference, Dresden (Deutschland), 06/15/2014 - 06/20/2014.
June 2014.

J. Grebenyuk et al.
Laser-driven Acceleration with External Injection at SINBAD.
5th International Particle Accelerator Conference, Dresden (Germany), 06/15/2014 - 06/20/2014.
June 2014.

M. Hansli et al.
A Beam Arrival Time Cavity for REGAE at DESY.
5th International Particle Accelerator Conference, Dresden (Germany), 06/15/2014 - 06/20/2014.
June 2014.

N. Hiller et al.
Status of Single-shot EOSD Measurement at ANKA.
5th International Particle Accelerator Conference, Dresden (Germany), 06/15/2014 - 06/20/2014.
June 2014.

V. Libov et al.
FLASHForward - Future-oriented wakefield-accelerator research and development at FLASH.
5th International Particle Accelerator Conference, Dresden (Germany), 06/15/2014 - 06/20/2014.
June 2014.

A. Lüdeke et al.
A Common Operation Metrics for Third Generation Light Sources.
5th International Particle Accelerator Conference, Dresden (Germany), 06/15/2014 - 06/20/2014.
June 2014.

A. Martinez de la Ossa et al.
Wakefield-Induced Ionization Injection.
5th International Particle Accelerator Conference, Dresden (Germany), 06/15/2014 - 06/20/2014.
June 2014.

M. Scholz et al.
Measurements of the Optical Functions at FLASH.
5th International Particle Accelerator Conference, Dresden (Germany), 06/15/2014 - 06/20/2014.
June 2014.

E. Syresin et al.
Synchrotron Radiation Test Validations of European XFEL MCP-based Detectors at DORIS Beamline BW1.
5th International Particle Accelerator Conference, Dresden (Germany), 06/15/2014 - 06/20/2014.
June 2014.

S. R. Uglov et al.
EUV Radiation Generated by a 5.7 MeV Electron Beam in Multilayer Periodical Structure.
5th International Particle Accelerator Conference, Dresden (Germany), 06/15/2014 - 06/20/2014.
June 2014.

H. Weise.
How to produce 100 Superconducting Modules for the European XFEL in Collaboration and with Industry.
5th International Particle Accelerator Conference, Dresden (Germany), 06/15/2014 - 06/20/2014.
June 2014.

DPG 2014

P. Boonpornprasert.
Simulation of Undulator Radiation for the THz Source Project at PITZ.
DPG Frühjahrstagung, Dresden (Germany), 03/30/2014 - 04/04/2014.
Mar. 2014.

I. Isaev.
Gun Conditioning at PITZ.
DPG Frühjahrstagung, Dresden (Germany), 03/30/2014 - 04/04/2014.
Mar. 2014.

O. Kononenko et al.
Controlled injection of plasma electrons into a beam-driven wakefield using the density downramp technique in the E-215 experiment at FACET.
DPG Frühjahrstagung, Dresden (Germany), 03/30/2014 - 04/04/2014.
Mar. 2014.

ICFA2014

R. Wanzenberg.
Tapered Transitions Dominating the PETRA III Impedance Model.
ICFA mini-Workshop on "Electromagnetic wake fields and impedances in particle accelerators", Erice, Sicily (Italy), 04/24/2014 - 04/28/2014.
Apr. 2014.

I. Zagorodnov.
Challenges for the XFEL Project at DESY.
ICFA mini-Workshop on "Electromagnetic wake fields and impedances in particle accelerators", Erice, Sicily (Italy), 04/24/2014 - 04/28/2014.
Apr. 2014.

I. Zagorodnov.
Wakefield Code ECHO 2(3)D.
ICFA mini-Workshop on "Electromagnetic wake fields and impedances in particle accelerators", Erice, Sicily (Italy), 04/24/2014 - 04/28/2014.
Apr. 2014.

LAOLA Workshop

M. Gross.
Status of the Self-Modulation Experiment at PITZ.
LAOLA Workshop, Wismar (Germany), 10/06/2014 - 10/06/2014.
Oct. 2014.

M. Khojoyan, A. M. d. l. Ossa and D. Malyutin.
Optimization and Transport of Electron Beam for Self-Modulation Experiments at PITZ.
LAOLA Workshop, Wismar (Germany), 10/06/2014 - 10/07/2014.
Oct. 2014.

M. Khojoyan.
Self-Modulation Studies: Electron Beam Longitudinal Phase Space after Beam-Plasma Interaction.
LAOLA Workshop, Wismar (Germany), 10/06/2014 - 10/07/2014.
Oct. 2014.

G. Pathak et al.
Simulation and Preliminary Experimental Study for Self-modulation Experiment at PITZ.
LAOLA Workshop, Wismar (Germany), 10/06/2014 - 10/07/2014.
Oct. 2014.

PITZ Collaboration Meeting

S. Schreiber.
News from FLASH.
PITZ Collaboration Meeting, Zeuthen (Germany), 05/27/2014 - 05/28/2014.
May 2014.

S. Schreiber.
News from FLASH.
PITZ Collaboration Meeting, Zeuthen (Germany), 12/02/2014 - 12/03/2014.
Dec. 2014.

Other Conference Presentations

R. Assmann.
A European Perspective on Plasma Acceleration.
Workshop on Plasma Acceleration STFC, London (England), 01/31/2014 - 01/31/2014.
Jan. 2014.

R. Assmann.
Accelerator $R\&D$ in Europe.
High Energy Physics Advisory Panel Accelerator $R\&D$ Sub-Panel Meeting at SLAC National Accelerator Laboratory, Stanford (USA), 08/29/2014 - 08/30/2014.
Aug. 2014.

R. Assmann.
European Network for Novel Accelerators (EuroNNAc2).
ICAN Meeting, Palaiseau (France), 04/28/2014 - 04/28/2014.
Apr. 2014.

R. Assmann and J. Grebenyuk.
Advanced Accelerator $R\&D$ at DESY and Roadmap Towards Applications.
Accelerator Test Facility II Upgrade Workshop, Brookhaven (USA), 10/16/2014 - 10/17/2014.
Oct. 2014.

M. Bieler.
A Common Operation Metrics for 3rd Generation Light Sources.
IAEA Technical Meeting on Management Strategies for Accelerator Facilities, Saint-Aubin (France), 09/15/2014 - 09/19/2014.
Sept. 2014.

M. Bieler.
HERA Experience or Lessons Learned at HERA, the Last e-p collider.
Electron Ion Colliders 2014, Newport News (USA), 03/17/2014 - 03/21/2014.
Mar. 2014.

M. Bieler.
PETRA III Installation Experience.
4th Diffraction Limited Storage Ring (DLSR) Workshop, Argonne (USA), 11/19/2014 - 11/21/2014.
Nov. 2014.

J. Boedewadt et al.
Plans for Seeding at FLASH.
DESY Photon Science User Meeting 2014, Hamburg (Germany), 01/30/2014 - 01/31/2014.
Jan. 2014.

J. Boedewadt et al.
Status and Strategies for Seeding at FLASH.
Opportunities for FLASH2 Beamlines, Hamburg (Germany), 01/28/2014 - 01/28/2014.
Jan. 2014.

S. Choroba.
The High Power RF System of the European XFEL.
Continuous Wave and High Average Power RF Workshop, Trieste (Italy), 05/13/2014 - 05/16/2014.
May 2014.

M. Dohlus.
Simulation of the Trickle Heating Effect.
6th Microbunching Instability Workshop, Triest (Italy), 10/06/2014 - 10/08/2014.
Oct. 2014.

M. Gross.
Accelerator Activities at PITZ.
LA3NET 3rd Topical Workshop on Novel Acceleration Techniques, Dresden-Rossendorf (Germany), 04/27/2014 - 04/30/2014.
Apr. 2014.

M. Krasilnikov.
Advanced Photo Cathode Laser Pulse Shaping for Ultimate XFEL Photo Injector Performance.
2nd ARD ST3 workshop, Dresden-Rossendorf (Germany), 02/26/2014 - 02/27/2014.
Feb. 2014.

M. Krasilnikov.
Deutsches Elektronen-Synchrotron DESY.
German-Russian Career Day, Uljanowsk (Russia), 04/29/2014 - 04/29/2014.
Apr. 2014.

M. Krasilnikov.
Development of a Photo Cathode Laser System for Quasi Ellipsoidal Bunches at a High Brightness Photo Injector.
HRJRG Workshop, , Moscow (Russia), 03/03/2014 - 03/03/2014.
Mar. 2014.

G. Kube.
Review of Petra-3 Diagnostics.
1st Diagnostics Experts of European Light Sources Workshop, Grenoble (France), 05/12/2014 - 05/13/2014.
May 2014.

B. Petersen.
Full cryogenic operation of AMTF-the first year.
6th International Workshop on cryogenic Operations, Daresbury (United Kingdom), 11/10/2014 - 11/12/2014.
Nov. 2014.

G. K. Sahoo et al.
Power Supplies Transient Recorders for Post-Mortem Analysis of BPM OrbitT Dumps at PETRA-III.
PCaPAC2014 - 10th International Workshop on Personal Computers and Particle Accelerator Controls, Karlsruhe (Germany), 10/13/2014 - 10/17/2014.
Oct. 2014.

S. Schreiber.
FLASH Facility: Accelerator.
Research field Matter - Programme MML - On-site visit, Hamburg (Germany), 03/17/2014 - 03/17/2014.
Mar. 2014.

S. Schreiber.
FLASH Operational Experience.
TESLA Technology Collaboration Meeting, Hamburg (Germany), 03/24/2014 - 03/27/2014.
Mar. 2014.

J.-P. Schwinkendorf et al.
FLASHForward - Future-orientated wakefield-accelerator research and development at FLASH.
HPL Christmas meeting 2014, Abingdon (United Kingdom), 12/15/2014 - 12/17/2014.
Dec. 2014.

N. J. Walker.
Energy-Frontier Colliders - the Road Ahead.
International Conference on High Energy Physics, Valencia (Spain), 07/02/2014 - 07/09/2014.
July 2014.

R. Wanzenberg.
PETRA III Status Report 2014.
XXII European Synchrotron Light Source Workshop, Grenoble (France), 11/24/2014 - 11/26/2014.
Nov. 2014.

H. Weise.
100 Superconducting Modules for the European XFEL.
International Workshop on Future Linear Colliders, Belgrad (Serbien), 10/06/2014 - 10/10/2014.
Oct. 2014.

H. Weise.
Status of the European XFEL Accelerator.
2014 European XFEL Users' Meeting, Hamburg (Germany), 01/29/2014 - 01/30/2014.
Jan. 2014.

K. Wittenburg.
Beam diagnostics for the detection and understanding of beam halo.
54th ICFA Advanced Beam Dynamics Workshop on High-Intensity and High-Brightness Hadron Beams, East Lansing (USA), 11/10/2014 - 11/14/2014.
Nov. 2014.

K. Wittenburg.
Halo Monitoring: Very High Dynamic Beam Profile Measurements.
Workshop on Beam Halo Monitoring, SLAC National Accelerator Laboratory (USA), 09/19/2014 - 09/19/2014.
Sept. 2014.

K. Wittenburg.
Homogene Dokumentation in einem heterogenen Forschungsinstitut.
NetWork’14, Leipzig (Germany), 04/29/2014 - 04/30/2014.
Apr. 2014.

Thesis

Ph.D. Thesis

S. Bayesteh.
Transverse Electron Beam Diagnostic at REGAE.
Universität Hamburg, 2014.

A. Ignatenko.
Development of Beam Halo Monitors for the European XFEL using radiation hard sensors and demonstration of the technology at FLASH.
BTU Cottbus-Senftenberg, 2014.

C. Liebig.
Design and Construction of an Injector for an Electron/Positron Linac Optimized for Positron Yield and Minimal Particle Loss.
Universität Hamburg, 2014.

D. Malyutin.
Time Resolved Transverse and Longitudinal Phase Space Measurements at the High Brightness Photo Injector PITZ.
University of Hamburg, Hamburg, 2014.

S. Pfeiffer.
Symmetric Grey Box Identification and Distributed Beam-Based Controller Design for Free-Electron Lasers.
Hamburg University of Technology, 2014.

S. Schulz.
Implementation of the Laser-Based Femtosecond Precision Synchronization System at FLASH.
Universität Hamburg, Hamburg, 2014.

Master Thesis

S. Philipp.
Investigation of the Mechanical Tuning for Electron Guns used in Free Electron Lasers - Finite Element Analysis of Plastic Deformation and Experimental Validation.
Ernst-Abbe-Hochschule Jena, 2014.

Photographs and graphics
Lars Berg, Hamburg
DESY
European XFEL
Marta Mayer (DESY)
Heiner Müller-Elsner, Hamburg
Dirk Nölle (DESY)
Reimo Schaaf, Hamburg
Edgar Weckert (DESY)

The figures were reproduced by permission of authors or journals.

Acknowledgement
We would like to thank all authors and everyone who helped in the creation of this annual report.

Imprint

Publishing and contact
Deutsches Elektronen-Synchrotron DESY
A Research Centre of the Helmholtz Association

Hamburg location:
Notkestr. 85, 22607 Hamburg, Germany
Tel.: +49 40 8998-0, Fax: +49 40 8998-3282
desyinfo@desy.de

Zeuthen location:
Platanenallee 6, 15738 Zeuthen, Germany
Tel.: +49 33762 7-70, Fax: +49 33762 7-7413
desyinfo.zeuthen@desy.de

www.desy.de
ISBN 978-3-935702-98-0

Editing
Klaus Balewski,
Ilka Flegel, Kapellendorf

Layout
Diana Schröder

Production
Britta Liebaug

Printing
EHS Druck GmbH, Schenefeld

Editorial deadline
28 February 2015

Editorial note
The authors of the individual scientific contributions published in this report are fully responsible for the contents.

HELMHOLTZ
ASSOCIATION

Deutsches Elektronen-Synchrotron
A Research Centre of the Helmholtz Association

The Helmholtz Association is a community of 18 scientific-technical and biological-medical research centres. These centres have been commissioned with pursuing long-term research goals on behalf of the state and society. The Association strives to gain insights and knowledge so that it can help to preserve and improve the foundations of human life. It does this by identifying and working on the grand challenges faced by society, science and industry. Helmholtz Centres perform top-class research in strategic programmes in six core fields: Energy, Earth and Environment, Health, Key Technologies, Structure of Matter, Aeronautics, Space and Transport.

www.helmholtz.de